A mass, energy, and helicity conserving dual-field discretization of the incompressible Navier-Stokes problem

A thesis presented by
MARKUS RENOLDNER

submitted to the
FACULTY OF MATHEMATICS
TECHNISCHE UNIVERSITÄT WIEN

to attain the degree of
DIPLOM-INGENIEUR (Dipl.-Ing.) / MASTER OF SCIENCE (MSc)

accepted on the recommendations of
Prof. Dr. Ralf Hiptmair, ETH Zürich

Dr. Markus Faustmann, TU Wien
Prof. Dr. Joachim Schöberl, TU Wien

April, 2023

Abstract

A structure-preserving dual-field discretization of the 3D incompressible Navier-Stokes problem is derived, which conserves mass, kinetic energy, and helicity on a periodic domain. In this approach, a conservative mixed variational formulation is introduced. It is based on two systems of equations with dual representations of velocity, vorticity, and pressure. Then, a staggered temporal discretization is constructed in order to integrate the evolution equations and to decouple the two systems. That way, the convective terms are linearzed, resulting in two discrete, algebraic systems. Furthermore, a spatial Galerkin Finite Element discretization is introduced, that follows a mimetic approach: The finite dimensional spaces form a discrete de Rham complex, which is essential to enable the conservation properties of the scheme. Conservation of mass, kinetic energy, and helicity at the discrete level is proven in the inviscid limit. The proposed method is expanded to a much more realistic, non-periodic Dirichlet problem, by adapting the finite-dimensional function spaces. It is proven, that mass and kinetic energy are still conserved. Numerical tests supporting the method in both the periodic and non-periodic setting are provided.

Acknowledgements

I want to thank my supervisors Prof. Ralf Hiptmair and Dr. Markus Faustmann whom I both had highly fruitful discussions with.
Moreover many thanks Wouter Tonnon, whose understanding of the technicalities of this project is only surpassed by his patience with me.
Thank you to my friends and family who supported me wherever they could.

Contents

Chapter 1

The incompressible Navier-Stokes equations

Incompressible flows can be modelled as a continuum described by the well-known Navier-Stokes equations. General, closed-form, analytic solutions for these partial differential equations have not been found so far. In fact, even the existence proof of smooth solutions seems to be out of reach currently. This motivates the construction of numerical methods that are 1) efficient to solve and 2) preserve relevant physical and mathematical structures in the discrete setting. One possible method that preserves mass, kinetic energy, and helicity of the flow-field will be discussed in this thesis.

First, consider the incompressible Navier-Stokes equations in rotational form

$$\begin{cases} \dfrac{\partial \boldsymbol{u}}{\partial t} + \boldsymbol{\omega} \times \boldsymbol{u} + \dfrac{1}{\mathrm{Re}} \nabla \times \boldsymbol{\omega} + \nabla p = \boldsymbol{f} \\ \boldsymbol{\omega} = \nabla \times \boldsymbol{u}, \\ \nabla \cdot \boldsymbol{u} = 0 \end{cases} \tag{1.1}$$

defined on a simply connected domain $\Omega \subset \mathbb{R}^d$ and time interval $(0, t)$ with the unknown velocity field $\boldsymbol{u} : \Omega \times (0,t) \to \mathbb{R}^d$, the unknown total pressure $p : \Omega \times (0,t) \to \mathbb{R}$, the vorticity $\boldsymbol{\omega}$, and given data $\boldsymbol{f} : \Omega \times (0,t) \to \mathbb{R}^d$. Re denotes the Reynolds number, a dimensionless coefficient, which is introduced in section 1.3. In this thesis, $d := 3$ is assumed, if not otherwise specified. Possible choices for boundary and initial conditions necessary for posing a meaningful problem will be discussed later.

The symbol p, denoting the unknown total pressure, includes the so-called Bernoulli pressure, as discussed in section 1.4.

The first equation is called momentum equation, the second one is the definition of the fluid vorticity and the third equation is the divergence-free condition. The latter enforces incompressibility of the fluid. A derivation is given in the following sections, based on chapters 8.6 and 8.7 of [Bar18].

1.1 Derivation of the divergence-free condition

In continuum mechanics, the continuity equation reads

$$\frac{\mathrm{d}}{\mathrm{d}t} \int_\Omega \phi + \int_{\partial\Omega} \boldsymbol{F}(\phi) = \int_\Omega \boldsymbol{b}. \tag{1.2}$$

Here, $\boldsymbol{F}$ is a general flux function and $\boldsymbol{b}$ is function representing all sources and sinks of the quantity ϕ. Applying the divergence theorem, defining $\boldsymbol{F} := \boldsymbol{u}\phi$ ("mass flux density") and observing that the equation has to hold for any volume Ω, one gets

$$\frac{\mathrm{d}\phi}{\mathrm{d}t} + \nabla \cdot (\boldsymbol{u}\phi) = \boldsymbol{b}.$$

For the continuity of mass, one chooses $\phi = \rho$, i.e. the mass density:

$$\frac{\mathrm{d}\rho}{\mathrm{d}t} + \rho\nabla \cdot \boldsymbol{u} + \boldsymbol{u} \cdot \nabla\rho = \boldsymbol{b}.$$

In case of incompressible flows ($\implies \frac{\mathrm{D}\rho}{\mathrm{D}t} := \frac{\mathrm{d}\rho}{\mathrm{d}t} + \boldsymbol{u} \cdot \nabla\rho = 0$) and with no mass in-/outflow, one obtains

$$\nabla \cdot \boldsymbol{u} = 0. \tag{1.3}$$

Here, $\frac{\mathrm{D}\rho}{\mathrm{D}t}$ is the total/material derivative of the quantity ρ along its movement trajectory.

1.2 Derivation of the momentum equation

Now one can apply the continuity equation to the momentum, i.e. choosing $\phi = \boldsymbol{u}\rho$ to get

$$\frac{\partial}{\partial t}(\boldsymbol{u}\rho) + \nabla \cdot (\rho\boldsymbol{u} \otimes \boldsymbol{u}) = \boldsymbol{b},$$

where one can use basic vector and tensor algebra rules to get

$$\nabla \cdot (\rho\boldsymbol{u} \otimes \boldsymbol{u}) = \nabla\rho \cdot \boldsymbol{u}\boldsymbol{u} + (\nabla \cdot \boldsymbol{u})\rho\boldsymbol{u} + (\nabla\boldsymbol{u})\rho\boldsymbol{u}.$$

By comparing the dimensions of the above quantities, one realizes, that $\boldsymbol{b}$ is in fact a force per unit volume. Reformulation gives

$$\mathbf{u}\left(\frac{\partial\rho}{\partial t} + \nabla \cdot (\rho\mathbf{u})\right) + \rho\left(\frac{\partial\mathbf{u}}{\partial t} + \mathbf{u} \cdot \nabla\mathbf{u}\right) = \boldsymbol{b}.$$

Using the mass continuity equation from before one obtains

$$\rho\left(\frac{\partial\mathbf{u}}{\partial t} + \mathbf{u} \cdot \nabla\mathbf{u}\right) \equiv \rho\frac{\mathrm{D}\boldsymbol{u}}{\mathrm{D}t} = \boldsymbol{b}. \tag{1.4}$$

The term $\mathbf{u} \cdot \nabla\mathbf{u}$ is also called convective term and is part of the material derivative of the velocity field. Now on to the right hand side: as derived in chapter 8.5 of [Bar18], in the right hand side of the momentum equation (also known as "equation of motion") of a continuum there appears the divergence of a tensor quantity called the Cauchy stress tensor. Its matrix representation in cartesian coordinates is

$$\boldsymbol{\sigma} = \begin{pmatrix} \sigma_{xx} & \tau_{xy} & \tau_{xz} \\ \tau_{yx} & \sigma_{yy} & \tau_{yz} \\ \tau_{zx} & \tau_{zy} & \sigma_{zz} \end{pmatrix}.$$

The term $\boldsymbol{b}$ is the sum of the divergence of this tensor and an external force term $\boldsymbol{f}$, i.e.

$$\boldsymbol{b} = \nabla \cdot \boldsymbol{\sigma} + \boldsymbol{f}.$$

Moreover, from the diagonal part of the stress tensor, one can extract the static pressure p_{stat}

$$\boldsymbol{\sigma} = -p_{\mathrm{stat}}\mathbb{I} + \boldsymbol{\tau}.$$

The pressure is actually the mean value of the trace of $\boldsymbol{\sigma}$: $p_{\text{stat}} = \frac{1}{d}\sum_i \sigma_{ii}$. This decomposition results in

$$\rho\left(\frac{\partial \mathbf{u}}{\partial t} + \mathbf{u}\cdot\nabla\mathbf{u}\right) = -\nabla p_{\text{stat}} + \nabla\cdot\boldsymbol{\tau} + \boldsymbol{f}. \tag{1.5}$$

To actually compute solutions for $\boldsymbol{u}$ and the new, explicitly visible unknown p_{stat}, one has to specify more properties of $\boldsymbol{\tau}$ (sometimes called "deviator stress tensor").
If $\boldsymbol{\tau}$ is proportional to the deformation rate/velocity difference per unit length of the $\boldsymbol{u}$-field, the flow is called "Newtonian". In 2D and for one component this yields

$$\tau_{ij} = \mu\frac{\mathrm{d}u_i}{\mathrm{d}x_j}.$$

The proportionality constant μ is called dynamic viscosity. In 3D one gets

$$\boldsymbol{\tau} = \mu\nabla\boldsymbol{u},$$

from which in the literature usually only the symmetric part $(\nabla\boldsymbol{u} + (\nabla\boldsymbol{u})^\intercal)$ is considered, as the antisymmetric part only describes a rotation of the flow, and not a deformation. This results in the incompressible Navier-Stokes momentum equation for Newtonian fluids:

$$\rho\left(\frac{\partial \mathbf{u}}{\partial t} + \mathbf{u}\cdot\nabla\mathbf{u}\right) = -\nabla p_{\text{stat}} + \mu\Delta\boldsymbol{u} + \boldsymbol{f}. \tag{1.6}$$

The term $\Delta\boldsymbol{u}$ is also called dissipative or diffusive term, as it results in energy dissipation. It also shows up in the heat equation.

1.3 Nondimensional formulation

A reference length, velocity, time and pressure (in capital letters) is introduced

$$\begin{aligned}
\tilde{\boldsymbol{r}} &= \frac{\boldsymbol{r}}{L}, \text{ and } \frac{1}{L}\tilde{\nabla} = \nabla,\\
\tilde{\boldsymbol{u}} &= \frac{\boldsymbol{u}}{U},\\
\tilde{t} &= \frac{t}{L/U},\\
\tilde{p}_{\text{stat}} &= \frac{p_{\text{stat}}}{\rho U^2},
\end{aligned}$$

one can substitute everything into the equation above and obtain

$$\frac{\partial\tilde{\boldsymbol{u}}}{\partial\tilde{t}} + \tilde{\boldsymbol{u}}\cdot\tilde{\nabla}\tilde{\boldsymbol{u}} = -\nabla\tilde{p}_{\text{stat}} + \frac{\mu}{\rho UL}\tilde{\nabla}^2\tilde{\boldsymbol{u}} + \boldsymbol{f}. \tag{1.7}$$

The coefficient preceding $\boldsymbol{f}$ has been incorporated into $\boldsymbol{f}$. Furthermore, in this thesis the tilde symbols will be ignored from now on. That means, the rest of this document will treat the Navier-Stokes equations in its non-dimensional form.

Now the Reynolds number is defined

$$\mathrm{Re} = \frac{\rho UL}{\mu}, \tag{1.8}$$

which is the single characteristic parameter of this equation. In the literature, Re is often introduced as the the ratio between inertial and viscous forces. A more straight-forward interpretation: it is the ratio of the dynamic pressure and the shear stress:

$$\mathrm{Re} \equiv \frac{\rho UL}{\mu} = \frac{\rho U^2}{\mu\frac{U}{L}} = 2\frac{p_{\text{dyn}}}{\tau_{\text{shear}}}.$$

This argument should illustrate the meaning of the phrase "ratio of pressure and stress" without going into too much details.
Flows with high Reynolds numbers show turbulent behaviour, low Reynolds numbers characterise creeping, laminar flows. The incompressible Navier-Stokes problem for Netwonian fluids then becomes

$$\begin{cases} \dfrac{\partial \mathbf{u}}{\partial t} + \mathbf{u} \cdot \nabla \mathbf{u} = -\nabla p_{\text{stat}} + \dfrac{1}{\text{Re}} \Delta \boldsymbol{u} + \boldsymbol{f}, \\ \nabla \cdot \boldsymbol{u} = 0. \end{cases} \tag{1.9}$$

1.4 Rotational formulation and the Bernoulli pressure

The Laplacian of a vector field is defined as

$$\Delta \boldsymbol{u} = \nabla(\nabla \cdot \boldsymbol{u}) - \nabla \times (\nabla \times \boldsymbol{u})$$

and the velocity is divergence-free. Further, it holds that

$$\boldsymbol{u} \cdot \nabla \boldsymbol{u} = \frac{1}{2} \nabla(\boldsymbol{u} \cdot \boldsymbol{u}) + (\nabla \times \boldsymbol{u}) \times \boldsymbol{u}.$$

This results in

$$\begin{cases} \dfrac{\partial \boldsymbol{u}}{\partial t} + \boldsymbol{\omega} \times \boldsymbol{u} + \dfrac{1}{2} \nabla(\boldsymbol{u} \cdot \boldsymbol{u}) + \dfrac{1}{\text{Re}} \nabla \times \boldsymbol{\omega} + \nabla p_{\text{stat}} = \boldsymbol{f}, \\ \boldsymbol{\omega} = \nabla \times \boldsymbol{u}, \\ \nabla \cdot \boldsymbol{u} = 0. \end{cases} \tag{1.10}$$

Here $\boldsymbol{\omega}$ denotes the vorticity of the fluid. The term $\frac{1}{2}(\boldsymbol{u} \cdot \boldsymbol{u})$ is (the dimensionless) Bernoulli pressure, also called dynamical pressure. Including physical constants, the Bernoulli pressure would be $\frac{1}{2}\rho(\boldsymbol{u} \cdot \boldsymbol{u})$.
Now, the total pressure of a fluid is the sum of the static and dynamic pressure

$$p_{\text{tot}} = p_{\text{stat}} + \frac{1}{2}(\boldsymbol{u} \cdot \boldsymbol{u}). \tag{1.11}$$

To simplify the momentum equation one can now treat this total pressure as an unknown of the problem. The momentum equation changes to

$$\frac{\partial \boldsymbol{u}}{\partial t} + \boldsymbol{\omega} \times \boldsymbol{u} + \frac{1}{\text{Re}} \nabla \times \boldsymbol{\omega} + \nabla p_{\text{tot}} = \boldsymbol{f}.$$

After computing a solution, one can easily recover the static pressure from $\boldsymbol{u}$ and p_{tot}, using the relation (1.11).
From here, this thesis will use the symbol p for the total pressure

$$p := p_{\text{tot}}.$$

The resulting system of equations is now:

$$\begin{cases} \dfrac{\partial \boldsymbol{u}}{\partial t} + \boldsymbol{\omega} \times \boldsymbol{u} + \dfrac{1}{\text{Re}} \nabla \times \boldsymbol{\omega} + \nabla p = \boldsymbol{f}, \\ \boldsymbol{\omega} = \nabla \times \boldsymbol{u}, \\ \nabla \cdot \boldsymbol{u} = 0, \end{cases} \tag{1.12}$$

which is exactly equivalent to the system (1.1) proposed in the introduction. To summarize: it is given an initial value for $\boldsymbol{u}^0$ and $\boldsymbol{\omega}^0$ as well as the forcing function $\boldsymbol{f}$ (also called data). The unknowns are the velocity field $\boldsymbol{u}$, vorticity field $\boldsymbol{\omega}$, and total pressure p.
To yield a meaningful problem, boundary conditions have to be prescribed.
Additionally, for $\text{Re} \to \infty$ (inviscid limit), the equations are also called Euler-equations.

1.5 Conservation properties of the Navier-Stokes equations

As $\nabla \cdot \boldsymbol{u} = 0$, mass (or rather: volume) is preserved. In the inviscid limit ($\mathrm{Re} \to \infty$), the above equations also conserve kinetic energy and helicity, assuming $\boldsymbol{f} = 0$.

Without loss of generality, $\boldsymbol{f} \neq 0$ can be assumed, if there exists a scalar-valued function ψ such that $\nabla\psi = \boldsymbol{f}$. In other words, if $\boldsymbol{f}$ is a "conservative" vector field, with scalar potential ψ. This works, as ψ can then be included in the total pressure (the forcing term is being interpreted as an extra pressure term) and later be subtracted again. See the previous subsection about the Bernoulli pressure as a comparison.

The kinetic energy is defined by

$$\mathcal{K} := \frac{1}{2}\int_\Omega \boldsymbol{u} \cdot \boldsymbol{u}, \tag{1.13}$$

and the helicity is given as

$$\mathcal{H} := \int_\Omega \boldsymbol{u} \cdot \boldsymbol{\omega}. \tag{1.14}$$

Now one can check the time rate of change for the kinetic energy

$$\frac{\mathrm{d}\mathcal{K}}{\mathrm{d}t} = \int_\Omega \frac{\partial \boldsymbol{u}}{\partial t} \cdot \boldsymbol{u}.$$

We start with the inviscid limit case ($\mathrm{Re} \to \infty$). Now the time derivative of $\boldsymbol{u}$ can be expressed using the momentum equation from (1.12):

$$\frac{\partial \boldsymbol{u}}{\partial t} = -\boldsymbol{\omega} \times \boldsymbol{u} - \nabla p.$$

Inserting that into the expression for the time derivative of $\mathcal{K}$ results in

$$\implies \frac{\mathrm{d}\mathcal{K}}{\mathrm{d}t} = -\int_\Omega (\boldsymbol{\omega} \times \boldsymbol{u}) \cdot \boldsymbol{u} - \int_\Omega \nabla p \cdot \boldsymbol{u} = -\int_\Omega (\boldsymbol{\omega} \times \boldsymbol{u}) \cdot \boldsymbol{u} + \int_\Omega p \nabla \cdot \boldsymbol{u} = 0.$$

In the last step, integration by parts and the divergence-free condition are applied, with the assumption, that the boundary integral vanishes. If this would not be the case, energy would not be conserved. One way to enforce this is by choosing suitable boundary conditions, which will be discussed in the following chapter. In the viscous case, the dissipation rate is

$$\frac{\mathrm{d}\mathcal{K}}{\mathrm{d}t} = -\frac{1}{\mathrm{Re}}\int_\Omega (\nabla \times \boldsymbol{\omega}) \cdot \boldsymbol{u} = -\frac{1}{\mathrm{Re}}\int_\Omega \boldsymbol{\omega} \cdot (\nabla \times \boldsymbol{u}) \equiv -\frac{2}{\mathrm{Re}}\mathcal{E}.$$

The integral over $\boldsymbol{\omega} \cdot \boldsymbol{\omega}$ is positive which is why $\mathcal{K}$ is strictly decreasing. Here, $\mathcal{E}$ is the enstrophy, which will be analized at the end of this section.
Next, one can check the helicity conservation:

$$\frac{\mathrm{d}\mathcal{H}}{\mathrm{d}t} = \int_\Omega \frac{\partial \boldsymbol{u}}{\partial t} \cdot \boldsymbol{\omega} + \int_\Omega \boldsymbol{u} \cdot \frac{\partial \boldsymbol{\omega}}{\partial t}.$$

The curl of the momentum equation is

$$\nabla \times \frac{\partial \boldsymbol{u}}{\partial t} + \nabla \times (\boldsymbol{\omega} \times \boldsymbol{u}) + \frac{1}{\mathrm{Re}}\nabla \times (\nabla \times \boldsymbol{\omega}) + \nabla \times (\nabla p) = \nabla \times \boldsymbol{f}.$$

Interchanging the differential operators to get $\boldsymbol{\omega} = \nabla \times \boldsymbol{u}$ and again assuming vanishing dissipative term and right hand side $\boldsymbol{f}$ yields

$$\frac{\partial \boldsymbol{\omega}}{\partial t} + \nabla \times (\boldsymbol{\omega} \times \boldsymbol{u}) = 0.$$

The last term is 0 as the curl of the gradient vanishes. This can now be plugged into the time rate of change of $\mathcal{H}$ shown before:

$$\begin{aligned}\frac{\mathrm{d}\mathcal{H}}{\mathrm{d}t} &= -\int_\Omega (\boldsymbol{\omega}\times\boldsymbol{u})\cdot\boldsymbol{\omega} - \int_\Omega \boldsymbol{u}\cdot\nabla\times(\boldsymbol{\omega}\times\boldsymbol{u}) - \int_\Omega \nabla p\cdot\boldsymbol{\omega} \\ &= -\int_\Omega (\boldsymbol{\omega}\times\boldsymbol{u})\cdot\boldsymbol{\omega} + \int_\Omega \boldsymbol{\omega}\cdot(\boldsymbol{\omega}\times\boldsymbol{u}) + \int_\Omega p\cdot\nabla\cdot\nabla\times\boldsymbol{u} = 0.\end{aligned}$$

In the first line, integration by parts was applied to the second and third term. Boundary integrals vanish as before and vanishing divergence of the curl was utilized for the third term in the second line. The dissipation rate in the viscous case is

$$\frac{\mathrm{d}\mathcal{H}}{\mathrm{d}t} = -\frac{2}{\mathrm{Re}}\int_\Omega \boldsymbol{\omega}\cdot(\nabla\times\boldsymbol{\omega}).$$

Now we can not argue anymore, that $\mathcal{H}$ is strictly decreasing over time, as we did with $\mathcal{K}$.
As a remark, also the enstrophy of the velocity field given by

$$\mathcal{E} := \frac{1}{2}\int_\Omega \boldsymbol{\omega}\cdot\boldsymbol{\omega}$$

is conserved by (1.12). Indeed, with $\mathrm{Re}\to 0$ and taking the curl of the momentum equation one gets

$$\frac{\mathrm{d}\mathcal{E}}{\mathrm{d}t} = \int_\Omega \frac{\mathrm{d}\boldsymbol{\omega}}{\mathrm{d}t}\boldsymbol{\omega} = -\int_\Omega \nabla\times(\boldsymbol{\omega}\times\boldsymbol{u})\cdot\boldsymbol{\omega} = -\frac{1}{2}\int_\Omega (\boldsymbol{u}\cdot\nabla\boldsymbol{\omega})\cdot\boldsymbol{\omega} - \frac{1}{2}\int_\Omega \nabla\cdot(\boldsymbol{u}\boldsymbol{\omega})\cdot\boldsymbol{\omega}.$$

Here the identity

$$\nabla\times(\boldsymbol{a}\times\boldsymbol{b}) = \frac{1}{2}(\boldsymbol{a}\cdot\nabla\boldsymbol{b} + \nabla\cdot(\boldsymbol{a}\boldsymbol{b}))$$

was applied. Integration by parts on the last term, or backwards integration by parts on the second to last term and utilizing vanishing boundary integrals shows that the last two integrals are in fact equal, yielding

$$\frac{\mathrm{d}\mathcal{E}}{\mathrm{d}t} = 0.$$

1.6 Literature overview and outline of the thesis

When reading the previous section, the reader might get the idea that conservation of physical quantities is an accidental property of the temporal evolution of the fluid system. This is only a very shallow interpretation. The research on structure-preserving methods has found a much deeper explanation: conservation properties of differential equations are an expression of their geometric structure.

Differential equations that can be formulated as a Hamiltonian system of differential equations, can be be analysed based on Noether's theorem. It states a relationship between geometric symmetries of a system and its conservation properties, see chapter 5.6 in [Bar18]. Temporal translation symmetry ("a different choice of time interval results in an equivalent problem") of a Hamiltonian system results in energy conservation. Spatial translation symmetry ("translating the spatial domain results in an equivalent problem") results in momentum conservation.
In the inviscid case, the rotational form of the incompressible Navier-Stokes equations (1.12) can be written as a Hamiltonian system, see [Olv82], implying conservation of energy. Conservation of helicity is less straight forward to show based on the Hamiltonian formulation of the system, see [YR22].

In fact, the construction of helicity conserving schemes is an active research area, e.g. see [Cap18] and [Val19]. There are two main reasons that motivate the current efforts of the scientific community to work on schemes that preserve both energy and helicity.

1. Simulating and investigating the joint cascade of energy and helicity.
   Papers like [CCE02] describe how in three-dimensional turbulence, energy and helicity are jointly cascaded into "small scales". The mechanism, which allows for the joint cascade, is shown to be facilitated by advection and vortex stretching. In [A A18], a comprehensive overview of these transfer mechanisms and cascades in turbulent flows is given. These papers also show why the preservation of helicity plays a crucial role in the generation and evolution of turbulence.

2. Higher numerical accuracy.
   The connection between energy and helicity cascades suggests that energy- and helicity-conserving schemes can contribute to even higher accuracy in simulations, see [Cap15]. This article describes the time-reversibility properties of various solvers for the incompressible Navier-Stokes problem. Next to time-stepping accuracy, the conservation of energy is also important to avoid numerical instability. The findings suggest that achieving accurate time-reversibility could serve as a benchmark for Navier-Stokes solvers. Similarly, in [MW08], the authors describe how energy-conserving discretizations are important for accurate simulations of turbulent flows. To avoid high computational costs of the well-known skew-symmetric splitting approach, a time-advancement strategy that retains conservation properties is developed using a certain type of Runge-Kutta schemes with different forms of the convective term at each stage.

The goal of this thesis is to derive and analyse a numerical scheme for the incompressible Navier-Stokes problem that conserves mass, kinetic energy, and helicity. It was first proposed on a periodic computational domain in [YR22]. The scheme is a Galerkin Finite Element method that is based on a variational formulation discussed in chapter 2. A temporal discretization is introduced in section 3.1 followed by a derivation of finite dimensional function spaces necessary for the spatial discretization in section 3.4.1. Numerical experiments on the periodic domain are being conducted in chapter 4.
As an extension from the method proposed in [YR22], we propose a novel Dirichlet scheme, that is applied to a much more realistic problem with essential boundary conditions. It allows the definition of essential boundary conditions on the velocity and vorticity field, and avoids the restrictive assumption of periodic domains. The associated continuous variational formulation is introduced in section 2.4. The discretization of that formulation is discussed in section 3.6 and results from numerical experiments are presented in sections 4.4 and 4.5.

Chapter 2

Continuous variational formulation

The goal of this chapter is to derive the continuous variational formulation of (1.12), based on [YR22]. This is necessary for the discretization procedure of the following chapter, while still preserving the conservation of mass, kinetic energy and helicity. First we introduce some variational theory, then we derive the formulation on a periodic domain. A non-periodic Dirichlet scenario will be discussed in section 2.4.

This chapter is based on the lecture notes [Fau22], [Hip22], as well as [Sch18]. A more in depth look into Finite Element theory can be found in [E A04], [Mon03], and [V G12].

2.1 Introduction

To generalize mathematical objects (like derivatives) to many variables, multi index notation can be used.

Definition 1 (Multi index notation for differential operators)**.** *A vector* $(\alpha_1, ..., \alpha_d) \in \mathbb{N}_0^d$ *is called a multi index and* $|\alpha| := \sum \alpha_i$*. The classic differential operator* D^α *for functions in* $C^\infty(\Omega)$ *is written as*

$$D^\alpha = \left(\frac{\partial}{\partial x_1}\right)^{\alpha_1} ... \left(\frac{\partial}{\partial x_d}\right)^{\alpha_d}.$$

Similar, as in the introduction of this thesis, $\Omega \subset \mathbb{R}^d$*, where* $d = 3$*, if not noted otherwise.*

Definition 2 (Smooth functions with compact support)**.** *The space* $C_0^\infty(\Omega)$ *is defined as*

$$C_0^\infty(\Omega) := \{\boldsymbol{u} \in C^\infty(\Omega) : \text{supp}(u) \subset \Omega\}. \tag{2.1}$$

The support of a function is the set defined as $\text{supp}(\boldsymbol{u}) := \{x \in \Omega : \boldsymbol{u}(x) \neq 0\}$.

If Ω is a bounded domain it holds: $\boldsymbol{u}|_{\partial\Omega} = 0 \iff \text{supp}(u) \subset \Omega$.

Definition 3 (Weak derivative)**.** *Let* u *be a locally integrable function, i.e.* $\boldsymbol{u} \in L^1(K)$ *for all compact* $K \subset \Omega$*. The function* $\boldsymbol{g}$ *is called weak derivative of* $\boldsymbol{u}$ *order* α*, if* $\boldsymbol{g}$ *is locally integrable, and satisfies*

$$\int_\Omega \boldsymbol{g} \cdot \boldsymbol{v} = (-1)^{|\alpha|} \int_\Omega \boldsymbol{u} \cdot D^\alpha \boldsymbol{v} \quad \forall \boldsymbol{v} \in C_0^\infty(\Omega). \tag{2.2}$$

With the notion of weak differentiability, the definition of so-called Sobolev function spaces are possible.

Definition 4 (The space H^1)**.** *The space* $H^1(\Omega)$ *is the space of all square-integrable functions* u*, whose weak first derivative* $D\boldsymbol{u}$ *is also square integrable, i.e.*

$$H^1(\Omega) := \left\{u \in L^2(\Omega) : Du \in L^2(\Omega)\right\}. \tag{2.3}$$

It is a normed space with the canonical norm

$$\|u\|^2_{H^1(\Omega)} := \|u\|^2_{L^2(\Omega)} + \|Du\|^2_{L^2(\Omega)}\,. \tag{2.4}$$

Moreover, $H^1(\Omega)$, is a Hilbert space with the inner product:

$$(u,v)_{H^1(\Omega)} := (u,v)_{L^2(\Omega)} + (Du,Dv)_{L^2(\Omega)} = \int_\Omega uv + DuDv \tag{2.5}$$

Because functions in $H^1(\Omega)$ are only known to have finite $H^1(\Omega)$-norms, pointwise definition of boundary values is not possible. The trace operator enables boundary value definitions on this space.

Theorem 5 (Trace operator)**.** *There exists a continuous trace operator*

$$\mathrm{tr} : H^1(\Omega) \to L^2(\partial\Omega)$$

such that there holds

$$u \in C^1(\Omega) \implies \mathrm{tr}(u) = u|_{\partial\Omega}.$$

Proof. See Thm. 44 and 45 in [Sch18] for the proof. □

The next theorem is highly important for the constructions of finite elements that consist of subdomains of Ω. The unknown solution will be interpolated on each element, and certain global continuity requirements have to be fulfilled also on the subdomain interfaces.

Theorem 6 (Subdomain interface condition for $H^1(\Omega)$)**.** *Let $u \in L^2(\Omega)$ and $\Omega = \Omega_1 \cup \Omega_2 \cup F_{12}$ s.t.*

- *$u_i := u|_{\Omega_i} \in H^1(\Omega_i)$, and $g_i := \nabla u_i$ is its weak gradient,*
- *traces on common interfaces of subdomains coincide: $\mathrm{tr}^{F_{12}}\, u_1 = \mathrm{tr}^{F_{12}}\, u_2$.*

Then, u belongs to $H^1(\Omega)$, i.e. globally for the whole domain Ω.

Proof. It suffices to show, that the weak gradient of u is in L^2. The idea is as follows: use the definition of the weak derivative/gradient, see definition (3). Apply Green's first integral formula on the subdomains Ω_i and use the fact that the outer normal vectors on common faces are oriented opposite to each other. The calculation steps can be found in the proof of Thm. 46 in [Sch18]. □

2.1.1 The space $H(\mathrm{curl}, \Omega)$

To derive a variational formulation of (1.12) including its curl and div operators, the notion of weak curl and divergence have to be introduced. The space of functions with a square-integrable weak curl is introduced first.

Definition 7 (Weak curl)**.** *Let $\boldsymbol{u} \in L^2(\Omega)$. The function $\boldsymbol{g} \in L^2(\Omega)$ is called the weak curl of $\boldsymbol{u}$, if*

$$\int_\Omega \boldsymbol{g}\cdot\boldsymbol{v} = \int_\Omega \boldsymbol{u}\cdot\mathrm{curl}\,\boldsymbol{v} \quad \forall \boldsymbol{v} \in [C_0^\infty(\Omega)]^d\,. \tag{2.6}$$

In the following "$\mathrm{curl}\,\boldsymbol{u}$" denotes either the strong or the weak curl of $\boldsymbol{u}$, depending on the context.

Definition 8 (The space $H(\mathrm{curl}, \Omega)$)**.**

$$H(\mathrm{curl},\Omega) := \left\{\boldsymbol{u} \in \left[L^2(\Omega)\right]^d : \mathrm{curl}\,\boldsymbol{u} \in \left[L^2(\Omega)\right]^d\right\}.$$

It turns out, like for the Sobolev space $H^1(\Omega)$, there is a trace operator, that allows to formulate boundary values in this function space.
The following two theorems can be found in section 3.2.1 of [Mon03], or as Thm. 2.11 in [V G12].

Theorem 9 (Trace theorem on $H(\mathrm{curl},\Omega)$)**.** *There exists a tangential trace operator*

$$\mathrm{tr_t} : H(\mathrm{curl},\Omega) \to L^2(\partial\Omega)$$

such that there holds

$$\boldsymbol{u} \in H(\mathrm{curl},\Omega) \cap [C^\infty(\Omega)]^d \implies \mathrm{tr_t}\,\boldsymbol{u} = \boldsymbol{n} \times \boldsymbol{u}|_{\partial\Omega}.$$

Theorem 10 (Tangential trace continuity on $H(\mathrm{curl},\Omega)$)**.** *Let $\Omega = \Omega_1 \cup \Omega_2$. Assume that $\boldsymbol{u}|_{\Omega_i} \in H(\mathrm{curl},\Omega_i)$, and the tangential traces are continuous across the interfaces $\gamma_{12} = \Omega_1 \cap \Omega_2$. Then, $\boldsymbol{u} \in H(\mathrm{curl},\Omega)$.*

2.1.2 The space $H(\mathrm{div},\Omega)$

Similar as in the previous section, we now introduce the notion of the weak divergence, and a proper function space for functions with square-integrable (weak) divergence.

Definition 11 (Weak divergence)**.** *Let $\boldsymbol{u} \in L^2(\Omega)$. The function $g \in L^2(\Omega)$ is called weak divergence of $\boldsymbol{u}$, if*

$$\int_\Omega \boldsymbol{g} \cdot \boldsymbol{v} = \int_\Omega \boldsymbol{u}\,\mathrm{div}\,\boldsymbol{v} \quad \forall \boldsymbol{v} \in [C_0^\infty(\Omega)]^d\,. \tag{2.7}$$

In the following "$\mathrm{div}\,\boldsymbol{u}$" denotes either the strong or the weak divergence of $\boldsymbol{u}$, depending on the context.

Definition 12 (The space $H(\mathrm{div},\Omega)$)**.**

$$H(\mathrm{div},\Omega) := \left\{\boldsymbol{u} \in \left[L^2(\Omega)\right]^d : \mathrm{div}\,\boldsymbol{u} \in \left[L^2(\Omega)\right]^d\right\}.$$

In order to formulate boundary conditions on this space, the following trace operator is introduced.

Theorem 13 (Trace theorem on $H(\mathrm{div},\Omega)$)**.** *There exists a normal-trace operator*

$$\mathrm{tr_n} : H(\mathrm{div},\Omega) \to L^2(\partial\Omega)$$

such that there holds

$$\boldsymbol{u} \in H(\mathrm{div},\Omega) \cap C^\infty(\Omega) \implies \mathrm{tr_n}\,\boldsymbol{u} = \boldsymbol{u} \cdot \boldsymbol{n}.$$

Proof. The proof can be found after Thm. 105 in [Sch18]. □

Theorem 14 (Normal trace continuity on $H(\mathrm{div},\Omega)$)**.** *Let $\Omega = \Omega_1 \cup \Omega_2$. Assume that $\boldsymbol{u}|_{\Omega_i} \in H(\mathrm{div},\Omega_i)$, and the normal traces are continuous across the interfaces $\gamma_{12} = \Omega_1 \cap \Omega_2$. Then, $\boldsymbol{u} \in H(\mathrm{div},\Omega)$.*

Proof. The idea of the proof is similar as in the case of the $H^1(\Omega)$-trace operator. It has to be shown, that the weak divergence is square-integrable for $\boldsymbol{u}$ to be element of $H(\mathrm{div},\Omega)$ globally. Again, this can be done using Green's integral identities. □

2.1.3 Integration by parts

The variational formulation of the original problem is derived by multiplying the equations by appropriate test functions and integrating by parts.

For sufficiently smooth (continuously or weakly differentiable) functions $u, \boldsymbol{v}$, there holds integration by parts:

$$\int_\Omega u \nabla \cdot \boldsymbol{v} = \int_{\partial\Omega} u \boldsymbol{v} \cdot \boldsymbol{n} - \int_\Omega \nabla u \cdot \boldsymbol{v}. \tag{2.8}$$

A similar property can be found for the curl operator:

Lemma 15 (Integration by parts for the curl operator)**.** *For sufficiently smooth functions* $\boldsymbol{u}, \boldsymbol{v}$ *and the* curl *operator, there holds integration by parts*

$$\int_\Omega (\nabla \times \boldsymbol{u}) \cdot \boldsymbol{v} = \int_\Omega \boldsymbol{u} \cdot (\nabla \times \boldsymbol{v}) - \int_{\partial\Omega} (\boldsymbol{v} \times \boldsymbol{u}) \cdot \boldsymbol{n}. \tag{2.9}$$

Proof. We start with the following vector identity in $\mathbb{R}^3$

$$\nabla \cdot (\boldsymbol{v} \times \boldsymbol{u}) = \boldsymbol{u} \cdot (\nabla \times \boldsymbol{v}) - \boldsymbol{v} \cdot (\nabla \times \boldsymbol{u}).$$

Integrating the above expression over the domain yields

$$\int_\Omega (\nabla \times \boldsymbol{u}) \cdot \boldsymbol{v} = \int_\Omega \boldsymbol{u} \cdot (\nabla \times \boldsymbol{v}) - \int_\Omega \nabla \cdot (\boldsymbol{v} \times \boldsymbol{u}).$$

Now one can apply Gauss' divergence theorem to the last term and get the above statement. □

2.2 Derivation of the continuous variational formulation

Finally, we can use the framework described in the previous sections to derive the variational formulation in the continuous setting. Again, at first we assume that Ω is a bounded, periodic domain in $\mathbb{R}^3$, meaning that instead of fixing values or gradient values of each unknown function (also called trial functions) at the boundary, it is assumed that each trial function has the same values at one end of the domain as at the "opposite" end.

The name variational formulation comes from the equivalence of these problems to the minimization of functionals studied by calculus of variations. Generally speaking, the variational formulation of a problem formulated as a set of partial differential equations is found by multiplying the orignal equations (strong form) with test functions, and integrating them over the computational domain. Integration by parts is being applied to shift differential operators to the test functions in order to reduce regularity requirements of the unknown function and to avoid the continuity requirement on f. The linearform $\int_\Omega f \cdot \tilde{\boldsymbol{u}}$ is now well defined for $f \in L^2$, as one can easily see using Cauchy-Schwarz:

$$\int_\Omega f \cdot \tilde{\boldsymbol{u}} \leq \sqrt{\int_\Omega f^2} \sqrt{\int_\Omega \tilde{\boldsymbol{u}}^2}. \tag{2.10}$$

Integrating the momentum equation from (1.12), multiplying with a test function $\tilde{\boldsymbol{u}}$ and performing integration by parts on the Reynolds term gives

$$\int_\Omega \frac{\partial \boldsymbol{u}}{\partial t} \cdot \tilde{\boldsymbol{u}} + \int_\Omega (\boldsymbol{\omega} \times \boldsymbol{u}) \cdot \tilde{\boldsymbol{u}} + \frac{1}{\mathrm{Re}} \int_\Omega (\nabla \times \boldsymbol{\omega}) \cdot \tilde{\boldsymbol{u}} + \int_\Omega \nabla p \cdot \tilde{\boldsymbol{u}} = \tag{2.11}$$

$$\int_\Omega \frac{\partial \boldsymbol{u}}{\partial t} \cdot \tilde{\boldsymbol{u}} + \int_\Omega (\boldsymbol{\omega} \times \boldsymbol{u}) \cdot \tilde{\boldsymbol{u}} + \frac{1}{\mathrm{Re}} \int_\Omega \boldsymbol{\omega} \cdot (\nabla \times \tilde{\boldsymbol{u}}) - \frac{1}{\mathrm{Re}} \int_{\partial\Omega} (\tilde{\boldsymbol{u}} \times \boldsymbol{\omega}) \cdot \boldsymbol{n} + \int_\Omega \nabla p \cdot \tilde{\boldsymbol{u}} = \int_\Omega \boldsymbol{f} \cdot \tilde{\boldsymbol{u}} \qquad \forall \tilde{\boldsymbol{u}}. \tag{2.12}$$

The new boundary integral vanishes, due to the assumption of a periodic domain: the unit normal vector $\boldsymbol{n}$ and the unknown $\boldsymbol{\omega}$ cancel out. The result is:

$$\int_\Omega \frac{\partial \boldsymbol{u}}{\partial t} \cdot \tilde{\boldsymbol{u}} + \int_\Omega (\boldsymbol{\omega} \times \boldsymbol{u}) \cdot \tilde{\boldsymbol{u}} + \frac{1}{\mathrm{Re}} \int_\Omega \boldsymbol{\omega} \cdot (\nabla \times \tilde{\boldsymbol{u}}) + \int_\Omega \nabla p \cdot \tilde{\boldsymbol{u}} = \int_\Omega \boldsymbol{f} \cdot \tilde{\boldsymbol{u}} \qquad \forall \tilde{\boldsymbol{u}} \tag{2.13}$$

The same procedure will be done with the vorticity constraint from (1.12):

$$\int_\Omega (\nabla \times \boldsymbol{u}) \cdot \tilde{\boldsymbol{\omega}} - \int_\Omega \boldsymbol{\omega} \cdot \tilde{\boldsymbol{\omega}} = 0 \qquad \forall \tilde{\boldsymbol{\omega}} \tag{2.14}$$

and with the divergence-free condition (again: the boundary integral vanishes):

$$\int_\Omega \boldsymbol{u} \cdot \nabla \tilde{p} = 0 \qquad \forall \tilde{p}. \tag{2.15}$$

The scheme that will be introduced is a dual-field scheme, which solves for the velocity, vorticity and pressure twice. This allows the weak form to conserve the quantities discussed in section 1.5. The unknowns are:

$\boldsymbol{u}$	velocity in $H(\mathrm{curl}, \Omega)$
$\boldsymbol{\omega}$	vorticity in $H(\mathrm{curl}, \Omega)$
$\boldsymbol{v}$	velocity in $H(\mathrm{div}, \Omega)$
$\boldsymbol{\zeta}$	vorticity in $H(\mathrm{div}, \Omega)$
p	pressure in $H^1(\Omega)$
q	pressure in $L^2(\Omega)$

The test functions are introduced in the following.

$\tilde{\boldsymbol{u}}$, $\tilde{\boldsymbol{\omega}}$	test functions in $H(\mathrm{curl}, \Omega)$
$\tilde{\boldsymbol{v}}$, $\tilde{\boldsymbol{\zeta}}$	test functions in $H(\mathrm{div}, \Omega)$
$\tilde{p}$	test function in $H^1(\Omega)$
$\tilde{q}$	test function in $L^2(\Omega)$

In addition to deriving equations (2.13), (2.14), and (2.15) a second time, with a different choice of function spaces and different terms being integrated by parts, the vorticities in the second term of the momentum equations will be exchanged to result in a coupled system.

2.2.1 Continuous variational formulation

The following formulation was first proposed by [YR22]. To achieve a more compact notation, the integrals are being denoted as inner products/bilinear forms (scalar functions with two arguments, that is linear in both):

$$\int_\Omega \boldsymbol{u} \cdot \boldsymbol{v} =: \langle \boldsymbol{u}, \boldsymbol{v} \rangle ,$$

and for boundary integrals round parentheses with subscript $\partial\Omega$:

$$\int_{\partial\Omega} \boldsymbol{u} \cdot \boldsymbol{v} =: (\boldsymbol{u}, \boldsymbol{v})_{\partial\Omega} .$$

Consider now the following dual-field mixed weak formulation for the rotational form of the incompressible Navier-Stokes equations on a periodic domain:

given $\boldsymbol{f} \in \left[L^2(\Omega)\right]^3$,
seek $(\boldsymbol{u}, \boldsymbol{\zeta}, p) \in H(\mathrm{curl}, \Omega) \times H(\mathrm{div}, \Omega) \times H^1(\Omega)$

and $(\boldsymbol{v}, \boldsymbol{\omega}, q) \in H(\mathrm{div}, \Omega) \times H(\mathrm{curl}, \Omega) \times L^2(\Omega)$
such that they satisfy the primal system

$$\left\langle \frac{\partial \boldsymbol{u}}{\partial t}, \tilde{\boldsymbol{u}} \right\rangle + \langle \boldsymbol{\omega} \times \boldsymbol{u}, \tilde{\boldsymbol{u}} \rangle + \frac{1}{\mathrm{Re}} \langle \boldsymbol{\zeta}, \nabla \times \tilde{\boldsymbol{u}} \rangle + \langle \nabla p, \tilde{\boldsymbol{u}} \rangle = \langle \boldsymbol{f}, \tilde{\boldsymbol{u}} \rangle \qquad \forall \tilde{\boldsymbol{u}} \in H(\mathrm{curl}, \Omega) \tag{2.16}$$

$$\left\langle \nabla \times \boldsymbol{u}, \tilde{\boldsymbol{\zeta}} \right\rangle - \left\langle \boldsymbol{\zeta}, \tilde{\boldsymbol{\zeta}} \right\rangle = 0 \qquad \forall \tilde{\boldsymbol{\zeta}} \in H(\mathrm{div}, \Omega) \tag{2.17}$$

$$\langle \boldsymbol{u}, \nabla \tilde{p} \rangle = 0 \qquad \forall \tilde{p} \in H^1(\Omega) \tag{2.18}$$

as well as the dual system

$$\left\langle \frac{\partial \boldsymbol{v}}{\partial t}, \tilde{\boldsymbol{v}} \right\rangle + \langle \boldsymbol{\zeta} \times \boldsymbol{v}, \tilde{\boldsymbol{v}} \rangle + \frac{1}{\mathrm{Re}} \langle \nabla \times \boldsymbol{\omega}, \tilde{\boldsymbol{v}} \rangle - \langle q, \nabla \cdot \tilde{\boldsymbol{v}} \rangle = \langle \boldsymbol{f}, \tilde{\boldsymbol{v}} \rangle \qquad \forall \tilde{\boldsymbol{v}} \in H(\mathrm{div}, \Omega) \tag{2.19}$$

$$\langle \boldsymbol{v}, \nabla \times \tilde{\boldsymbol{\omega}} \rangle - \langle \boldsymbol{\omega}, \tilde{\boldsymbol{\omega}} \rangle = 0 \qquad \forall \tilde{\boldsymbol{\omega}} \in H(\mathrm{curl}, \Omega) \tag{2.20}$$

$$\langle \nabla \cdot \boldsymbol{v}, \tilde{q} \rangle = 0 \qquad \forall \tilde{q} \in L^2(\Omega) \tag{2.21}$$

Interpretation:

- The scheme is dual-field, as there are two momentum equations with two constraints each. Velocity, vorticity, and pressure are solved twice. Following the derivation from the previous section backwards shows that both velocities, vorticities, and pressures solve the Navier-Stokes equations.
- It is now visible how $\boldsymbol{\omega} \in H(\mathrm{curl}, \Omega)$ and $\boldsymbol{\zeta} \in H(\mathrm{div}, \Omega)$ are coupling the two momentum equations. E.g. $\boldsymbol{\omega}$ is the vorticity corresponding to the dual velocity $\boldsymbol{v}$ (enforced by constraint (2.20)), but it still appears in the primal momentum equation (2.16).
- Equation (2.17) would allow to replace each $\boldsymbol{\zeta}$ with $\nabla \times \boldsymbol{u}$. That way, the number of unknowns would be reduced to five. We will still keep working with the larger, "symmetric"-looking formulation, which is mathematically equivalent.
- It is not clear, whether the second term of the momentum equations is square-integrable. It is not possible to just apply Cauchy-Schwarz like in (2.10). It turns out, the finite dimensional representation of these terms is integrable, see section 3.4.1.
- The pressure is only defined up to a constant. This could be solved by adding constraints to the system, e.g. using a Lagrange multiplier formulation. A possible choice for such a constraint would be to require that the integral over the pressure vanishes: $\int_\Omega p = 0$. Another option was chosen for the numeric tests in chapter 4. There, a MINRES solver computing the minimum residual solution was utilized.

2.3 Conservation on periodic domains

The function spaces that were introduced in section 2 and then have been used in equations (2.16) to (2.21) form an exact sequence: the so called de Rham sequence. These spaces and differential operators have a very peculiar structure.

2.3.1 de Rham complex

It holds that

$$H^1(\Omega) \xrightarrow{\nabla} H(\mathrm{curl}, \Omega) \xrightarrow{\mathrm{curl}} H(\mathrm{div}, \Omega) \xrightarrow{\mathrm{div}} L^2(\Omega). \tag{2.22}$$

The notation $A \xrightarrow{\odot} B$ means that the operator $\odot$ maps elements from space A to space B. For simply-connected domains, the de Rham sequence shown above has the following properties:

- Gradients of $H^1(\Omega)$-functions are element of $H(\mathrm{curl}, \Omega)$, as the curl of any gradient is 0 and therefore square-integrable and therefore also element of $H(\mathrm{curl}, \Omega)$.
- Curls of $H(\mathrm{curl}, \Omega)$ functions are element of $H(\mathrm{div}, \Omega)$ as the divergence of any curl is 0 and therefore also square-integrable and hence an element of $H(\mathrm{div}, \Omega)$.
- By definition the divergence of an $H(\mathrm{div}, \Omega)$ function is square integrable, which is the last property of the de Rham squence.

A simply connected domain has the property that any path between two endpoints is completely inside of the domain and can be transformed into any other path on the domain by a continuous mapping while preserving the endpoints.
The observations above can be summarized quite elegantly into a very short phrase: The kernel of the right differential operator is exactly the range of the left one. Because of this reason, the de Rham sequence is a so called "exact sequence".

This property means, for example:

$$\mathrm{range}(\nabla) = \ker(\mathrm{curl})$$

with

$$\begin{aligned} \mathrm{range}(\nabla) &:= \{\boldsymbol{u} \in H(\mathrm{curl}, \Omega) : \boldsymbol{u} = \nabla p, p \in H^1(\Omega)\}, \\ \ker(\mathrm{curl}) &:= \{\boldsymbol{u} \in H(\mathrm{curl}, \Omega) : \mathrm{curl}\, \boldsymbol{u} = 0\}. \end{aligned}$$

Moreover, this fundamental property of the function spaces used for the weak problem proposed before, allows to prove the conservation properties from section 1.5 also for this weak formulation.

We now assume the inviscid limit case ($\mathrm{Re} \to \infty$) and $\boldsymbol{f} = 0$ to observe conservation.

2.3.2 Mass

Mass conservation holds in the weak sense for $\boldsymbol{u}$ and strongly for $\boldsymbol{v}$ due to the two constraints of the weak formulation of the scheme, see (2.18) and (2.21).

2.3.3 Energy

The kinetic energies are

$$\mathcal{K}_1 := \frac{1}{2} \langle \boldsymbol{u}, \boldsymbol{u} \rangle \tag{2.23}$$

$$\mathcal{K}_2 := \frac{1}{2} \langle \boldsymbol{v}, \boldsymbol{v} \rangle \tag{2.24}$$

and their time-rate of change:

$$\frac{\mathrm{d}\mathcal{K}_1}{\mathrm{d}t} = \left\langle \frac{\partial \boldsymbol{u}}{\partial t}, \boldsymbol{u} \right\rangle, \qquad \frac{\mathrm{d}\mathcal{K}_2}{\mathrm{d}t} = \left\langle \frac{\partial \boldsymbol{v}}{\partial t}, \boldsymbol{v} \right\rangle. \tag{2.25}$$

Consider the momentum equation (2.16) and replace $\tilde{\boldsymbol{u}} := \boldsymbol{u}$

$$\left\langle \frac{\partial \boldsymbol{u}}{\partial t}, \boldsymbol{u} \right\rangle + \langle \boldsymbol{\omega} \times \boldsymbol{u}, \boldsymbol{u} \rangle + \langle \nabla p, \boldsymbol{u} \rangle = 0. \tag{2.26}$$

The second term vanishes due to orthogonality of the cross product and the third term because of (2.18). Therefore

$$\frac{\mathrm{d}\mathcal{K}_1}{\mathrm{d}t} = 0. \tag{2.27}$$

and similarly for $\mathcal{K}_2$. It is also possible to predict the time-rate of change (dissipation rate) for a finite Reynolds number, which is equal to the viscous/dissipative term. Defining the enstrophies

$$\mathcal{E}_\zeta := \frac{1}{2}\left\langle \boldsymbol{\zeta}, \boldsymbol{\zeta} \right\rangle, \tag{2.28}$$

$$\mathcal{E}_\omega := \frac{1}{2}\left\langle \boldsymbol{\omega}, \boldsymbol{\omega} \right\rangle, \tag{2.29}$$

one obtains

$$\frac{\mathrm{d}\mathcal{K}_1}{\mathrm{d}t} = \left\langle \frac{\partial \boldsymbol{u}}{\partial t}, \boldsymbol{u} \right\rangle = -\frac{1}{\mathrm{Re}}\left\langle \boldsymbol{\zeta}, \nabla \times \boldsymbol{u} \right\rangle = -\frac{1}{\mathrm{Re}}\left\langle \boldsymbol{\zeta}, \boldsymbol{\zeta} \right\rangle = -\frac{2}{\mathrm{Re}}\mathcal{E}_\zeta \leq 0,$$

and similar, using (2.20)

$$\frac{\mathrm{d}\mathcal{K}_2}{\mathrm{d}t} = \left\langle \frac{\partial \boldsymbol{v}}{\partial t}, \boldsymbol{v} \right\rangle = -\frac{1}{\mathrm{Re}}\left\langle \nabla \times \boldsymbol{\omega}, \boldsymbol{v} \right\rangle = -\frac{1}{\mathrm{Re}}\left\langle \boldsymbol{\omega}, \boldsymbol{\omega} \right\rangle = -\frac{2}{\mathrm{Re}}\mathcal{E}_\omega \leq 0.$$

This is aligned with the results from section 1.5.

2.3.4 Helicity

The fluid helicities are given as the following integrals:

$$\mathcal{H}_1 := \left\langle \boldsymbol{u}, \boldsymbol{\omega} \right\rangle, \tag{2.30}$$

$$\mathcal{H}_2 := \left\langle \boldsymbol{v}, \boldsymbol{\zeta} \right\rangle, \tag{2.31}$$

where $\boldsymbol{u}, \boldsymbol{\omega} \in H(\mathrm{curl}, \Omega)$ and $\boldsymbol{v}, \boldsymbol{\zeta} \in H(\mathrm{div}, \Omega)$. The goal is to show

$$\frac{\mathrm{d}\mathcal{H}_1}{\mathrm{d}t} = \left\langle \frac{\partial \boldsymbol{u}}{\partial t}, \boldsymbol{\omega} \right\rangle + \left\langle \boldsymbol{u}, \frac{\partial \boldsymbol{\omega}}{\partial t} \right\rangle = 0 \tag{2.32}$$

and similar for $\mathcal{H}_2$. Now we use equation (2.16) and set $\tilde{\boldsymbol{u}} := \boldsymbol{\omega} \in H(\mathrm{curl}, \Omega)$, which gives

$$\left\langle \frac{\partial \boldsymbol{u}}{\partial t}, \boldsymbol{\omega} \right\rangle + \left\langle \boldsymbol{\omega} \times \boldsymbol{u}, \boldsymbol{\omega} \right\rangle + \left\langle \boldsymbol{\omega}, \nabla p \right\rangle = 0. \tag{2.33}$$

The second term vanishes because the two arguments of the bilinear form are orthogonal due to the cross product. Equation (2.20) provides:

$$-\left\langle \boldsymbol{v}, \nabla \times \tilde{\boldsymbol{\omega}} \right\rangle + \left\langle \boldsymbol{\omega}, \tilde{\boldsymbol{\omega}} \right\rangle = 0 \quad \forall \tilde{\boldsymbol{\omega}} \in H(\mathrm{curl}, \Omega). \tag{2.34}$$

As $p \in H_1(\Omega) \implies \nabla p \in H(\mathrm{curl}, \Omega)$ due to the de Rham sequence (2.22) the choice $\tilde{\boldsymbol{\omega}} := \nabla p$ is valid. This yields:

$$-\left\langle \boldsymbol{v}, \nabla \times \nabla p \right\rangle + \left\langle \boldsymbol{\omega}, \nabla p \right\rangle = 0$$

and because of $\nabla \times \nabla(\cdot) \equiv 0$ this gives

$$\left\langle \boldsymbol{\omega}, \nabla p \right\rangle = 0.$$

This is the third term of equation (2.33) and

$$\left\langle \frac{\partial \boldsymbol{u}}{\partial t}, \boldsymbol{\omega} \right\rangle = 0 \tag{2.35}$$

follows immediately. Now consider the second term of (2.32). To show that this term is zero, we start by taking the time derivative of (2.34), which is

$$-\left\langle \frac{\partial \boldsymbol{v}}{\partial t}, \nabla \times \tilde{\boldsymbol{\omega}} \right\rangle + \left\langle \frac{\partial \boldsymbol{\omega}}{\partial t}, \tilde{\boldsymbol{\omega}} \right\rangle - \left\langle \boldsymbol{v}, \nabla \times \frac{\partial \boldsymbol{\omega}}{\partial t} \right\rangle + \left\langle \boldsymbol{\omega}, \frac{\partial \tilde{\boldsymbol{\omega}}}{\partial t} \right\rangle = 0 \quad \forall \tilde{\boldsymbol{\omega}} \in H(\mathrm{curl}, \Omega), \tag{2.36}$$

due to the product rule. But as this expression holds for all $\tilde{\boldsymbol{\omega}} \in H(\mathrm{curl}, \Omega)$, the third and forth term vanish because of (2.20). This gives

$$-\left\langle \frac{\partial \boldsymbol{v}}{\partial t}, \nabla \times \tilde{\boldsymbol{\omega}} \right\rangle + \left\langle \frac{\partial \boldsymbol{\omega}}{\partial t}, \tilde{\boldsymbol{\omega}} \right\rangle = 0 \quad \forall \tilde{\boldsymbol{\omega}} \in H(\mathrm{curl}, \Omega). \tag{2.37}$$

Also $\tilde{\boldsymbol{\omega}} \in H(\mathrm{curl}, \Omega) \implies \nabla \times \tilde{\boldsymbol{\omega}} \in H(\mathrm{div}, \Omega)$ due to (2.22) allowing to take (2.19) with $\tilde{\boldsymbol{v}} := \nabla \times \tilde{\boldsymbol{\omega}}$:

$$\left\langle \frac{\partial \boldsymbol{v}}{\partial t}, \nabla \times \tilde{\boldsymbol{\omega}} \right\rangle + \langle \boldsymbol{\zeta} \times \boldsymbol{v}, \nabla \times \tilde{\boldsymbol{\omega}} \rangle - \langle q, \nabla \cdot \nabla \times \tilde{\boldsymbol{\omega}} \rangle = 0 \quad \forall \tilde{\boldsymbol{\omega}} \in H(\mathrm{curl}, \Omega). \tag{2.38}$$

Combining (2.37) and (2.38) yields

$$\left\langle \frac{\partial \boldsymbol{\omega}}{\partial t}, \tilde{\boldsymbol{\omega}} \right\rangle + \langle \boldsymbol{\zeta} \times \boldsymbol{v}, \nabla \times \tilde{\boldsymbol{\omega}} \rangle - \langle q, \nabla \cdot \nabla \times \tilde{\boldsymbol{\omega}} \rangle = 0 \quad \forall \tilde{\boldsymbol{\omega}} \in H(\mathrm{curl}, \Omega). \tag{2.39}$$

Choosing $\tilde{\boldsymbol{\omega}} := \boldsymbol{u} \in H(\mathrm{curl}, \Omega)$ results in

$$\left\langle \frac{\partial \boldsymbol{\omega}}{\partial t}, \boldsymbol{u} \right\rangle + \langle \boldsymbol{\zeta} \times \boldsymbol{v}, \nabla \times \boldsymbol{u} \rangle - \langle q, \nabla \cdot \nabla \times \boldsymbol{u} \rangle = 0. \tag{2.40}$$

The variational formulation enforces $\boldsymbol{\zeta} = \nabla \times \boldsymbol{u}$ pointwise (see (2.17)) so replace that in (2.40). Hence, the second term vanishes due to orthogonality and the third term as $\nabla \cdot \nabla \times (\cdot) \equiv 0$. This is nice, because now it is clear why (2.32) is fulfilled.

To analyze $\mathcal{H}_2$, consider the dual vorticity constraint (2.20) with $\tilde{\boldsymbol{\omega}} := \boldsymbol{u}$

$$\langle \boldsymbol{v}, \nabla \times \boldsymbol{u} \rangle - \langle \boldsymbol{\omega}, \boldsymbol{u} \rangle = 0. \tag{2.41}$$

And finally, we get

$$\mathcal{H}_2 = \langle \boldsymbol{v}, \boldsymbol{\zeta} \rangle = \langle \boldsymbol{v}, \nabla \times \boldsymbol{u} \rangle = \langle \boldsymbol{u}, \boldsymbol{\omega} \rangle = \mathcal{H}_1. \tag{2.42}$$

Similar as for the energy, the dissipation rate can be found by considering a finite Reynolds number and following the exact same steps as for the inviscid case. This gives

$$\frac{\mathrm{d}\mathcal{H}_1}{\mathrm{dt}} = \frac{\mathrm{d}\mathcal{H}_2}{\mathrm{dt}} = -\frac{2}{\mathrm{Re}} \langle \boldsymbol{\zeta}, \nabla \times \boldsymbol{\omega} \rangle .$$

Again this is aligned with the results from section 1.5.

2.4 The Dirichlet problem

In the following, the scheme is adapted to allow for Dirichlet boundary conditions. This is done by changing the trial and test spaces of the dual equations (2.19) and (2.20). We use the spaces $H_0(\mathrm{div}, \Omega)$ and $H_0(\mathrm{curl}, \Omega)$ that only contain functions with a zero normal/tangential trace on the boundary $\partial\Omega$:

Definition 16 (The space $H_0(\mathrm{curl}, \Omega)$)**.**

$$H_0(\mathrm{curl}, \Omega) := \{\boldsymbol{u} \in H(\mathrm{curl}, \Omega) : \boldsymbol{u} \times \boldsymbol{n}|_{\partial\Omega} = 0\}$$

Definition 17 (The space $H_0(\mathrm{div}, \Omega)$)**.**

$$H_0(\mathrm{div}, \Omega) := \{\boldsymbol{u} \in H(\mathrm{div}, \Omega) : \boldsymbol{u} \cdot \boldsymbol{n}|_{\partial\Omega} = 0\}$$

Further, as now the periodic setting is not active anymore, the boundary integrals in (2.16) and (2.17) do not necessarily vanish anymore. The other 2 equations remain the same.

Given $\boldsymbol{f} \in \left[L^2(\Omega)\right]^3$,
seek $(\boldsymbol{u}, \boldsymbol{\zeta}, p) \in H(\mathrm{curl}, \Omega) \times H(\mathrm{div}, \Omega) \times H^1(\Omega)$
and $(\boldsymbol{v}, \boldsymbol{\omega}, q) \in H_0(\mathrm{div}, \Omega) \times H_0(\mathrm{curl}, \Omega) \times L^2(\Omega)$
such that they satisfy

$$\left\langle \frac{\partial \boldsymbol{u}}{\partial t}, \tilde{\boldsymbol{u}} \right\rangle + \langle \boldsymbol{\omega} \times \boldsymbol{u}, \tilde{\boldsymbol{u}} \rangle + \frac{1}{\mathrm{Re}} \langle \boldsymbol{\zeta}, \nabla \times \tilde{\boldsymbol{u}} \rangle + \langle \nabla p, \tilde{\boldsymbol{u}} \rangle = \langle \boldsymbol{f}, \tilde{\boldsymbol{u}} \rangle + \frac{1}{\mathrm{Re}} (\boldsymbol{\zeta} \times \boldsymbol{n}), \tilde{\boldsymbol{u}})_{\partial\Omega} \qquad \forall \tilde{\boldsymbol{u}} \in H(\mathrm{curl}, \Omega) \tag{2.43}$$

$$\left\langle \nabla \times \boldsymbol{u}, \tilde{\boldsymbol{\zeta}} \right\rangle - \left\langle \boldsymbol{\zeta}, \tilde{\boldsymbol{\zeta}} \right\rangle = 0 \qquad \forall \tilde{\boldsymbol{\zeta}} \in H(\mathrm{div}, \Omega) \tag{2.44}$$

$$\langle \boldsymbol{u}, \nabla \tilde{p} \rangle = (\boldsymbol{u} \cdot \boldsymbol{n}, \tilde{p})_{\partial\Omega} \qquad \forall \tilde{p} \in H^1(\Omega) \tag{2.45}$$

and further

$$\left\langle \frac{\partial \boldsymbol{v}}{\partial t}, \tilde{\boldsymbol{v}} \right\rangle + \langle \boldsymbol{\zeta} \times \boldsymbol{v}, \tilde{\boldsymbol{v}} \rangle + \frac{1}{\mathrm{Re}} \langle \nabla \times \boldsymbol{\omega}, \tilde{\boldsymbol{v}} \rangle - \langle q, \nabla \cdot \tilde{\boldsymbol{v}} \rangle = \langle \boldsymbol{f}, \tilde{\boldsymbol{v}} \rangle \qquad \forall \tilde{\boldsymbol{v}} \in H_0(\mathrm{div}, \Omega) \tag{2.46}$$

$$\langle \boldsymbol{v}, \nabla \times \tilde{\boldsymbol{\omega}} \rangle - \langle \boldsymbol{\omega}, \tilde{\boldsymbol{\omega}} \rangle = 0 \qquad \forall \tilde{\boldsymbol{\omega}} \in H_0(\mathrm{curl}, \Omega) \tag{2.47}$$

$$\langle \nabla \cdot \boldsymbol{v}, \tilde{q} \rangle = 0 \qquad \forall \tilde{q} \in L^2(\Omega) \tag{2.48}$$

Interpretation:

- Because the dual test functions $\tilde{\boldsymbol{v}}$ and $\tilde{\boldsymbol{\omega}}$ are in the spaces $H_0(\mathrm{div}, \Omega)$ and $H_0(\mathrm{curl}, \Omega)$, the boundary integrals on the dual system vanish.
- If the boundary data g on the velocity fields and h on the vorticity fields does not vanish in all components, the problem stated above should rather seek for $\boldsymbol{v} \in H_g(\mathrm{div}, \Omega)$ and $\boldsymbol{\omega} \in H_h(\mathrm{curl}, \Omega)$. Technically these spaces are affine spaces, and do not fulfil the vector space properties anymore. This issue can be handled with the "offset function trick" described in [Hip22]. We stick to the notation with 0, also for non-homogeneous boundary data.
- The boundary integrals on equation (2.43) and (2.45) contain given information to the problem and are therefore part of the right hand side. If the boundary data is time-dependent, the boundary integrals have to be updated in each time step using the newest available values of $\boldsymbol{\zeta}$, and $\boldsymbol{u}$.

2.5 Conservation in the corrected spaces

2.5.1 Mass

Mass conservation holds in the weak sense for $\boldsymbol{u}$, in case of vanishing normal-component of $\boldsymbol{u}$ on the boundary. Otherwise, the weak divergence of the primal velocity is equal to the boundary contribution.
The divergence-free condition holds strongly/point-wise for $\boldsymbol{v}$ due to the constraint (2.48).

2.5.2 Energy

The kinetic energies are

$$\mathcal{K}_1 := \langle \boldsymbol{u}, \boldsymbol{u} \rangle, \qquad \mathcal{K}_2 := \langle \boldsymbol{v}, \boldsymbol{v} \rangle, \tag{2.49}$$

and their time-rate of change:

$$\frac{\mathrm{d}\mathcal{K}_1}{\mathrm{d}t} = 2\left\langle \frac{\partial \boldsymbol{u}}{\partial t}, \boldsymbol{u} \right\rangle, \qquad \frac{\mathrm{d}\mathcal{K}_2}{\mathrm{d}t} = 2\left\langle \frac{\partial \boldsymbol{v}}{\partial t}, \boldsymbol{v} \right\rangle. \tag{2.50}$$

If one now takes equation (2.43) with the choice

$$\tilde{\boldsymbol{u}} := \boldsymbol{u} \in H(\mathrm{curl}, \Omega)$$

one gets

$$\left\langle \frac{\partial \boldsymbol{u}}{\partial t}, \boldsymbol{u} \right\rangle + \langle \boldsymbol{\omega} \times \boldsymbol{u}, \boldsymbol{u} \rangle + \frac{1}{\mathrm{Re}} \langle \boldsymbol{\zeta}, \nabla \times \boldsymbol{u} \rangle + \langle \nabla p, \boldsymbol{u} \rangle = \frac{1}{\mathrm{Re}} \left((\boldsymbol{\zeta} \times \boldsymbol{n}), \boldsymbol{u} \right)_{\partial\Omega}. \tag{2.51}$$

The second term is zero due to orthogonality, and the fourth term is equal to the boundary contribution of (2.45):

$$\left\langle \frac{\partial \boldsymbol{u}}{\partial t}, \boldsymbol{u} \right\rangle = -\frac{1}{\mathrm{Re}} \langle \boldsymbol{\zeta}, \nabla \times \boldsymbol{u} \rangle - (\boldsymbol{u} \cdot \boldsymbol{n}, \tilde{p})_{\partial\Omega} + \frac{1}{\mathrm{Re}} \left((\boldsymbol{\zeta} \times \boldsymbol{n}), \boldsymbol{u} \right)_{\partial\Omega}. \tag{2.52}$$

In case of zero normal component of $\boldsymbol{u}$ and zero tangential component $\boldsymbol{\zeta}$, the time-rate of change of energy is equal to the dissipative term. Similarly, for $\boldsymbol{v}$ one gets

$$\left\langle \frac{\partial \boldsymbol{v}}{\partial t}, \boldsymbol{v} \right\rangle = -\frac{1}{\mathrm{Re}} \langle \nabla \times \boldsymbol{\omega}, \boldsymbol{v} \rangle. \tag{2.53}$$

Both this and the dissipation of $\mathcal{K}_1$ are proportional to $\mathcal{E}$, see (2.44) and (2.47).

2.5.3 Helicity

In general, helicity is not conserved for the Dirichlet problem, like it was for the periodic case (see 2.3.4). To show this, it is important to remember, that only on the dual variables $\boldsymbol{v} \in H_0(\mathrm{div}, \Omega)$ and $\boldsymbol{\omega} \in H_0(\mathrm{curl}, \Omega)$ essential boundary values are enforced. The primal velocity and vorticity do not have essential boundary values.

Again, it is required that

$$\frac{\mathrm{d}\mathcal{H}_1}{\mathrm{d}t} = \left\langle \frac{\partial \boldsymbol{u}}{\partial t}, \boldsymbol{\omega} \right\rangle + \left\langle \boldsymbol{u}, \frac{\partial \boldsymbol{\omega}}{\partial t} \right\rangle = 0. \tag{2.54}$$

Starting with the first term: take (2.43) in the inviscid limit without forcing and set $\boldsymbol{\omega} =: \tilde{\boldsymbol{u}} \in H(\mathrm{curl}, \Omega)$ which is allowed, as $H_0(\mathrm{curl}, \Omega) \subset H(\mathrm{curl}, \Omega)$

$$\left\langle \frac{\partial \boldsymbol{u}}{\partial t}, \boldsymbol{\omega} \right\rangle + \langle \boldsymbol{\omega} \times \boldsymbol{u}, \boldsymbol{\omega} \rangle + \langle \boldsymbol{\omega}, \nabla p \rangle = 0. \tag{2.55}$$

The second term vanishes due to orthogonality. The next step utilizes the corrected constraint from equation (2.47), which reads as

$$\langle \boldsymbol{v}, \nabla \times \tilde{\boldsymbol{\omega}} \rangle - \langle \boldsymbol{\omega}, \tilde{\boldsymbol{\omega}} \rangle = 0 \quad \forall \tilde{\boldsymbol{\omega}} \in H_0(\mathrm{curl}, \Omega).$$

However, setting $\tilde{\boldsymbol{\omega}} := \nabla p$ is not possible, because $\nabla p \notin H_0(\mathrm{curl}, \Omega)$. One would have to choose p in a way, such that $\nabla p \in H_0(\mathrm{curl}, \Omega)$. This would be the case for $p \in H_0^1(\Omega)$.

If one continues the steps from the helicity conservation proof for the periodic problem in section 2.3.4, one will find the following requirements to be necessary:

- restricting the testfunction $\tilde{\boldsymbol{u}}$ such that $\nabla \times \tilde{\boldsymbol{u}} \in H_0(\mathrm{div}, \Omega)$,

- restricting $\boldsymbol{u}$ the same way,
- enforcing $\boldsymbol{u} \in H_0(\mathrm{curl}, \Omega)$ (which would imply the previous condition)
- and both $\tilde{\boldsymbol{\zeta}}$ as well as $\boldsymbol{\zeta}$ have to be element of $\in H_0(\mathrm{div}, \Omega)$.

These requirements on the test and trial functions would be satisfied by an adapted de Rham complex with essential boundary conditions (see Remark 3.17 in [Zag06]). It is given as

$$H_0^1(\Omega) \xrightarrow{\nabla} H_0(\mathrm{curl}, \Omega) \xrightarrow{\mathrm{curl}} H_0(\mathrm{div}, \Omega) \xrightarrow{\mathrm{div}} L_0^2(\Omega). \tag{2.56}$$

Whether this choice of boundary conditions, namely to have essential boundary conditions on all trial functions, is also valid implementation-wise and leads to a numerically stable algorithm is still to be investigated.
The formulation introduced in section 2.4 does in general not conserve helicity.

Chapter 3

Discrete variational formulation

This chapter, especially sections 3.3 and 3.4, is again based on the lecture notes [Fau22], [Hip22], as well as [Sch18].

Having discussed the continuous formulation of the scheme in the previous chapter, it is now time to discretize it and transform it into linear algebra format so that a computer can solve it. The goal of the discretization is to preserve the conservation of mass, kinetic energy and helicity similarly as the continuous formulation.

First, the time discretization is discussed, then appropriate finite dimensional subspaces of the previously discussed function spaces are being constructed so that the unknowns/trial functions can be interpolated using the respective basis functions of these subspaces. Finally, the notion of finite elements is discussed. It would also be possible to do a spatial discretization first. As this chapter is again based on [YR22], we stick to the described method of discretization.

3.1 Temporal semi-discretization

For the temporal discretization of the evolution equation (2.16), integer time steps are used, and for (2.18), half-integer time steps are being used. That way, each equation can use the solution values of the other equation from half a time step before. The time sequences are restricted to constant time intervals. Function evaluations at time step t_k will be denoted with a superscript

$$f^k := f(t_k)$$

and the uniform time step length is

$$\Delta t := t^k - t^{k-1} = t^{k+\frac{1}{2}} - t^{k-\frac{1}{2}}.$$

The integrator applied to a first order ODE of the form

$$\frac{\mathrm{d}f(t)}{dt} = h(f(t), t)$$

yields

$$\frac{f^k - f^{k-1}}{\Delta t} = h\left(f^{k-\frac{1}{2}}, t^{k-1} + \frac{\Delta t}{2}\right).$$

Furthermore, the midpoint rule is used, which states

$$f^{k-\frac{1}{2}} := \frac{f^k + f^{k-1}}{2}. \tag{3.1}$$

Applying these definitions to equations (2.19), (2.20) and (2.21) yields the following time-discrete problem:

given $\left(\boldsymbol{\omega}^{k-1}, \boldsymbol{v}^{k-1}, \boldsymbol{f}^{k-\frac{1}{2}}, \boldsymbol{\zeta}^{k-\frac{1}{2}}\right) \in H(\mathrm{curl}, \Omega) \times H(\mathrm{div}, \Omega) \times \left[L^2(\Omega)\right]^d \times H(\mathrm{div}, \Omega)$
seek $\left(\boldsymbol{\omega}^{k}, \boldsymbol{v}^{k}, q^{k-\frac{1}{2}}\right) \in H(\mathrm{curl}, \Omega) \times H(\mathrm{div}, \Omega) \times L^2(\Omega)$
such that they satisfy

$$\left\langle \frac{\boldsymbol{v}^k - \boldsymbol{v}^{k-1}}{\Delta t}, \tilde{\boldsymbol{v}} \right\rangle + \left\langle \boldsymbol{\zeta}^{k-\frac{1}{2}} \times \frac{\boldsymbol{v}^k + \boldsymbol{v}^{k-1}}{2}, \tilde{\boldsymbol{v}} \right\rangle + \frac{1}{\mathrm{Re}} \left\langle \nabla \times \frac{\boldsymbol{\omega}^k + \boldsymbol{\omega}^{k-1}}{2}, \tilde{\boldsymbol{v}} \right\rangle - \left\langle q^{k-\frac{1}{2}}, \nabla \cdot \tilde{\boldsymbol{v}} \right\rangle = \left\langle \boldsymbol{f}^{k-\frac{1}{2}}, \tilde{\boldsymbol{v}} \right\rangle \quad \forall \tilde{\boldsymbol{v}} \in H(\mathrm{div}, \Omega) \tag{3.2}$$

$$\left\langle \boldsymbol{v}^k, \nabla \times \tilde{\boldsymbol{\omega}} \right\rangle - \left\langle \boldsymbol{\omega}^k, \tilde{\boldsymbol{\omega}} \right\rangle = 0 \quad \forall \tilde{\boldsymbol{\omega}} \in H(\mathrm{curl}, \Omega) \tag{3.3}$$

$$\left\langle \nabla \cdot \boldsymbol{v}^k, \tilde{q} \right\rangle = 0 \quad \forall \tilde{q} \in L^2(\Omega) \tag{3.4}$$

Moreover one makes use of the above definitions to discretize equations (2.16) to (2.18). The time-discrete problem is

given $\left(\boldsymbol{u}^{k-\frac{1}{2}}, \boldsymbol{\zeta}^{k-\frac{1}{2}}, \boldsymbol{f}^{k}, \boldsymbol{\omega}^{k}\right) \in H(\mathrm{curl}, \Omega) \times H(\mathrm{div}, \Omega) \times \left[L^2(\Omega)\right]^d \times H(\mathrm{curl}, \Omega)$

seek $\left(p^{k}, \boldsymbol{u}^{k+\frac{1}{2}}, \boldsymbol{\zeta}^{k+\frac{1}{2}}\right) \in H^1(\Omega) \times H(\mathrm{curl}, \Omega) \times H(\mathrm{div}, \Omega)$
such that they satisfy

$$\left\langle \frac{\boldsymbol{u}^{k+\frac{1}{2}} - \boldsymbol{u}^{k-\frac{1}{2}}}{\Delta t}, \tilde{\boldsymbol{u}} \right\rangle + \left\langle \boldsymbol{\omega}^{k} \times \frac{\boldsymbol{u}^{k+\frac{1}{2}} + \boldsymbol{u}^{k-\frac{1}{2}}}{2}, \tilde{\boldsymbol{u}} \right\rangle + \frac{1}{\mathrm{Re}} \left\langle \frac{\boldsymbol{\zeta}^{k+\frac{1}{2}} + \boldsymbol{\zeta}^{k-\frac{1}{2}}}{2}, \nabla \times \tilde{\boldsymbol{u}} \right\rangle - \left\langle \nabla p^k, \tilde{\boldsymbol{u}} \right\rangle = \left\langle \boldsymbol{f}^{k}, \tilde{\boldsymbol{u}} \right\rangle \quad \forall \tilde{\boldsymbol{u}} \in H(\mathrm{curl}, \Omega) \tag{3.5}$$

$$\left\langle \nabla \times \boldsymbol{u}^{k+\frac{1}{2}}, \tilde{\boldsymbol{\zeta}} \right\rangle - \left\langle \boldsymbol{\zeta}^{k+\frac{1}{2}}, \tilde{\boldsymbol{\zeta}} \right\rangle = 0 \quad \forall \tilde{\boldsymbol{\zeta}} \in H(\mathrm{div}, \Omega) \tag{3.6}$$

$$\left\langle \boldsymbol{u}^{k+\frac{1}{2}}, \nabla \tilde{p} \right\rangle = 0 \quad \forall \tilde{p} \in H^1(\Omega) \tag{3.7}$$

These two sets of three equations each are being solved alternately. For that, the value $\boldsymbol{\zeta}^{k-\frac{1}{2}}$ in equation (3.2) is computed in equations (3.5) to (3.7). Further, the value $\boldsymbol{\omega}^{k}$ in equation (3.4) is computed in equations (3.2) to (3.4).

To start the iteration, i.e. to find $\boldsymbol{u}^{\frac{1}{2}}, \boldsymbol{\zeta}^{\frac{1}{2}}$, an initialization step is necessary. A possibility is to apply an explicit Euler method to equation (2.16).

3.1.1 Explicit Euler method for the first half time step

To find $\boldsymbol{u}^{\frac{1}{2}}, \boldsymbol{\zeta}^{\frac{1}{2}}$, the only available values are the initial values of the velocities and vorticities (not the pressures!): $\boldsymbol{u}^0, \boldsymbol{\zeta}^0, \boldsymbol{v}^0, \boldsymbol{\omega}^0$.

The explicit Euler method applied to an ODE of the form

$$\frac{\mathrm{d}f(t)}{dt} = h(f(t), t)$$

yields

$$\frac{f^k - f^{k-1}}{\Delta t} = h(f^{k-1}, t^{k-1}),$$

which is an explicit integration method: the new time step is solely dependent on old, previously computed values.
The Euler method applied to the Navier-Stokes problem reads as follows:

given $\left(\boldsymbol{u}^0, \boldsymbol{f}^0, \boldsymbol{\omega}^0\right) \in H(\mathrm{curl}, \Omega) \times \left[L^2(\Omega)\right]^d \times H(\mathrm{curl}, \Omega)$

seek $\left(p^0, \boldsymbol{u}^{\frac{1}{2}}, \boldsymbol{\zeta}^{\frac{1}{2}}\right) \in H^1(\Omega) \times H(\mathrm{curl}, \Omega) \times H(\mathrm{div}, \Omega)$
such that they satisfy

$$\left\langle \frac{\boldsymbol{u}^{\frac{1}{2}} - \boldsymbol{u}^0}{\frac{1}{2}\Delta t}, \tilde{\boldsymbol{u}} \right\rangle + \left\langle \boldsymbol{\omega}^0 \times \boldsymbol{u}^0, \tilde{\boldsymbol{u}} \right\rangle$$
$$+ \frac{1}{\mathrm{Re}} \left\langle \boldsymbol{\zeta}^{\frac{1}{2}}, \nabla \times \tilde{\boldsymbol{u}} \right\rangle - \left\langle \nabla p^0, \tilde{\boldsymbol{u}} \right\rangle = \left\langle \boldsymbol{f}^0, \tilde{\boldsymbol{u}} \right\rangle \qquad \forall \tilde{\boldsymbol{u}} \in H(\mathrm{curl}, \Omega) \tag{3.8}$$
$$\left\langle \nabla \times \boldsymbol{u}^{\frac{1}{2}}, \tilde{\boldsymbol{\zeta}} \right\rangle - \left\langle \boldsymbol{\zeta}^{\frac{1}{2}}, \tilde{\boldsymbol{\zeta}} \right\rangle = 0 \qquad \forall \tilde{\boldsymbol{\zeta}} \in H(\mathrm{div}, \Omega) \tag{3.9}$$
$$\left\langle \nabla \cdot \boldsymbol{u}^{\frac{1}{2}}, \tilde{p} \right\rangle = 0 \qquad \forall \tilde{p} \in L^2(\Omega) \tag{3.10}$$

To make sense of the time stepping algorithm and to understand which values are available at which time step, consider the following table.

time step	solved at k	required at k	previously computed
$k = 0$	-	-	$\boldsymbol{u}^0, \boldsymbol{\zeta}^0, \boldsymbol{v}^0, \boldsymbol{\omega}^0$
$k = \frac{1}{2}$	$\boldsymbol{u}^{\frac{1}{2}}, \boldsymbol{\zeta}^{\frac{1}{2}}$	$\boldsymbol{u}^0, \boldsymbol{\omega}^0$	$\boldsymbol{u}^0, \boldsymbol{\zeta}^0, \boldsymbol{\omega}^0, \boldsymbol{v}^0$
$k = 1$	$\boldsymbol{v}^1, \boldsymbol{\omega}^1$	$\boldsymbol{v}^0, \boldsymbol{\omega}^0, \boldsymbol{\zeta}^{\frac{1}{2}}$	$\boldsymbol{u}^{\frac{1}{2}}, \boldsymbol{\zeta}^{\frac{1}{2}}, \boldsymbol{\omega}^0, \boldsymbol{v}^0$
$k = \frac{3}{2}$	$\boldsymbol{u}^{\frac{3}{2}}, \boldsymbol{\zeta}^{\frac{3}{2}}$	$\boldsymbol{u}^{\frac{1}{2}}, \boldsymbol{\zeta}^{\frac{1}{2}}, \boldsymbol{\omega}^1$	$\boldsymbol{u}^{\frac{1}{2}}, \boldsymbol{\zeta}^{\frac{1}{2}}, \boldsymbol{\omega}^1, \boldsymbol{v}^1$
...	...	...	...

Its easy to see how the two systems are coupled by their vorticities and how the systems are solved alternately.

3.2 Conservation in the semi-discrete setting

3.2.1 Mass

The conservation of the divergence-free property of $\boldsymbol{v} \in H(\mathrm{div}, \Omega)$ is still fulfilled pointwise/strongly due to condition (3.4). In contrast to that, the corresponding condition for $\boldsymbol{u} \in H(\mathrm{curl}, \Omega)$ is again only satisfied weakly through integration by parts.

3.2.2 Energy

For this, $\boldsymbol{f} = 0$ (or nonzero, but conservative, see the comment on that in section 1.5) and $\mathrm{Re} = \infty$ is assumed. The goal is to show that

$$\mathcal{K}_1^{k+\frac{1}{2}} = \frac{1}{2} \left\langle \boldsymbol{u}^{k+\frac{1}{2}}, \boldsymbol{u}^{k+\frac{1}{2}} \right\rangle, \tag{3.11}$$
$$\mathcal{K}_2^{k} = \frac{1}{2} \left\langle \boldsymbol{v}^{k}, \boldsymbol{v}^{k} \right\rangle \tag{3.12}$$

are conserved, i.e:

$$\mathcal{K}_1^k = \mathcal{K}_1^{k-1}, \qquad \mathcal{K}_2^k = \mathcal{K}_2^{k-1}.$$

In other words:

$$\left\langle \boldsymbol{u}^{k+\frac{1}{2}}, \boldsymbol{u}^{k+\frac{1}{2}} \right\rangle - \left\langle \boldsymbol{u}^{k-\frac{1}{2}}, \boldsymbol{u}^{k-\frac{1}{2}} \right\rangle = 0.$$

Adding and subtracting a term to rearrange the expression yields

$$\left\langle \boldsymbol{u}^{k+\frac{1}{2}}, \boldsymbol{u}^{k+\frac{1}{2}} \right\rangle - \left\langle \boldsymbol{u}^{k-\frac{1}{2}}, \boldsymbol{u}^{k-\frac{1}{2}} \right\rangle + \left\langle \boldsymbol{u}^{k+\frac{1}{2}}, \boldsymbol{u}^{k-\frac{1}{2}} \right\rangle - \left\langle \boldsymbol{u}^{k-\frac{1}{2}}, \boldsymbol{u}^{k+\frac{1}{2}} \right\rangle = 0,$$

applying linearity of the bilinear forms results in

$$\left\langle \boldsymbol{u}^{k+\frac{1}{2}}, \boldsymbol{u}^{k+\frac{1}{2}} + \boldsymbol{u}^{k-\frac{1}{2}} \right\rangle - \left\langle \boldsymbol{u}^{k-\frac{1}{2}}, \boldsymbol{u}^{k+\frac{1}{2}} + \boldsymbol{u}^{k-\frac{1}{2}} \right\rangle = 0$$

and applying linearity again gives

$$\left\langle \boldsymbol{u}^{k+\frac{1}{2}} - \boldsymbol{u}^{k-\frac{1}{2}}, \boldsymbol{u}^{k+\frac{1}{2}} + \boldsymbol{u}^{k-\frac{1}{2}} \right\rangle = 0.$$

After adding constants to match the expression with the momentum equations (3.5) and (3.2) one obtains

$$\left\langle \frac{\boldsymbol{u}^{k+\frac{1}{2}} - \boldsymbol{u}^{k-\frac{1}{2}}}{\Delta t}, \frac{\boldsymbol{u}^{k+\frac{1}{2}} + \boldsymbol{u}^{k-\frac{1}{2}}}{2} \right\rangle = 0, \tag{3.13}$$

$$\left\langle \frac{\boldsymbol{v}^{k} - \boldsymbol{v}^{k-1}}{\Delta t}, \frac{\boldsymbol{v}^{k} + \boldsymbol{v}^{k-1}}{2} \right\rangle = 0. \tag{3.14}$$

If these expressions vanish, (3.11) and (3.12) are fulfilled. As mentioned, these terms appear in the momentum equations (3.5) and (3.2). Taking the first momentum equation and choosing

$$\tilde{\boldsymbol{u}} := \frac{\boldsymbol{u}^{k+\frac{1}{2}} + \boldsymbol{u}^{k-\frac{1}{2}}}{2}$$

yields

$$\left\langle \frac{\boldsymbol{u}^{k+\frac{1}{2}} - \boldsymbol{u}^{k-\frac{1}{2}}}{\Delta t}, \frac{\boldsymbol{u}^{k+\frac{1}{2}} + \boldsymbol{u}^{k-\frac{1}{2}}}{2} \right\rangle + \left\langle \boldsymbol{\omega}^{k} \times \frac{\boldsymbol{u}^{k+\frac{1}{2}} + \boldsymbol{u}^{k-\frac{1}{2}}}{2}, \frac{\boldsymbol{u}^{k+\frac{1}{2}} + \boldsymbol{u}^{k-\frac{1}{2}}}{2} \right\rangle - \left\langle \nabla p^{k}, \frac{\boldsymbol{u}^{k+\frac{1}{2}} + \boldsymbol{u}^{k-\frac{1}{2}}}{2} \right\rangle = 0. \tag{3.15}$$

Again like in the continuous setting, the second term vanishes due to orthogonality properties of the general cross product and the third term vanishes because

$$\left\langle \nabla p^{k}, \frac{\boldsymbol{u}^{k+\frac{1}{2}} + \boldsymbol{u}^{k-\frac{1}{2}}}{2} \right\rangle = \frac{1}{2} \left\langle \nabla p^{k}, \boldsymbol{u}^{k+\frac{1}{2}} \right\rangle + \frac{1}{2} \left\langle \nabla p^{k}, \boldsymbol{u}^{k-\frac{1}{2}} \right\rangle.$$

both of which are zero due to equation (3.7). The exact same procedure can be followed for the conservation of $\mathcal{K}_2$. The dissipation rate for a finite Reynolds number can also be predicted, which gives

$$\left\langle \frac{\boldsymbol{u}^{k+\frac{1}{2}} - \boldsymbol{u}^{k-\frac{1}{2}}}{\Delta t}, \frac{\boldsymbol{u}^{k+\frac{1}{2}} + \boldsymbol{u}^{k-\frac{1}{2}}}{2} \right\rangle = -\frac{1}{\mathrm{Re}} \left\langle \frac{\boldsymbol{\zeta}^{k+\frac{1}{2}} + \boldsymbol{\zeta}^{k-\frac{1}{2}}}{2}, \frac{\boldsymbol{\zeta}^{k+\frac{1}{2}} + \boldsymbol{\zeta}^{k-\frac{1}{2}}}{2} \right\rangle = -\frac{2}{\mathrm{Re}} \mathcal{E}_{\zeta}^{k}, \tag{3.16}$$

$$\left\langle \frac{\boldsymbol{v}^{k} - \boldsymbol{v}^{k-1}}{\Delta t}, \frac{\boldsymbol{v}^{k} + \boldsymbol{v}^{k-1}}{2} \right\rangle = -\frac{1}{\mathrm{Re}} \left\langle \frac{\boldsymbol{\omega}^{k} + \boldsymbol{\omega}^{k-1}}{2}, \frac{\boldsymbol{\omega}^{k} + \omega^{k-1}}{2} \right\rangle = -\frac{2}{\mathrm{Re}} \mathcal{E}_{\omega}^{k+\frac{1}{2}}. \tag{3.17}$$

As $\mathcal{E}_i \leq 0$, energy is being dissipated also in the discrete setting.

3.2.3 Helicity

Again, first $\mathrm{Re} \to \infty$ and zero forcing term is assumed. We take (3.5), choose the test function $\tilde{\boldsymbol{u}} := \boldsymbol{\omega}$, and apply the same process as in the continuous setting, see section 2.3.4. This yields

$$\left\langle \frac{\boldsymbol{u}^{k+\frac{1}{2}} - \boldsymbol{u}^{k-\frac{1}{2}}}{\Delta t}, \boldsymbol{\omega}^k \right\rangle = 0. \tag{3.18}$$

This is the discrete equivalent of the first term of (2.32). For the equivalent of the second term of said equation one gets

$$\left\langle \frac{\boldsymbol{\omega}^k - \boldsymbol{\omega}^{k-1}}{\Delta t}, \boldsymbol{u}^{k-\frac{1}{2}} \right\rangle = 0. \tag{3.19}$$

Equation (3.18) can be rewritten as

$$\left\langle \frac{\boldsymbol{u}^{k+\frac{1}{2}} - \boldsymbol{u}^{k-\frac{1}{2}}}{\Delta t}, \boldsymbol{\omega}^k \right\rangle = \left\langle \frac{\boldsymbol{u}^{k+\frac{1}{2}}}{\Delta t}, \boldsymbol{\omega}^k \right\rangle - \left\langle \frac{\boldsymbol{u}^{k-\frac{1}{2}}}{\Delta t}, \boldsymbol{\omega}^k \right\rangle = 0, \tag{3.20}$$

and similar calculations hold for (3.19). Consequentially, one concludes

$$\left\langle \boldsymbol{u}^{k+\frac{1}{2}}, \boldsymbol{\omega}^k \right\rangle = \left\langle \boldsymbol{u}^{k-\frac{1}{2}}, \boldsymbol{\omega}^k \right\rangle = \left\langle \boldsymbol{u}^{k-\frac{1}{2}}, \boldsymbol{\omega}^{k-1} \right\rangle. \tag{3.21}$$

As (3.18) holds for all k, it also implies that

$$\left\langle \frac{\boldsymbol{u}^{k-\frac{1}{2}} - \boldsymbol{u}^{k-\frac{3}{2}}}{\Delta t}, \boldsymbol{\omega}^{k-1} \right\rangle = 0, \tag{3.22}$$

and

$$\left\langle \boldsymbol{u}^{k+\frac{1}{2}}, \boldsymbol{\omega}^k \right\rangle = \left\langle \boldsymbol{u}^{k-\frac{1}{2}}, \boldsymbol{\omega}^k \right\rangle = \left\langle \boldsymbol{u}^{k-\frac{1}{2}}, \boldsymbol{\omega}^{k-1} \right\rangle = \left\langle \boldsymbol{u}^{k-\frac{3}{2}}, \boldsymbol{\omega}^{k-1} \right\rangle \tag{3.23}$$

follows immediately. Now this implies that

$$\left\langle \boldsymbol{u}^{k+\frac{1}{2}}, \boldsymbol{\omega}^k \right\rangle + \left\langle \boldsymbol{u}^{k-\frac{1}{2}}, \boldsymbol{\omega}^k \right\rangle = 2 \left\langle \boldsymbol{u}^{k-\frac{1}{2}}, \boldsymbol{\omega}^k \right\rangle$$

Define the primal velocity at integer time steps $\boldsymbol{u}^k$ by the midpoint rule (3.1) and get

$$\boldsymbol{u}^k = \frac{\boldsymbol{u}^{k+\frac{1}{2}} + \boldsymbol{u}^{k-\frac{1}{2}}}{2} \tag{3.24}$$

and by linearity

$$\left\langle \boldsymbol{u}^k, \boldsymbol{\omega}^k \right\rangle = \left\langle \boldsymbol{u}^{k-\frac{1}{2}}, \boldsymbol{\omega}^k \right\rangle. \tag{3.25}$$

Applying this procedure to $\boldsymbol{u}^{k-1}$ yields

$$\mathcal{H}_1^k \equiv \left\langle \boldsymbol{u}^k, \boldsymbol{\omega}^k \right\rangle = \left\langle \boldsymbol{u}^{k-1}, \boldsymbol{\omega}^{k-1} \right\rangle \equiv \mathcal{H}_1^{k-1}. \tag{3.26}$$

Now take (3.3) and choose $\tilde{\boldsymbol{\omega}} := \boldsymbol{u}^k$, which leads to

$$\left\langle \boldsymbol{\omega}^k, \boldsymbol{u}^k \right\rangle = \left\langle \boldsymbol{v}^k, \nabla \times \boldsymbol{u}^k \right\rangle = \left\langle \boldsymbol{v}^k, \nabla \times \frac{\boldsymbol{u}^{k+\frac{1}{2}} + \boldsymbol{u}^{k-\frac{1}{2}}}{2} \right\rangle = \left\langle \boldsymbol{v}^k, \frac{\boldsymbol{\zeta}^{k+\frac{1}{2}} + \boldsymbol{\zeta}^{k-\frac{1}{2}}}{2} \right\rangle \tag{3.27}$$

as $\boldsymbol{\zeta} = \nabla \times \boldsymbol{u}$ pointwise. Finally by (3.1), there holds

$$\left\langle \boldsymbol{v}^k, \frac{\boldsymbol{\zeta}^{k+\frac{1}{2}} + \boldsymbol{\zeta}^{k-\frac{1}{2}}}{2} \right\rangle = \left\langle \boldsymbol{v}^k, \boldsymbol{\zeta}^k \right\rangle. \tag{3.28}$$

(3.26) and the previous two equations imply

$$\mathcal{H}_2^k \equiv \left\langle \boldsymbol{v}^k, \boldsymbol{\zeta}^k \right\rangle = \left\langle \boldsymbol{u}^k, \boldsymbol{\omega}^k \right\rangle \equiv \mathcal{H}_1^k, \tag{3.29}$$

which shows the conservation. Similarly as before the dissipation rate can be analyzed: For $\mathrm{Re} < \infty$, one obtains, instead of (3.18) and (3.19)

$$\left\langle \frac{\boldsymbol{u}^{k+\frac{1}{2}} - \boldsymbol{u}^{k-\frac{1}{2}}}{\Delta t}, \boldsymbol{\omega}^k \right\rangle = -\frac{1}{\mathrm{Re}} \left\langle \frac{\boldsymbol{\zeta}^{k+\frac{1}{2}} + \boldsymbol{\zeta}^{k-\frac{1}{2}}}{2}, \nabla \times \boldsymbol{\omega}^k \right\rangle, \tag{3.30}$$

$$\left\langle \frac{\boldsymbol{\omega}^k - \boldsymbol{\omega}^{k-1}}{\Delta t}, \boldsymbol{u}^{k-\frac{1}{2}} \right\rangle = -\frac{1}{\mathrm{Re}} \left\langle \nabla \times \frac{\boldsymbol{\omega}^k + \boldsymbol{\omega}^{k-1}}{2}, \boldsymbol{\zeta}^{k-\frac{1}{2}} \right\rangle. \tag{3.31}$$

Summation of the equations, use of linearity, canceling out $\frac{1}{\Delta t}\left\langle \boldsymbol{u}^{k-\frac{1}{2}}, \boldsymbol{\omega}^k \right\rangle$ on the left, and application of (3.1) to $\boldsymbol{\zeta}$ and $\boldsymbol{\omega}$ on the right provides

$$\frac{1}{\Delta t}\left\langle \boldsymbol{u}^{k+\frac{1}{2}}, \boldsymbol{\omega}^k \right\rangle - \frac{1}{\Delta t}\left\langle \boldsymbol{u}^{k-\frac{1}{2}}, \boldsymbol{\omega}^{k-1} \right\rangle = -\frac{1}{\mathrm{Re}}\left\langle \boldsymbol{\zeta}^k, \nabla \times \boldsymbol{\omega}^k \right\rangle - \frac{1}{\mathrm{Re}}\left\langle \nabla \times \boldsymbol{\omega}^{k-\frac{1}{2}}, \boldsymbol{\zeta}^{k-\frac{1}{2}} \right\rangle. \tag{3.32}$$

Similarly, (3.30) also holds for the timestep $k-1$, which reads as

$$\left\langle \frac{\boldsymbol{u}^{k-\frac{1}{2}} - \boldsymbol{u}^{k-\frac{3}{2}}}{\Delta t}, \boldsymbol{\omega}^{k-1} \right\rangle = -\frac{1}{\mathrm{Re}} \left\langle \frac{\boldsymbol{\zeta}^{k-\frac{1}{2}} + \boldsymbol{\zeta}^{k-\frac{3}{2}}}{2}, \nabla \times \boldsymbol{\omega}^{k-1} \right\rangle.$$

Add this to (3.31), apply linearity, cancel out $\frac{1}{\Delta t}\left\langle \boldsymbol{u}^{k-\frac{1}{2}}, \boldsymbol{\omega}^{k-\frac{1}{2}} \right\rangle$ on the left, apply (3.1) to $\boldsymbol{\zeta}$ and $\boldsymbol{\omega}$ on the right yields:

$$\begin{aligned}\frac{1}{\Delta t}\left\langle \boldsymbol{u}^{k-\frac{1}{2}}, \boldsymbol{\omega}^k \right\rangle - \frac{1}{\Delta t}\left\langle \boldsymbol{u}^{k-\frac{3}{2}}, \boldsymbol{\omega}^{k-1} \right\rangle = &-\frac{1}{\mathrm{Re}}\left\langle \boldsymbol{\zeta}^{k-1}, \nabla \times \boldsymbol{\omega}^{k-1} \right\rangle \\ &- \frac{1}{\mathrm{Re}}\left\langle \nabla \times \boldsymbol{\omega}^{k-\frac{1}{2}}, \boldsymbol{\zeta}^{k-\frac{1}{2}} \right\rangle.\end{aligned} \tag{3.33}$$

Now the left hand sides of (3.32) and (3.33) are summed, and $\boldsymbol{u}^k$ and $\boldsymbol{u}^{k-1}$ are inserted using (3.1)

$$\frac{\left\langle \boldsymbol{u}^{k+\frac{1}{2}} + \boldsymbol{u}^{k-\frac{1}{2}}, \boldsymbol{\omega}^k \right\rangle}{\Delta t} - \frac{\left\langle \boldsymbol{u}^{k-\frac{1}{2}} + \boldsymbol{u}^{k-\frac{3}{2}}, \boldsymbol{\omega}^{k-1} \right\rangle}{\Delta t} = 2\frac{\left\langle \boldsymbol{u}^k, \boldsymbol{\omega}^k \right\rangle - \left\langle \boldsymbol{u}^{k-1}, \boldsymbol{\omega}^{k-1} \right\rangle}{\Delta t}. \tag{3.34}$$

By definition, this expression is equal to

$$2\frac{\mathcal{H}_1^k - \mathcal{H}_1^{k-1}}{\Delta t} =: 2\mathcal{D},$$

where $\mathcal{D}$ is the dissipation rate. The summed right hand sides of (3.32) and (3.33) are

$$-\frac{2}{\mathrm{Re}}\left\langle \nabla \times \boldsymbol{\omega}^{k-\frac{1}{2}}, \boldsymbol{\zeta}^{k-\frac{1}{2}} \right\rangle - \frac{\left\langle \boldsymbol{\zeta}^k, \nabla \times \boldsymbol{\omega}^k \right\rangle + \left\langle \boldsymbol{\zeta}^{k-1}, \nabla \times \boldsymbol{\omega}^{k-1} \right\rangle}{\mathrm{Re}}. \tag{3.35}$$

Also in the case of finite Reynolds number (3.29) still holds, and therefore implies

$$\frac{\mathcal{H}_1^k - \mathcal{H}_1^{k-1}}{\Delta t} = \frac{\mathcal{H}_2^k - \mathcal{H}_2^{k-1}}{\Delta t} \equiv \mathcal{D}, \tag{3.36}$$

and because of the previous calculations, one arrives at

$$\mathcal{D} = -\frac{\left\langle \nabla \times \boldsymbol{\omega}^{k-\frac{1}{2}}, \boldsymbol{\zeta}_2^{k-\frac{1}{2}} \right\rangle}{\mathrm{Re}} - \frac{\left\langle \boldsymbol{\zeta}_2^k, \nabla \times \boldsymbol{\omega}^k \right\rangle + \left\langle \boldsymbol{\zeta}_2^{k-1}, \nabla \times \boldsymbol{\omega}^{k-1} \right\rangle}{2\,\mathrm{Re}}. \tag{3.37}$$

3.3 Spatial Finite Element discretization

The finite element method is a powerful numerical method that will be used to find solutions to the given problem in the previous section. Its objective is to approximate the unknown functions by interpolation on a finite number of elements, that make up the domain. In the following, finite elements are formally defined.

Definition 18 (Ciarlet Finite Element)**.** *A finite element is a triple* (T, V^T, Ψ^T) *with*

- T *being a bounded set,*
- V^T *being an* N*-dimensional function space on* T*,*
- $\Psi^T = \{\psi_1^T, ...\psi_N^T\}$ *being a set of* N *linearly independent functionals on* V^T*.*

The functionals (also called degrees of freedom) on the finite element space V^T can be used to construct a basis $\{\boldsymbol{\phi}_1^T, ...\boldsymbol{\phi}_N^T\}$ on the function space, by requiring

$$\psi_i^T(\boldsymbol{\phi}_j^T) = \delta_{ij}. \tag{3.38}$$

The basis functions allow the interpolation/basis expansion of the unknown function.

Definition 19 (Local interpolation operator)**.** *The local interpolation operator is defined as*

$$\begin{aligned} I_T : C(T) &\to V^T \\ \boldsymbol{u} &\mapsto \sum_{j=1}^{N_T} \psi_j^T(\boldsymbol{u})\boldsymbol{\phi}_j^T. \end{aligned} \tag{3.39}$$

Note that it is idempotent/it is a projection, i.e. $I_T(I_T\boldsymbol{u}) = I_T\boldsymbol{u}$*.*

The domain in which the given problem will be solved is being denoted by $\Omega \subset \mathbb{R}^d$. It will be divided into a finite number of elements. The result of dividing the domain into subdomains (corresponding to the bounded set T in definition 18) is called a mesh or a triangulation.

Definition 20 (Mesh/Triangulation)**.** *A regular mesh* $\mathcal{T} = \{T_1, ...T_N\}$ *of a domain* $\Omega \subset \mathbb{R}^d$ *is a subdivision of* Ω *such that* $\Omega = \bigcup_i T_i$ *and that* $T_i \cap T_{j\neq i}$ *is empty for non-neighbour elements or exactly one common vertex/edge/face for neighbour elements.*

To reduce computational complexity, the functionals and therefore also the basis functions will be defined and computed on one standardised reference element and then transformed to each element.

Definition 21 (Transformation to reference element)**.** *For the reference element* $\hat{T}$ *and another element* T*, let the transformation be such that*

- $T = F^T(\hat{T})$
- $u = \hat{u} \circ (F^T)^{-1}$ *for* $u \in V^T$*,* $\hat{u} \in V^{\hat{T}}$*,*
- $\psi^T(u) = \psi^{\hat{T}}(u \circ F^T)$*,*
- F^T *is affine linear.*

If such an F^T *exists, then the two elements* (T, V^T, Ψ^T) *and* $(\hat{T}, V^{\hat{T}}, \Psi^{\hat{T}})$ *are called affine equivalent.*

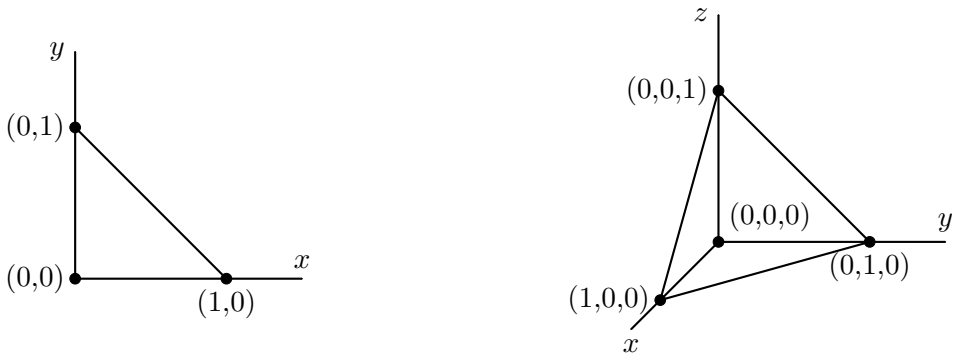

Figure 3.1: The reference triangle on the left and the reference tetrahedron on the right.

In the following, several types of finite elements for different function spaces (so far denoted as V^T) will be defined. Aside from the function spaces, they also differ in how the functionals/degrees of freedom are defined, and how continuity conditions on element boundaries are formulated.

The following definitions are still to be understood locally on one (reference) element, indicated by the symbol T.

3.3.1 $H^1(\Omega)$-conforming finite elements

The lowest order element for $H^1(\Omega)$-functions is defined on the local finite element space P^1. In 2D and 3D this space is respectively:

$$P^1(T) := \text{span}\left\{x^i y^j : i + j \leq 1, \text{ and } (x, y) \in T \subset \mathbb{R}^2\right\}, \tag{3.40}$$

$$P^1(T) := \text{span}\left\{x^i y^j z^k : i + j + k \leq 1, \text{ and } (x, y, z) \in T \subset \mathbb{R}^3\right\}. \tag{3.41}$$

In the above definitions, i, j are exponents, and not indices. It holds that

$$P^1(T) \subseteq H^1(T). \tag{3.42}$$

For so called Lagrangian finite elements, the functionals on P^1 are defined as point evaluations on the nodes of the element T:

$$\psi_i^T(u) := u|_{N_i} \tag{3.43}$$

with N_i denoting the i^{th} node of element T. Now, a local basis of $P^1(T)$ can be constructed.

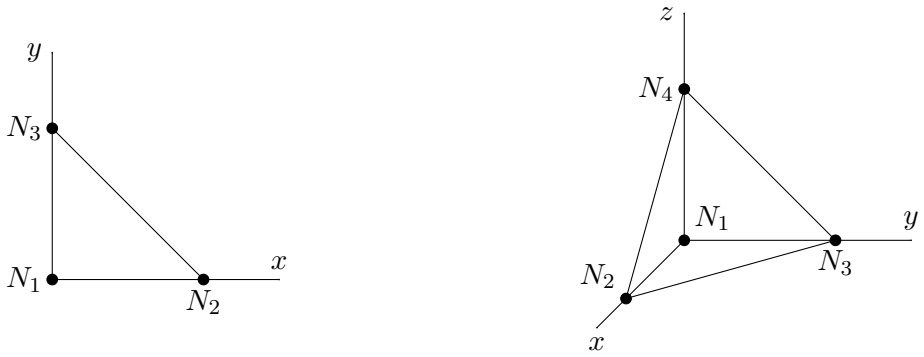

Figure 3.2: Node numbering of reference elements.

Lemma 22 (Lagrange basis functions on the reference triangle)**.** *Let T be the reference triangle. Then, the Lagrange basis functions on $P^1(T)$ are*

$$\gamma_1 : (x, y, z) \mapsto 1 - x - y, \tag{3.44}$$
$$\gamma_2 : (x, y, z) \mapsto x, \tag{3.45}$$
$$\gamma_3 : (x, y, z) \mapsto y, \tag{3.46}$$

Proof. A numbering of the nodes as in figure 3.2 above is being used.
Note that $\gamma_i \in P^1(T) \implies \gamma_i = a_i + b_i x + c_i y$ with $a_i, b_i, c_i \in \mathbb{R}$. Using condition (3.38), one can write down equations to find the basis functions.

$$\begin{aligned}
\psi_1^T(\gamma_1) = \gamma_1(0,0) = a_1 &\overset{!}{=} 1, \\
\psi_2^T(\gamma_1) = \gamma_1(1,0) = a_1 + b_1 x &\overset{!}{=} 0, \\
\psi_3^T(\gamma_1) = \gamma_1(0,1) = a_1 + c_1 y &\overset{!}{=} 0.
\end{aligned}$$

which gives $a_1 = 1$, $b_1 = c_1 = -1$. Writing down the conditions for γ_2, γ_3 yields all basis functions. The space $P^1(T)$ has dimension 3, and the 3 basis functions are linearly independent. □

Lemma 23 (Lagrange basis functions on reference tetrahedron)**.** *Let T be the reference tetrahedron. Then, the basis functions are*

$$\gamma_1 : (x, y, z) \mapsto 1 - x - y - z, \tag{3.47}$$
$$\gamma_2 : (x, y, z) \mapsto x, \tag{3.48}$$
$$\gamma_3 : (x, y, z) \mapsto y, \tag{3.49}$$
$$\gamma_4 : (x, y, z) \mapsto z. \tag{3.50}$$

Proof. Using the node numbering from figure 3.2 and utilizing condition (3.38), gives the respective basis functions. The space $P^1(T)$ has dimension 4, and the 4 basis functions are linearly independent. □

So far, we have only talked about objects that are defined locally on one element. For $H^1(\Omega)$ functions (on the whole domain Ω), the conforming function space is introduced in the following.

Definition 24 (Globally $H^1(\Omega)$-conforming space)**.**

$$X^{P1}(\Omega) := \{u \in H^1(\Omega) : u|_T \in P^1(T) \quad \forall T \in \mathcal{T}\}$$

In theorem 6 we have mentioned that the continuity condition for $H^1(\Omega)$ functions on subdomains is the fact that the traces on common interfaces coincide. For elements T_1, T_2 with $T_1 \cap T_2 =: \gamma \neq 0$, this means that

$$\mathrm{tr}^\gamma\, u|_{T_1} = \mathrm{tr}^\gamma\, u|_{T_2}.$$

The global interpolation operator for $H^1(\Omega)$ functions is such that its restriction to an element coincides with the local interpolation operator (introduced in (3.39)). This means

$$(I^{P1}u)|_T = I^T(u|_T) \quad \forall T \in \mathcal{T}.$$

3.3.2 $H(\mathrm{curl}, \Omega)$-conforming finite elements

The lowest order $H(\mathrm{curl}, \Omega)$-conforming finite element is called Nédélec-element. The respective local finite element space is given as

$$ND(T) := \mathrm{span}\left\{\lambda_i \nabla\lambda_j - \nabla\lambda_i \lambda_j : \lambda_i(N_j) = \delta_{ij} \text{ for } \lambda_i \in P^1(T)\right\}, \tag{3.51}$$

which is a 3- or 6-dimensional space that includes all constant, and a subset of all affine-linear functions. It holds that

$$ND(T) \subseteq H(\mathrm{curl}, T). \tag{3.52}$$

The degrees of freedom on each element are the functionals on the finite element space, which are defined as the line integral of a function over the edges E_i of the element:

$$\psi_i^T(\boldsymbol{u}) := \int_{E_i} \boldsymbol{u}. \tag{3.53}$$

The choice of the functional is the reason why this element is also categorized as an edge element. It is essential to realize, that the edges of the element are oriented! When enforcing tangential continuity at the intersections of two elements, the edge orientation of an element needs to be aligned properly relative to its neighbour. In order to project functions onto $ND(T)$, one needs to construct a basis.

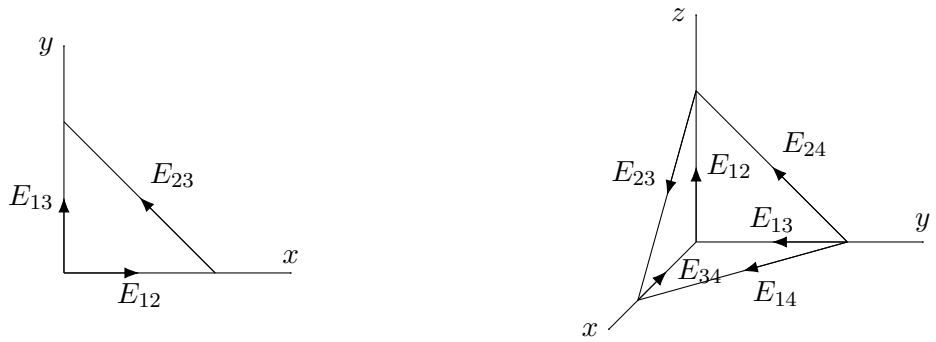

Figure 3.3: Edge/tangential vector numbering of reference elements

As mentioned in section 2.1.1, functions in $H(\mathrm{curl}, \Omega)$ fulfill tangential continuity. For a finite dimensional space to be conforming to $H(\mathrm{curl}, \Omega)$, this property is also required. The degrees of freedom on the edges E_i therefore have to be aligned with neighbour elements properly.

Lemma 25 (Nédélec basis functions for the reference triangle)**.** *For the reference triangle, the Nédélec basis functions are*

$$\boldsymbol{\tau}_{12} : (x, y) \mapsto \begin{pmatrix} 1 - y \\ x \end{pmatrix}, \quad \boldsymbol{\tau}_{13} : (x, y) \mapsto \begin{pmatrix} y \\ 1 - x \end{pmatrix}, \quad \boldsymbol{\tau}_{23} : (x, y) \mapsto \begin{pmatrix} -y \\ x \end{pmatrix}.$$

Proof. The hat functions/barycentric coordinates are mappings given as

$$\lambda_1 : (x, y) \mapsto 1 - x - y, \tag{3.54}$$
$$\lambda_2 : (x, y) \mapsto x, \tag{3.55}$$
$$\lambda_3 : (x, y) \mapsto y. \tag{3.56}$$

The nodes are numbered like for the Lagrange elements in figure 3.2. Using the definition of the space ND in (3.51) one can find the basis functions.

It is also straight-forward to show condition (3.38), i.e. $(\psi_i^T(\boldsymbol{\tau}_j) = \delta_{ij})$.
As an example, the basis function $\boldsymbol{\tau}_{12}$ is considered. The evaluation of the associated functional with $\boldsymbol{\tau}_{12}$ yields

$$\begin{aligned}
\psi_{12}^T(\boldsymbol{\tau}_{12}) &= \int_{E_{12}} \boldsymbol{\tau}_{12} \mathrm{d}\boldsymbol{s} \\
&= \frac{1}{2} \left(\boldsymbol{\tau}_{12}(E_2) + \boldsymbol{\tau}_{12}(E_1)\right) \cdot \boldsymbol{t}_{12} \\
&= \frac{1}{2} \left(\boldsymbol{\tau}_{12}(1,0) + \boldsymbol{\tau}_{12}(0,0)\right) \cdot (1,0)^\intercal \\
&= \frac{1}{2} \left[\begin{pmatrix} 1 \\ 1 \end{pmatrix} + \begin{pmatrix} 1 \\ 0 \end{pmatrix} \right] \cdot \begin{pmatrix} 1 \\ 0 \end{pmatrix} \\
&= 1.
\end{aligned}$$

Any other functional, such as for example functional ψ_{13}^T yields

$$\begin{aligned}
\psi_{13}^T(\boldsymbol{\tau}_{12}) &= \int_{E_{13}} \boldsymbol{\tau}_{12} \mathrm{d}\boldsymbol{s} \\
&= \frac{1}{2} \left(\boldsymbol{\tau}_{12}(E_3) + \boldsymbol{\tau}_{12}(E_1)\right) \cdot \boldsymbol{t}_{13} \\
&= \frac{1}{2} \left(\boldsymbol{\tau}_{12}(0,1) + \boldsymbol{\tau}_{12}(0,0)\right) \cdot (0,1)^\intercal \\
&= \frac{1}{2} \left[\begin{pmatrix} 0 \\ 0 \end{pmatrix} + \begin{pmatrix} 1 \\ 0 \end{pmatrix} \right] \cdot \begin{pmatrix} 0 \\ 1 \end{pmatrix} \\
&= 0.
\end{aligned}$$

$ND(T)$ has dimension 3 and there are 3 linearly independent basis functions, which implies $ND(T) = \mathrm{span}\{\boldsymbol{\tau}_i\}$. □

Lemma 26 (Nédélec basis functions for the reference tetrahedron)**.** *The Nédélec basis functions of the reference tetrahedron T are*

$$\boldsymbol{\tau}_{12} : (x,y,z) \mapsto \begin{pmatrix} 1-y-z \\ x \\ x \end{pmatrix}, \quad \boldsymbol{\tau}_{13} : (x,y,z) \mapsto \begin{pmatrix} y \\ 1-x-z \\ y \end{pmatrix}, \quad \boldsymbol{\tau}_{14} : (x,y,z) \mapsto \begin{pmatrix} z \\ z \\ 1-x-y \end{pmatrix}$$

$$\boldsymbol{\tau}_{23} : (x,y,z) \mapsto \begin{pmatrix} -y \\ x \\ 0 \end{pmatrix}, \quad \boldsymbol{\tau}_{24} : (x,y,z) \mapsto \begin{pmatrix} -z \\ 0 \\ x \end{pmatrix}, \quad \boldsymbol{\tau}_{34} : (x,y,z) \mapsto \begin{pmatrix} 0 \\ -z \\ y \end{pmatrix}.$$

Proof. The hat functions/barycentric coordinate functions on the reference tetrathedron are

$$\lambda_1 : (x,y,z) \mapsto 1-x-y-z, \tag{3.57}$$
$$\lambda_2 : (x,y,z) \mapsto x, \tag{3.58}$$
$$\lambda_3 : (x,y,z) \mapsto y, \tag{3.59}$$
$$\lambda_4 : (x,y,z) \mapsto z. \tag{3.60}$$

The nodes of the element are numbered like in figure 3.2. As in 2D, one uses the definition of the space $ND(T)$ in (3.51) to construct the $\boldsymbol{\tau}_i$.

The condition (3.38) is also fulfilled. The basis function $\boldsymbol{\tau}_{12}$ is being considered as an example. The evaluation of a functional with its associated basis function yields

$$\begin{aligned}
\psi_{12}^T(\boldsymbol{\tau}_{12}) &= \int_{E_{12}} \boldsymbol{\tau}_{12} \mathrm{d}\boldsymbol{s} \\
&= \frac{1}{2}\left(\boldsymbol{\tau}_{12}(E_2) + \boldsymbol{\tau}_{12}(E_1)\right) \cdot \boldsymbol{t}_{12} \\
&= \frac{1}{2}\left(\boldsymbol{\tau}_{12}(1,0,0) + \boldsymbol{\tau}_{12}(0,0,0)\right) \cdot (1,0,0)^\intercal \\
&= \frac{1}{2}\left[\begin{pmatrix}1\\1\\1\end{pmatrix} + \begin{pmatrix}1\\0\\0\end{pmatrix}\right] \cdot \begin{pmatrix}1\\0\\0\end{pmatrix} \\
&= 1.
\end{aligned}$$

The basis function evaluated by any other functional yields 0. As an example ψ_{13}^T is considered

$$\begin{aligned}
\psi_{13}^T(\boldsymbol{\tau}_{12}) &= \int_{E_{13}} \boldsymbol{\tau}_{12} \mathrm{d}\boldsymbol{s} \\
&= \frac{1}{2}\left(\boldsymbol{\tau}_{12}(E_3) + \boldsymbol{\tau}_{12}(E_1)\right) \cdot \boldsymbol{t}_{13} \\
&= \frac{1}{2}\left(\boldsymbol{\tau}_{12}(0,1,0) + \boldsymbol{\tau}_{12}(0,0,0)\right) \cdot (0,1,0)^\intercal \\
&= \frac{1}{2}\left[\begin{pmatrix}0\\0\\0\end{pmatrix} + \begin{pmatrix}1\\0\\0\end{pmatrix}\right] \cdot \begin{pmatrix}0\\1\\0\end{pmatrix} \\
&= 0.
\end{aligned}$$

Checking all combinations of ψ_i^T and $\boldsymbol{\tau}_j$ proves the statement. The space $ND(T)$ has dimension 6 and there are 6 linearly independent basis functions, implying $ND(T) = \mathrm{span}\{\boldsymbol{\tau}_i\}$. □

Similar as in the previous section, we can now introduce the global function space for the whole domain Ω.

Definition 27 (Globally $H(\mathrm{curl}, \Omega)$-conforming space)**.**

$$X^{ND}(\Omega) := \{u \in H(\mathrm{curl}, \Omega) : u|_T \in ND(T) \quad \forall T \in \mathcal{T}\}$$

In theorem 10 we have mentioned the continuity condition for $H(\mathrm{curl}, \Omega)$ functions on subdomains. Again, the traces on common interfaces have to coincide. For elements T_1, T_2 with $T_1 \cap T_2 =: \gamma \neq 0$, this means that

$$\mathrm{tr}_t^\gamma\, u|_{T_1} = \mathrm{tr}_t^\gamma\, u|_{T_2}.$$

The global interpolation operator for $H(\mathrm{curl}, \Omega)$ functions is such that its restriction to an element coincides with the local interpolation operator (introduced in (3.39)). This means

$$(I^{ND}u)|_T = I^T(u|_T) \quad \forall T \in \mathcal{T}.$$

3.3.3 $H(\mathrm{div}, \Omega)$-conforming finite elements

For the space $H(\mathrm{div}, \Omega)$, the cheapest (lowest order) finite element is the so called Raviart Thomas element of order 0 (RT^0). The order denotes the regularity, a term that describes the

number of continuous derivatives between elements. In this case, 0-regularity implies that the normal component of the function values is continuous on the element intersections, but not their derivatives.
The space $RT^0(T)$ is defined as the set of all constant functions plus some linear functions:

$$RT^0(T) := \left\{ \boldsymbol{a} + b\boldsymbol{x} : \boldsymbol{a} \in \mathbb{R}^d, b \in \mathbb{R} \right\}. \tag{3.61}$$

It holds that

$$RT^0(T) \subseteq H(\mathrm{div}, T). \tag{3.62}$$

In 2D the space is 3 dimensional and has therefore 3 functionals/degrees of freedom in its dual space. In 3D the space is 4 dimensional and has 4 functionals. They are defined as the integral over the normal trace along the element faces (faces and edges coincide in 2D):

$$\psi_i^T(\boldsymbol{u}) := \int_{F_i} \boldsymbol{u}.$$

Because of definition 18 the element is well defined and one can construct the basis of $RT^0(T)$.

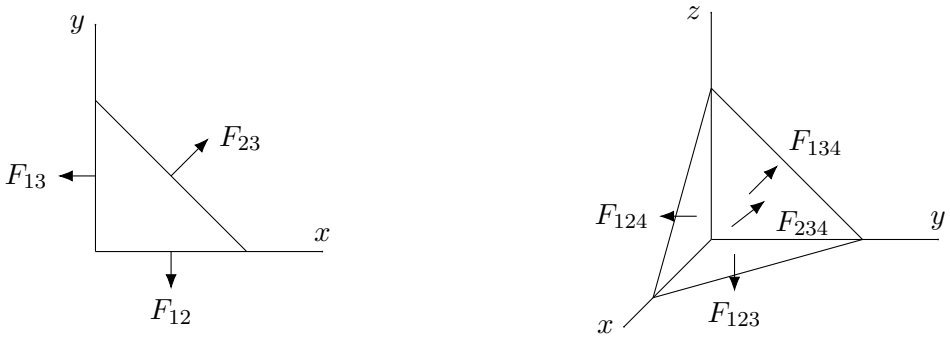

Figure 3.4: Face/normal vector numbering of reference elements.

As mentioned in section 2.1.2, functions in $H(\mathrm{div}, \Omega)$ fulfil normal continuity. For a finite dimensional space to be conforming to $H(\mathrm{div}, \Omega)$, this property is also required. The degrees of freedom on the faces F_i have therefore be aligned with neighbour elements properly.
Note that on the 2D reference triangle, faces and edges are the same geometrical objects.

Lemma 28 ($RT^0(T)$ basis functions for the reference triangle)**.** *The $RT^0(T)$ basis functions are given as*

$$\boldsymbol{\sigma}_1 : (x, y) \mapsto \begin{pmatrix} -x \\ 1 - y \end{pmatrix}, \quad \boldsymbol{\sigma}_2 : (x, y) \mapsto \begin{pmatrix} -x \\ -y \end{pmatrix}, \quad \boldsymbol{\sigma}_3 : (x, y) \mapsto \begin{pmatrix} x - 1 \\ y \end{pmatrix}. \tag{3.63}$$

Proof. One has $\psi_i^T(\boldsymbol{\sigma}_j) = \delta_{ij}$ (condition (3.38)) as well as $\boldsymbol{\sigma}_i = \begin{pmatrix} a_i \\ b_i \end{pmatrix} + c_i \begin{pmatrix} x \\ y \end{pmatrix}$ with $a_i, b_i, c_i \in \mathbb{R}$, which leads to

$$\psi_1^T(\boldsymbol{\sigma}_1) = \int_{F_{12}} \boldsymbol{\sigma}_1 \cdot \boldsymbol{n}_1 \mathrm{d}s = \int_0^1 \left[\begin{pmatrix} a_1 \\ b_1 \end{pmatrix} + c_1 \begin{pmatrix} t \\ 0 \end{pmatrix} \right] \cdot \begin{pmatrix} 0 \\ -1 \end{pmatrix} \mathrm{d}t \stackrel{!}{=} 1,$$

$$\psi_2^T(\boldsymbol{\sigma}_1) = \int_{F_{23}} \boldsymbol{\sigma}_1 \cdot \boldsymbol{n}_2 \mathrm{d}s = \int_0^1 \left[\begin{pmatrix} a_1 \\ b_1 \end{pmatrix} + c_1 \begin{pmatrix} t \\ 1-t \end{pmatrix} \right] \cdot \frac{1}{\sqrt{2}} \begin{pmatrix} 1 \\ 1 \end{pmatrix} \mathrm{d}t \stackrel{!}{=} 0,$$

$$\psi_3^T(\boldsymbol{\sigma}_1) = \int_{F_{13}} \boldsymbol{\sigma}_1 \cdot \boldsymbol{n}_3 \mathrm{d}s = \int_0^1 \left[\begin{pmatrix} a_1 \\ b_1 \end{pmatrix} + c_1 \begin{pmatrix} 0 \\ t \end{pmatrix} \right] \cdot \begin{pmatrix} -1 \\ 0 \end{pmatrix} \mathrm{d}t \stackrel{!}{=} 0.$$

The numbering of the faces (=edges in 2D) can be seen in figure 3.4.
The same 3 equations can be written down for $\boldsymbol{\sigma}_2$ and $\boldsymbol{\sigma}_3$. With these 9 equations, one finds the 9 unknown coefficients. This gives 3 linearly independent functions, which implies $\mathrm{span}(\boldsymbol{\sigma}_i) = RT^0(T)$. □

Lemma 29 ($RT^0(T)$ basis functions for the reference tetrahedron)**.** *The $RT^0(T)$ basis functions are given as*

$$\boldsymbol{\sigma}_1 : (x,y,z) \mapsto \begin{pmatrix} 2x \\ 2y \\ 2z \end{pmatrix}, \quad \boldsymbol{\sigma}_2 : (x,y,z) \mapsto \begin{pmatrix} 2-2x \\ -2y \\ -2z \end{pmatrix}, \tag{3.64}$$

$$\boldsymbol{\sigma}_3 : (x,y,z) \mapsto \begin{pmatrix} 2x \\ 2y-2 \\ 2z \end{pmatrix}, \quad \boldsymbol{\sigma}_4 : (x,y,z) \mapsto \begin{pmatrix} -2x \\ -2y \\ 2-2z \end{pmatrix}. \tag{3.65}$$

Proof. From condition (3.38) as well as $\boldsymbol{\sigma}_i = \begin{pmatrix} a_i \\ b_i \\ c_i \end{pmatrix} + d_i \begin{pmatrix} x \\ y \\ z \end{pmatrix}$, one gets

$$\psi_1^T(\boldsymbol{\sigma}_1) = \int_{F_{123}} \boldsymbol{\sigma}_1 \cdot \boldsymbol{n}_1 \mathrm{d}A = \int_0^1 \int_0^{s-1} \left[\begin{pmatrix} a_1 \\ b_1 \\ c_1 \end{pmatrix} + d_1 \begin{pmatrix} t \\ s \\ 0 \end{pmatrix} \right] \cdot \begin{pmatrix} 0 \\ 0 \\ -1 \end{pmatrix} \mathrm{d}t\mathrm{d}s \stackrel{!}{=} 1$$

$$\psi_2^T(\boldsymbol{\sigma}_1) = \int_{F_{124}} \boldsymbol{\sigma}_1 \cdot \boldsymbol{n}_2 \mathrm{d}A = \int_0^1 \int_0^{s-1} \left[\begin{pmatrix} a_2 \\ b_2 \\ c_2 \end{pmatrix} + d_2 \begin{pmatrix} t \\ 0 \\ s \end{pmatrix} \right] \cdot \begin{pmatrix} 0 \\ -1 \\ 0 \end{pmatrix} \mathrm{d}t\mathrm{d}s \stackrel{!}{=} 0$$

etc.

For each $\boldsymbol{\sigma}_i$ one has 4 equations for 4 unknown coefficients, which provides the 4 linearly independent functions, which implies $\mathrm{span}(\boldsymbol{\sigma}_i) = RT^0(T)$. □

Similar as in the previous section, we can now introduce the global function space for the whole domain Ω.

Definition 30 (Globally $H(\mathrm{div},\Omega)$-conforming space)**.**

$$X^{RT0}(\Omega) := \{u \in H(\mathrm{div},\Omega) : u|_T \in RT^0(T) \quad \forall T \in \mathcal{T}\}$$

In theorem 14 we have mentioned the continuity condition for $H(\mathrm{div},\Omega)$ functions on subdomains. Again, the traces on common interfaces have to coincide. For elements T_1, T_2 with $T_1 \cap T_2 =: \gamma \neq 0$, this means that

$$\mathrm{tr}_n^\gamma\, u|_{T_1} = \mathrm{tr}_n^\gamma\, u|_{T_2}.$$

The global interpolation operator for $H(\mathrm{div},\Omega)$ functions is such that its restriction to an element coincides with the local interpolation operator (introduced in (3.39)). This means

$$(I^{RT0}u)|_T = I^T(u|_T) \quad \forall T \in \mathcal{T}.$$

3.3.4 $L^2(\Omega)$-conforming finite elements

In the space $L^2(\Omega)$, piecewise-constant finite elements are used. The local finite element space P^0 is the space of all constant polynomials.
It holds that

$$P^0(T) \subset L^2(T). \tag{3.66}$$

The functionals on $P^0(T)$ are

$$\psi_i^T(u) := u(\boldsymbol{r}_c), \tag{3.67}$$

where $\boldsymbol{r}_c$ denotes the center of mass of T. On the 2D reference triangle $\boldsymbol{r}_c = \left(\frac{1}{3},\frac{1}{3}\right)$, on the 3D reference tetrahedron $\boldsymbol{r}_c = \left(\frac{1}{4},\frac{1}{4},\frac{1}{4}\right)$.
As the functionals on this space are point evaluations, they are again called Lagrange-elements.

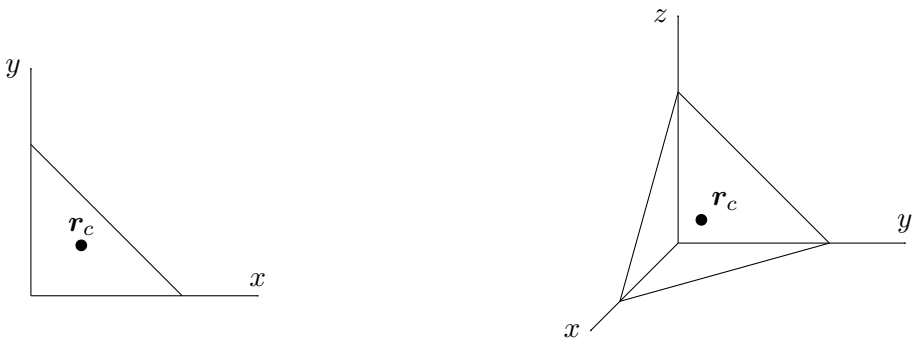

Figure 3.5: Sketch of degrees of freedom.

The basis functions χ_i in this space are constant functions. In $L^2(\Omega)$ there is no continuity requirement on the element boundaries.

Definition 31 (Global $L^2(\Omega)$-conforming space)**.** *We denote the global function space as $X^{P0}(\Omega)$ and the corresponding global interpolation operator as I^{P0}.*

3.4 Assembly of the global system

Based on the discussion in the previous sections, the weak formulation (2.16) to (2.21) can now be projected/interpolated into the global finite dimensional functions spaces setting.
The unknown functions $\boldsymbol{u}, \boldsymbol{\zeta}, \boldsymbol{v}, \boldsymbol{\omega}, p$ and q are represented in these spaces by the means of the global interpolation operators I^{P1}, I^{ND}, I^{RT0}, and I^{P0}.
These operators interpolate the functions using the basis functions γ, $\boldsymbol{\tau}$, $\boldsymbol{\sigma}$, and χ introduced in the last sections. However, these basis functions were defined locally on one element and we

need global basis functions. By identifying (i.e. removing "duplicate") functionals that coincide on element interfaces and requiring (3.38) globally, for example

$$\psi_i^{ND}(\boldsymbol{\tau}_j) = \delta_{ij}$$

one obtains global functionals, and a global function basis. We use the same symbol for a global basis function that we have used for the local ones, i.e.

$$\gamma \in X^{P1}(\Omega), \quad \boldsymbol{\tau} \in X^{ND}(\Omega), \quad \boldsymbol{\sigma} \in X^{RT}(\Omega), \quad \chi \in X^{P0}(\Omega).$$

However, the index now runs over all global functionals/degrees of freedom. We denote the number of global functionals of the function space X^Y with N_Y.
As an example consider

$$I^{ND}\boldsymbol{u} = \sum_{i=1}^{N_{ND}} \psi_i^{ND}(\boldsymbol{u})\boldsymbol{\tau}_i = \sum_{i=1}^{N_{ND}} \boldsymbol{\tau}_i \underbrace{\int_E \boldsymbol{u}}_{=:u_i} = \sum_{i=1}^{N_{ND}} u_i \boldsymbol{\tau}_i \in X^{ND}(\Omega), \tag{3.68}$$

with ψ_i^{ND} being the global functionals on X^{ND}. Similarly for the other trial functions, there holds:

$$I^{RT0}\boldsymbol{\zeta} = \sum_{i=1}^{N_{RT}} \zeta_i \boldsymbol{\sigma}_i \in X^{RT0}(\Omega), \tag{3.69}$$

$$I^{P1}p = \sum_{i=1}^{N_{P1}} p_i \gamma_i \in X^{P1}(\Omega), \tag{3.70}$$

$$I^{RT0}\boldsymbol{v} = \sum_{i=1}^{N_{RT}} v_i \boldsymbol{\sigma}_i \in X^{RT0}(\Omega), \tag{3.71}$$

$$I^{ND}\boldsymbol{\omega} = \sum_{i=1}^{N_{ND}} \omega_i \boldsymbol{\tau}_i \in X^{ND}(\Omega), \tag{3.72}$$

$$I^{P0}q = \sum_{i=1}^{N_{P0}} p_i \chi_i \in X^{P0}(\Omega). \tag{3.73}$$

Instead of testing with the infinite-dimensional test functions from the continuous setting $\tilde{\boldsymbol{u}}, \tilde{\boldsymbol{\zeta}}, \tilde{\boldsymbol{v}}, \tilde{\boldsymbol{\omega}}, \tilde{p}$ and $\tilde{q}$, the Galerkin method suggests to use the basis functions of the respective discrete function spaces $X^{P1}(\Omega), X^{ND}(\Omega), X^{RT}(\Omega)$, and $X^{P0}(\Omega)$. The expansions (3.69) - (3.73) can be plugged into the continuous variational formulation (2.16) to (2.21). Again, taking $\boldsymbol{u}$ as an example, consider equation (2.16):

$$\left\langle \frac{\partial}{\partial t} \sum_{i=1}^{N} u_i \boldsymbol{\tau}_i, \boldsymbol{\tau}_j \right\rangle + \left\langle \boldsymbol{\omega} \times \left(\sum_{i=1}^{N} u_i \boldsymbol{\tau}_i \right), \boldsymbol{\tau}_j \right\rangle + \frac{1}{\mathrm{Re}} \left\langle \sum_{i=1}^{N} \zeta_i \boldsymbol{\sigma}_i, \nabla \times \boldsymbol{\tau}_j \right\rangle$$
$$+ \left\langle \nabla \left(\sum_{i=1}^{N} p_i \gamma_i \right), \boldsymbol{\tau}_j \right\rangle = \langle \boldsymbol{f}_i, \boldsymbol{\tau}_j \rangle \qquad \forall \boldsymbol{\tau}_j \in X^{ND}(\Omega). \tag{3.74}$$

Remarks:

- The time discretization introduced in (3.2)-(3.7) has not been applied, to make the equations simpler and to demonstrate the spatial discretization.
- The coefficients u_i, ζ_i, p_i (and q_i) are the unknowns, and therefore defined at the "new" timestep. They are real numbers.

- The basis functions $\boldsymbol{\tau_i}, \boldsymbol{\sigma_i}, \gamma_i$ (and χ_i for $X^{P0}(\Omega)$) do not change in time.
- The function $\boldsymbol{\omega}$ is borrowed from the second momentum equation, and is therefore from the last time step. It is a known function in $X^{ND}(\Omega)$.

As a last step, the unknown coefficients u_i, ζ_i, p_i can be factored out from the bilinearforms. Together with the time discretization (3.5) the momentum equation becomes:

$$\frac{1}{\Delta t}\left\langle \sum_{i=1}^{N_{ND}} \boldsymbol{\tau}_i, \boldsymbol{\tau}_j \right\rangle \left(u_i^{k+\frac{1}{2}} - u_i^{k-\frac{1}{2}} \right) + \frac{1}{2}\left\langle \boldsymbol{\omega}^k \times \left(\sum_{i=1}^{N_{ND}} \boldsymbol{\tau}_i \right), \boldsymbol{\tau}_j \right\rangle \left(u_i^{k+\frac{1}{2}} + u_i^{k-\frac{1}{2}} \right)$$
$$+ \frac{1}{2\mathrm{Re}}\left\langle \sum_{i=1}^{N_{RT}} \boldsymbol{\sigma}_i, \nabla \times \boldsymbol{\tau}_j \right\rangle \left(\boldsymbol{\zeta}_i^{k+\frac{1}{2}} + \boldsymbol{\zeta}_i^{k-\frac{1}{2}} \right) - \left\langle \sum_{i=1}^{N_{P1}} \nabla\gamma_i, \boldsymbol{\tau_j} \right\rangle p_i^k = \left\langle \boldsymbol{f}^k, \boldsymbol{\tau}_j \right\rangle \quad \forall \boldsymbol{\tau}_j \in X^{ND}(\Omega).$$

The old time steps can be moved to the right, and the whole equation can be written in matrix-vector products.

3.4.1 Fully discrete system

In the following, the symbol $\vec{u}$ denotes vectors in linear algebra formulation of the assembled system of equations. There, each component u_i is the expansion coefficient of the discrete variable from (3.68). The matrices induced by the inner products are given as

$$\begin{aligned}
\mathrm{M}_{ij} &= \langle \boldsymbol{\tau}_j, \boldsymbol{\tau}_i \rangle \\
\mathrm{N}_{ij} &= \langle \boldsymbol{\sigma}_j, \boldsymbol{\sigma}_i \rangle \\
\mathrm{C}_{ij} &= \langle \nabla \times \boldsymbol{\tau}_j, \boldsymbol{\sigma}_i \rangle \\
\mathrm{D}_{ij} &= \langle \nabla \cdot \boldsymbol{\sigma}_j, \chi_i \rangle \\
\mathrm{G}_{ij} &= \langle \nabla\gamma_j, \boldsymbol{\tau}_i \rangle \\
\mathrm{R}_{ij}^{k-\frac{1}{2}} &= \left\langle \boldsymbol{\zeta}^{k-\frac{1}{2}} \times \boldsymbol{\sigma}_j, \boldsymbol{\sigma}_i \right\rangle \\
\mathrm{R}_{ij}^{k} &= \left\langle \boldsymbol{\omega}^{k} \times \boldsymbol{\tau}_j, \boldsymbol{\tau}_i \right\rangle \\
\mathbf{f}_i^{k-\frac{1}{2}} &= \left\langle \boldsymbol{f}^{k-\frac{1}{2}}, \boldsymbol{\sigma}_i \right\rangle \\
\mathbf{f}_i^{k} &= \left\langle \boldsymbol{f}^{k}, \boldsymbol{\tau}_i \right\rangle
\end{aligned}$$

Notice the index ordering: each matrix is defined in a "transposed" way. This way, the matrix-vector product formulation works out. This procedure leads to two fully discrete, linear systems. The problem becomes:

given $\left(\vec{\omega}^{k-1}, \vec{v}^{k-1}, \mathbf{f}^{k-\frac{1}{2}}, \vec{\zeta}^{k-\frac{1}{2}}\right) \in X^{ND}(\Omega) \times X^{RT}(\Omega) \times X^{P0}(\Omega) \times X^{RT}(\Omega)$
seek $\left(\vec{\omega}^{k}, \vec{v}^{k}, \vec{q}^{k-\frac{1}{2}}\right) \in X^{ND}(\Omega) \times X^{RT}(\Omega) \times X^{P0}(\Omega)$
such that they satisfy

$$\begin{cases}
\mathrm{N}\dfrac{\vec{v}^k - \vec{v}^{k-1}}{\Delta t} + \mathrm{R}^{k-\frac{1}{2}}\dfrac{\vec{v}^k + \vec{v}^{k-1}}{2} + \dfrac{1}{\mathrm{Re}}\mathrm{C}\dfrac{\vec{\omega}^k + \vec{\omega}^{k-1}}{2} - \mathrm{D}^\intercal \vec{p}^{k-\frac{1}{2}} = \mathbf{f}^{k-\frac{1}{2}} \\
\mathrm{C}^\intercal \vec{v}^k - \mathrm{M}\vec{\omega}^k = \mathbf{0} \\
\mathrm{D}\vec{v}^k = \mathbf{0}
\end{cases}$$

and further, given $\left(\vec{u}^{k-\frac{1}{2}}, \vec{\zeta}^{k-\frac{1}{2}}, \mathbf{f}^k, \vec{\omega}^k\right) \in X^{ND}(\Omega) \times X^{RT}(\Omega) \times X^{P0}(\Omega) \times X^{ND}(\Omega)$

seek $\left(p^k, \vec{u}^{k+\frac{1}{2}}, \vec{\zeta}^{k+\frac{1}{2}}\right) \in X^{P1}(\Omega) \times X^{ND}(\Omega) \times X^{RT}(\Omega)$
such that they satisfy

$$\begin{cases} \mathrm{M}\dfrac{\vec{u}^{k+\frac{1}{2}} - \vec{u}^{k-\frac{1}{2}}}{\Delta t} + \mathrm{R}^k \dfrac{\vec{u}^{k+\frac{1}{2}} + \vec{u}^{k-\frac{1}{2}}}{2} + \dfrac{1}{\mathrm{Re}}\mathrm{C}^\intercal \dfrac{\vec{\zeta}^{k+\frac{1}{2}} + \vec{\zeta}^{k-\frac{1}{2}}}{2} + \mathrm{G}\vec{p}^k = \mathbf{f}^k \\ \mathrm{C}_1^{k+\frac{1}{2}} - \mathrm{N}\vec{\zeta}^{k+\frac{1}{2}} = \mathbf{0} \\ \mathrm{G}^\intercal \vec{u}^{k+\frac{1}{2}} = \mathbf{0} \end{cases}$$

The matrices and vectors from above can be written in two large blockmatrix systems:

$$\begin{bmatrix} \frac{1}{\Delta t}\,\mathrm{N} + \frac{1}{2}\mathrm{R}^{k-\frac{1}{2}} & \frac{1}{2\mathrm{Re}}\mathrm{C} & -\mathrm{D}^\intercal \\ \mathrm{C}^\intercal & -\mathrm{M} & \mathbf{0} \\ \mathrm{D} & \mathbf{0} & \mathbf{0} \end{bmatrix} \begin{bmatrix} \vec{v}^k \\ \vec{\omega}^k \\ \vec{q}^{k-\frac{1}{2}} \end{bmatrix} = \begin{bmatrix} \left(\frac{1}{\Delta t}\,\mathrm{N} - \frac{1}{2}\mathrm{R}^{k-\frac{1}{2}}\right)\vec{v}^{k-1} - \frac{1}{2\mathrm{Re}}\mathrm{C}\vec{\omega}^{k-1} + \mathbf{f}^{k-\frac{1}{2}} \\ \mathbf{0} \\ \mathbf{0} \end{bmatrix}$$

$$\begin{bmatrix} \frac{1}{\Delta t}\mathrm{M} + \frac{1}{2}\mathrm{R}^k & \frac{1}{2\mathrm{Re}}\mathrm{C}^\intercal & \mathrm{G} \\ \mathrm{C} & -\mathrm{N} & \mathbf{0} \\ \mathrm{G}^\intercal & \mathbf{0} & \mathbf{0} \end{bmatrix} \begin{bmatrix} \vec{u}^{k+\frac{1}{2}} \\ \vec{\zeta}^{k+\frac{1}{2}} \\ \vec{p}^k \end{bmatrix} = \begin{bmatrix} \left(\frac{1}{\Delta t}\mathrm{M} - \frac{1}{2}\mathrm{R}^k\right)\vec{u}^{k-\frac{1}{2}} - \frac{1}{2\mathrm{Re}}\mathrm{C}^\intercal\vec{\zeta}^{k-\frac{1}{2}} + \mathbf{f}^k \\ \mathbf{0} \\ \mathbf{0} \end{bmatrix}.$$

Interpretation:

- The fact, that the coupling of the two fields by the two vorticities $\boldsymbol{\omega}$ and $\boldsymbol{\zeta}$ is removed, leads to a much faster computation time. In each time step only one of the two systems is solved.
- Aside from linearizing the convective terms, another benefit of the dual representation of each unknown is that the difference between the two solutions can be used as an error indicator.
- In the continuous setting, the nonlinear convective terms where not well-defined, see section 2.2.1. The discrete representation of these convective terms, R^k, and $\mathrm{R}^{k+\frac{1}{2}}$, are now well-defined. This is because in the discrete setting, the functions $\boldsymbol{\omega}, \boldsymbol{\zeta}, \boldsymbol{\sigma}$, and $\boldsymbol{\tau}$ are interpolations of the respective continuous functions.

3.4.2 Euler step in the discrete setting

As mentioned in section 3.1.1, the first time step of the primal variables has to be done by using an explicit integration scheme, such as the Euler method. The proposed Euler step from before can also be converted into the fully discrete linear algebra language.

$$\begin{bmatrix} \frac{2}{\Delta t}\mathrm{M} + \mathrm{R}^0 & \frac{1}{\mathrm{Re}}\mathrm{C}^\intercal & \mathrm{G} \\ \mathrm{C} & -\mathrm{N} & \mathbf{0} \\ \mathrm{G}^\intercal & \mathbf{0} & \mathbf{0} \end{bmatrix} \begin{bmatrix} \vec{u}^{\frac{1}{2}} \\ \vec{\zeta}^{\frac{1}{2}} \\ \vec{p}^0 \end{bmatrix} = \begin{bmatrix} \frac{2}{\Delta t}\mathrm{M}\vec{u}^0 + \mathbf{f}^0 \\ \mathbf{0} \\ \mathbf{0} \end{bmatrix}$$

The submatrices are the same as defined before.

3.5 Conservation in the fully discrete setting

3.5.1 Discrete de Rham complex

Equation 2.22, the de Rham complex, is essential for the following conservation proofs. To construct structure-preserving discretizations, these properties have to be transported into the discrete setting. The sections 3.3.1 - 3.3.4 have introduced spaces that fulfil a discrete de Rham complex. It holds that

$$\begin{array}{ccccccc} H^1(\Omega) & \xrightarrow{\nabla} & H(\mathrm{curl},\Omega) & \xrightarrow{\mathrm{curl}} & H(\mathrm{div},\Omega) & \xrightarrow{\mathrm{div}} & L^2(\Omega) \\ \downarrow{\scriptstyle I^{P1}} & & \downarrow{\scriptstyle I^{ND}} & & \downarrow{\scriptstyle I^{RT0}} & & \downarrow{\scriptstyle I^{P0}} \\ X^{P1}(\Omega) & \xrightarrow{\nabla} & X^{ND}(\Omega) & \xrightarrow{\mathrm{curl}} & X^{RT0}(\Omega) & \xrightarrow{\mathrm{div}} & X^{P0}(\Omega) \end{array} \tag{3.75}$$

The diagram commutes. Again, e.g.:

$$\mathrm{range}(\nabla) = \ker(\mathrm{curl}),$$

which now also works for the "lower" line of the de Rham complex that contains the discrete spaces.

3.5.2 Transfer of conservation properties

As also discussed in [YR22], the choice of the finite-dimensional subspaces (Finite Element spaces) which form a discrete de Rham sequence, allows the transfer of the conservation properties into the fully discrete setting.
Based on the continuity requirements of the trace operators introduced in the beginning of chapter 2 (theorems 6, 10, and 14), the conditions for element interfaces in the global finite dimensional spaces were discussed (see sections 3.3.1 to 3.3.3). Therefore, the basis functions used to interpolate the trial functions have a certain type of continuity on these interfaces. As the lower line of the de Rham complex (the "discrete de Rham complex") in (3.75) also holds, all proofs carried out in section 3.2 can be carried out equally in the finite dimensional function spaces, and therefore in the fully discrete setting.

3.6 The semi-discrete Dirichlet problem

Similar as in section 3.1, a temporal semi-discretization is derived from (2.43) to (2.48). The ordering of equations is now flipped to represent the ordering in which the unknowns are being computed.

Given $\left(\boldsymbol{\omega}^{k-1}, \boldsymbol{v}^{k-1}, \boldsymbol{f}^{k-\frac{1}{2}}, \boldsymbol{\zeta}^{k-\frac{1}{2}}\right) \in H_0(\mathrm{curl},\Omega) \times H_0(\mathrm{div},\Omega) \times \left[L^2(\Omega)\right]^d \times H(\mathrm{div},\Omega)$
seek $\left(\boldsymbol{\omega}^{k}, \boldsymbol{v}^{k}, q^{k-\frac{1}{2}}\right) \in H_0(\mathrm{curl},\Omega) \times H_0(\mathrm{div},\Omega) \times L^2(\Omega)$
such that they satisfy

$$\left\langle \frac{\boldsymbol{v}^k - \boldsymbol{v}^{k-1}}{\Delta t}, \tilde{\boldsymbol{v}} \right\rangle + \left\langle \boldsymbol{\zeta}^{k-\frac{1}{2}} \times \frac{\boldsymbol{v}^k + \boldsymbol{v}^{k-1}}{2}, \tilde{\boldsymbol{v}} \right\rangle$$
$$\frac{1}{\mathrm{Re}} \left\langle \nabla \times \frac{\boldsymbol{\omega}^k + \boldsymbol{\omega}^{k-1}}{2}, \tilde{\boldsymbol{v}} \right\rangle - \left\langle q^{k-\frac{1}{2}}, \nabla \cdot \tilde{\boldsymbol{v}} \right\rangle = \left\langle \boldsymbol{f}^{k-\frac{1}{2}}, \tilde{\boldsymbol{v}} \right\rangle \quad \forall \tilde{\boldsymbol{v}} \in H_0(\mathrm{div},\Omega) \tag{3.76}$$

$$\left\langle \boldsymbol{v}^k, \nabla \times \tilde{\boldsymbol{\omega}} \right\rangle - \left\langle \boldsymbol{\omega}^k, \tilde{\boldsymbol{\omega}} \right\rangle = 0 \quad \forall \tilde{\boldsymbol{\omega}} \in H_0(\mathrm{curl},\Omega) \tag{3.77}$$

$$\left\langle \nabla \cdot \boldsymbol{v}^k, \tilde{q} \right\rangle = 0 \quad \forall \tilde{q} \in L^2(\Omega) \tag{3.78}$$

And for the second system (equations (2.43) to (2.45)) we get the following problem:

given $\left(\boldsymbol{u}^{k-\frac{1}{2}}, \boldsymbol{\zeta}^{k-\frac{1}{2}}, \boldsymbol{f}^k, \boldsymbol{\omega}^k\right) \in H(\mathrm{curl}, \Omega) \times H(\mathrm{div}, \Omega) \times \left[L^2(\Omega)\right]^d \times H(\mathrm{curl}, \Omega)$

seek $\left(p^k, \boldsymbol{u}^{k+\frac{1}{2}}, \boldsymbol{\zeta}^{k+\frac{1}{2}}\right) \in H^1(\Omega) \times H(\mathrm{curl}, \Omega) \times H(\mathrm{div}, \Omega)$
such that

$$\begin{aligned}
&\left\langle \frac{\boldsymbol{u}^{k+\frac{1}{2}} - \boldsymbol{u}^{k-\frac{1}{2}}}{\Delta t}, \tilde{\boldsymbol{u}} \right\rangle \\
&+ \left\langle \boldsymbol{\omega}^k \times \frac{\boldsymbol{u}^{k+\frac{1}{2}} + \boldsymbol{u}^{k-\frac{1}{2}}}{2}, \tilde{\boldsymbol{u}} \right\rangle \\
&+ \frac{1}{\mathrm{Re}} \left\langle \frac{\boldsymbol{\zeta}^{k+\frac{1}{2}} + \boldsymbol{\zeta}^{k-\frac{1}{2}}}{2}, \nabla \times \tilde{\boldsymbol{u}} \right\rangle - \left\langle \nabla p^k, \tilde{\boldsymbol{u}} \right\rangle = \left\langle \boldsymbol{f}^k, \tilde{\boldsymbol{u}} \right\rangle \\
&\qquad + \frac{1}{\mathrm{Re}} \left((\boldsymbol{\zeta}^k \times \boldsymbol{n}), \tilde{\boldsymbol{u}} \right)_{\partial\Omega} \qquad \forall \tilde{\boldsymbol{u}} \in H(\mathrm{curl}, \Omega) \qquad (3.79) \\
&\left\langle \nabla \times \boldsymbol{u}^{k+\frac{1}{2}}, \tilde{\boldsymbol{\zeta}} \right\rangle - \left\langle \boldsymbol{\zeta}^{k+\frac{1}{2}}, \tilde{\boldsymbol{\zeta}} \right\rangle = 0 \qquad \forall \tilde{\boldsymbol{\zeta}} \in H(\mathrm{div}, \Omega) \qquad (3.80) \\
&\left\langle \boldsymbol{u}^{k+\frac{1}{2}}, \nabla \tilde{p} \right\rangle = \left(\boldsymbol{u}^k \cdot \boldsymbol{n}, \tilde{p} \right)_{\partial\Omega} \qquad \forall \tilde{p} \in H^1(\Omega) \qquad (3.81)
\end{aligned}$$

Interpretation

- As before, these two sets of three equations each are being solved alternately.
- The value $\boldsymbol{\zeta}^{k-\frac{1}{2}}$ in equation (3.76) is computed in equations (3.79) to (3.81).
- The value $\boldsymbol{\omega}^k$ in equation (3.78) is computed in equations (3.76) to (3.78).
- In order to find $\boldsymbol{u}^{\frac{1}{2}}, \boldsymbol{\zeta}^{\frac{1}{2}}$, an explicit Euler method is applied to equation (2.43).
- The values $\boldsymbol{\zeta}^k$ and $\boldsymbol{u}^k$ are computed using boundary data.

3.7 Conservation properties

We continue with the discussion of the conservation properties of the temporally discretized Dirichlet scheme.

3.7.1 Mass

The conservation of the divergence-free property of $\boldsymbol{v} \in H(\mathrm{div}, \Omega)$ is still fulfilled pointwise (or strongly), due to condition (3.76). In contrast to that, the corresponding condition for $\boldsymbol{u} \in H(\mathrm{curl}, \Omega)$ is only satisfied weakly and only up to the boundary contribution from (3.81).

3.7.2 Energy

Again, $\boldsymbol{f} = 0$. Like derived in section 3.2 the goal is to show

$$\left\langle \frac{\boldsymbol{u}^{k+\frac{1}{2}} - \boldsymbol{u}^{k-\frac{1}{2}}}{\Delta t}, \frac{\boldsymbol{u}^{k+\frac{1}{2}} + \boldsymbol{u}^{k-\frac{1}{2}}}{2} \right\rangle = 0, \qquad (3.82)$$

$$\left\langle \frac{\boldsymbol{v}^k - \boldsymbol{v}^{k-1}}{\Delta t}, \frac{\boldsymbol{v}^k + \boldsymbol{v}^{k-1}}{2} \right\rangle = 0. \qquad (3.83)$$

For that, consider equation (3.79) and choose

$$\tilde{\boldsymbol{u}} := \frac{\boldsymbol{u}^{k+\frac{1}{2}} + \boldsymbol{u}^{k-\frac{1}{2}}}{2},$$

which results in a rather lengthy expression:

$$\begin{aligned}\left\langle \frac{\boldsymbol{u}^{k+\frac{1}{2}} - \boldsymbol{u}^{k-\frac{1}{2}}}{\Delta t}, \frac{\boldsymbol{u}^{k+\frac{1}{2}} + \boldsymbol{u}^{k-\frac{1}{2}}}{2} \right\rangle + \left\langle \boldsymbol{\omega}^k \times \frac{\boldsymbol{u}^{k+\frac{1}{2}} + \boldsymbol{u}^{k-\frac{1}{2}}}{2}, \frac{\boldsymbol{u}^{k+\frac{1}{2}} + \boldsymbol{u}^{k-\frac{1}{2}}}{2} \right\rangle \\ + \frac{1}{\mathrm{Re}} \left\langle \frac{\boldsymbol{\zeta}^{k+\frac{1}{2}} + \boldsymbol{\zeta}^{k-\frac{1}{2}}}{2}, \nabla \times \frac{\boldsymbol{u}^{k+\frac{1}{2}} + \boldsymbol{u}^{k-\frac{1}{2}}}{2} \right\rangle - \left\langle \nabla p^k, \frac{\boldsymbol{u}^{k+\frac{1}{2}} + \boldsymbol{u}^{k-\frac{1}{2}}}{2} \right\rangle \\ = \left\langle \boldsymbol{f}^k, \frac{\boldsymbol{u}^{k+\frac{1}{2}} + \boldsymbol{u}^{k-\frac{1}{2}}}{2} \right\rangle + \frac{1}{\mathrm{Re}} \left((\boldsymbol{\zeta}^k \times \boldsymbol{n}), \frac{\boldsymbol{u}^{k+\frac{1}{2}} + \boldsymbol{u}^{k-\frac{1}{2}}}{2} \right)_{\partial\Omega}.\end{aligned}$$

The second term vanishes due to orthogonality. The forth term is equal to:

$$\begin{aligned}\left\langle \nabla p^k, \frac{\boldsymbol{u}^{k+\frac{1}{2}} + \boldsymbol{u}^{k-\frac{1}{2}}}{2} \right\rangle &= \frac{1}{2} \left\langle \nabla p^k, \boldsymbol{u}^{k+\frac{1}{2}} \right\rangle + \frac{1}{2} \left\langle \nabla p^k, \boldsymbol{u}^{k-\frac{1}{2}} \right\rangle \\ &= \frac{1}{2} \left(\boldsymbol{u}^{k-\frac{1}{2}} \cdot \boldsymbol{n}, \tilde{p} \right)_{\partial\Omega} + \frac{1}{2} \left(\boldsymbol{u}^{k-\frac{3}{2}} \cdot \boldsymbol{n}, \tilde{p} \right)_{\partial\Omega},\end{aligned}$$

see (3.81). The fifth term is zero as $\boldsymbol{f} = 0$ and the last term remains. Therefore:

$$\begin{aligned}\left\langle \frac{\boldsymbol{u}^{k+\frac{1}{2}} - \boldsymbol{u}^{k-\frac{1}{2}}}{\Delta t}, \frac{\boldsymbol{u}^{k+\frac{1}{2}} + \boldsymbol{u}^{k-\frac{1}{2}}}{2} \right\rangle = -\frac{1}{\mathrm{Re}} \left\langle \frac{\boldsymbol{\zeta}^{k+\frac{1}{2}} + \boldsymbol{\zeta}^{k-\frac{1}{2}}}{2}, \nabla \times \frac{\boldsymbol{u}^{k+\frac{1}{2}} + \boldsymbol{u}^{k-\frac{1}{2}}}{2} \right\rangle \\ - \frac{1}{2} \left(\boldsymbol{u}^{k-\frac{1}{2}} \cdot \boldsymbol{n}, \tilde{p} \right)_{\partial\Omega} - \frac{1}{2} \left(\boldsymbol{u}^{k-\frac{3}{2}} \cdot \boldsymbol{n}, \tilde{p} \right)_{\partial\Omega} + \frac{1}{\mathrm{Re}} \left((\boldsymbol{\zeta}^k \times \boldsymbol{n}), \frac{\boldsymbol{u}^{k+\frac{1}{2}} + \boldsymbol{u}^{k-\frac{1}{2}}}{2} \right)_{\partial\Omega}. \quad (3.84)\end{aligned}$$

In case of zero-normal velocity $\boldsymbol{u}$ on the boundary and zero-tangential vorticity $\boldsymbol{\zeta}$ on the boundary, the dissipation rate is again proportional to the inverse of the Reynolds number and the enstrophy $\mathcal{E}$. Therefore, the energy is either conserved or dissipated, as $\mathcal{E} > 0$.
In case of the dual velocity $\boldsymbol{v}$, the result can be obtained similarly, except without the boundary integrals. One obtains

$$\left\langle \frac{\boldsymbol{v}^k - \boldsymbol{v}^{k-1}}{\Delta t}, \frac{\boldsymbol{v}^k + \boldsymbol{v}^{k-1}}{2} \right\rangle = -\frac{1}{\mathrm{Re}} \left\langle \nabla \times \frac{\boldsymbol{\omega}^k + \boldsymbol{\omega}^{k-1}}{2}, \frac{\boldsymbol{v}^k + \boldsymbol{v}^{k-1}}{2} \right\rangle. \quad (3.85)$$

When applying constraints (3.77) and (3.80), one sees that these dissipation rates is in fact proportional to $\mathcal{E}$, as defined in end of section 1.5.

3.7.3 Helicity

As discussed in section 2.5.3, in general helicity is not conserved.

3.8 The fully discrete Dirichlet problem

In addition to the matrices introduced at the beginning of section 3.4.1, two more terms have to be included in the discrete system: the boundary terms from equations (3.79), and (3.81). These new terms read as:

$$\begin{aligned}\mathbf{r}_i^k &= \frac{1}{\mathrm{Re}} \left(\boldsymbol{\zeta}^k \times \boldsymbol{n}, \boldsymbol{\tau}_i \right)_{\partial\Omega}, \\ \mathbf{g}_i^k &= \left(\boldsymbol{u}^k \cdot \boldsymbol{n}, \gamma_i \right)_{\partial\Omega}.\end{aligned}$$

As mentioned at the end of section 2.4, these terms get added to the right hand side and result in the following problem:

given $\left(\vec{\omega}^{k-1}, \vec{v}^{k-1}, \mathbf{f}^{k-\frac{1}{2}}, \vec{\zeta}^{k-\frac{1}{2}}\right) \in X^{ND}(\Omega) \times X^{RT}(\Omega) \times X^{P0}(\Omega) \times X^{RT}(\Omega)$
seek $\left(\vec{\omega}^{k}, \vec{v}^{k}, \vec{q}^{k-\frac{1}{2}}\right) \in X^{ND}(\Omega) \times X^{RT}(\Omega) \times X^{P0}(\Omega)$
such that they satisfy:

$$\begin{cases} \mathrm{N}\dfrac{\vec{v}^{k} - \vec{v}^{k-1}}{\Delta t} + \mathrm{R}^{k-\frac{1}{2}}\dfrac{\vec{v}^{k} + \vec{v}^{k-1}}{2} + \dfrac{1}{\mathrm{Re}}\mathrm{C}\dfrac{\vec{\omega}^{k} + \vec{\omega}^{k-1}}{2} - \mathrm{D}^{\intercal}\vec{p}^{k-\frac{1}{2}} = \mathbf{f}^{k-\frac{1}{2}} \\ \mathrm{C}^{\intercal}\vec{v}^{k} - \mathrm{M}\vec{\omega}^{k} = \mathbf{0} \\ \mathrm{D}\vec{v}^{k} = \mathbf{0} \end{cases}$$

and further, given $\left(\vec{u}^{k-\frac{1}{2}}, \vec{\zeta}^{k-\frac{1}{2}}, \mathbf{f}^{k}, \vec{\omega}^{k}, \mathbf{r}^{k}, \mathbf{g}^{k}\right) \in X^{ND}(\Omega) \times X^{RT}(\Omega) \times X^{P0}(\Omega) \times X^{ND}(\Omega) \times X^{P0}(\Omega) \times X^{P0}(\Omega)$
seek $\left(p^{k}, \vec{u}^{k+\frac{1}{2}}, \vec{\zeta}^{k+\frac{1}{2}}\right) \in X^{P1}(\Omega) \times X^{ND}(\Omega) \times X^{RT}(\Omega)$
such that they satisfy:

$$\begin{cases} \mathrm{M}\dfrac{\vec{u}^{k+\frac{1}{2}} - \vec{u}^{k-\frac{1}{2}}}{\Delta t} + \mathrm{R}^{k}\dfrac{\vec{u}^{k+\frac{1}{2}} + \vec{u}^{k-\frac{1}{2}}}{2} + \dfrac{1}{\mathrm{Re}}\mathrm{C}^{\intercal}\dfrac{\vec{\zeta}^{k+\frac{1}{2}} + \vec{\zeta}^{k-\frac{1}{2}}}{2} + \mathrm{G}\vec{p}^{k} = \mathbf{f}^{k} + \mathbf{r}^{k} \\ \mathrm{C}_{1}^{k+\frac{1}{2}} - \mathrm{N}\vec{\zeta}^{k+\frac{1}{2}} = \mathbf{0} \\ \mathrm{G}^{\intercal}\vec{u}^{k+\frac{1}{2}} = \mathbf{g}^{k} \end{cases}$$

As in the periodic case, we reformulate the above equations into a large matrix system:

$$\begin{bmatrix} \frac{1}{\Delta t}\,\mathrm{N} + \frac{1}{2}\mathrm{R}^{k-\frac{1}{2}} & \frac{1}{2\mathrm{Re}}\mathrm{C} & -\mathrm{D}^{\intercal} \\ \mathrm{C}^{\intercal} & -\mathrm{M} & \mathbf{0} \\ \mathrm{D} & \mathbf{0} & \mathbf{0} \end{bmatrix} \begin{bmatrix} \vec{v}^{k} \\ \vec{\omega}^{k} \\ \vec{q}^{k-\frac{1}{2}} \end{bmatrix} = \begin{bmatrix} \left(\frac{1}{\Delta t}\,\mathrm{N} - \frac{1}{2}\mathrm{R}^{k-\frac{1}{2}}\right)\vec{v}^{k-1} - \frac{1}{2\mathrm{Re}}\mathrm{C}\vec{\omega}^{k-1} + \mathbf{f}^{k-\frac{1}{2}} \\ \mathbf{0} \\ \mathbf{0} \end{bmatrix},$$

$$\begin{bmatrix} \frac{1}{\Delta t}\mathrm{M} + \frac{1}{2}\mathrm{R}^{k} & \frac{1}{2\mathrm{Re}}\mathrm{C}^{\intercal} & \mathrm{G} \\ \mathrm{C} & -\mathrm{N} & \mathbf{0} \\ \mathrm{G}^{\intercal} & \mathbf{0} & \mathbf{0} \end{bmatrix} \begin{bmatrix} \vec{u}^{k+\frac{1}{2}} \\ \vec{\zeta}^{k+\frac{1}{2}} \\ \vec{p}^{k} \end{bmatrix} = \begin{bmatrix} \left(\frac{1}{\Delta t}\mathrm{M} - \frac{1}{2}\mathrm{R}^{k}\right)\vec{u}^{k-\frac{1}{2}} - \frac{1}{2\mathrm{Re}}\mathrm{C}^{\intercal}\vec{\zeta}^{k-\frac{1}{2}} + \mathbf{f}^{k} + \mathbf{r}^{k} \\ \mathbf{0} \\ \mathbf{g}^{k} \end{bmatrix},$$

and present the adapted Euler step

$$\begin{bmatrix} \frac{2}{\Delta t}\mathrm{M} + \mathrm{R}^{0} & \frac{1}{\mathrm{Re}}\mathrm{C}^{\intercal} & \mathrm{G} \\ \mathrm{C} & -\mathrm{N} & \mathbf{0} \\ \mathrm{G}^{\intercal} & \mathbf{0} & \mathbf{0} \end{bmatrix} \begin{bmatrix} \vec{u}^{\frac{1}{2}} \\ \vec{\zeta}^{\frac{1}{2}} \\ \vec{p}^{0} \end{bmatrix} = \begin{bmatrix} \frac{2}{\Delta t}\mathrm{M}\vec{u}^{0} + \mathbf{f}^{0} + \mathbf{r}^{0} \\ \mathbf{0} \\ \mathbf{g}^{0} \end{bmatrix},$$

which computes $\vec{u}^{\frac{1}{2}}$ and $\vec{\zeta}^{\frac{1}{2}}$ from the initial data.

3.9 Conservation properties

As mentioned in section 3.5, the discrete de Rham complex (3.75) plays an essential role in transferring conservation properties from the continuous level into the finite dimensional function spaces. Section 3.7 showed, that mass and energy are conserved by the adapted scheme for the Dirichlet problem, while helicity is not in general. Based on a similar reasoning as laid out in section 3.5, these two quantities are also conserved in the discrete setting.

Chapter 4

Numerical experiments

Both the periodic as well as the Dirichlet scheme is implemented in the C++ software library `MFEM`. More information can be found following this link: https://mfem.org. The implementation of both schemes is available under this link: https://github.com/markusrenoldner/MEHCscheme.

As mentioned in the introduction of chapter 1, a general solution to the Navier-Stokes equations is not available. To test numerical methods that compute approximate solutions, one is faced with the challenge of determining whether a method produces a "good" approximation to this unknown solutions. Typically, convergence tests are employed that compute whether a certain error of the approximation gets smaller by refining the mesh size. However, one cannot just compare the numerical approximation to the exact solution, as the latter is not available. One popular approach is the idea of manufactured/forced solutions.

4.1 Manufactured solutions

We consider a generic differential equation problem, with an unknown solution u, a differential operator L and a right hand side f, with

$$L(u) = f.$$

If an arbitrary solution u^* is set in advance, then plugging this into L results in the right hand side f^*:

$$f^* := L(u^*).$$

u^* has to have enough regularity. Moreover, it must fulfil the boundary conditions, the vorticity contraint, and divergence-free condition. Ideally, it should also be representable by elementary functions or a programming routine. The problem to find u which solves

$$L(u) = f^*$$

with the very particular chosen right hand side, has the known solution

$$u = u^*.$$

Now the scheme can be tested by setting a manufactured solution u^*, finding the corresponding right hand side f^*, setting the correct initial value $u^*|_{t=0}$ and boundary values $u^*|_{\partial\Omega}$, and then checking, if the scheme finds this solution.

4.2 Convergence tests on periodic domains

For the convergence tests of the scheme, the so called Taylor-Green vortex solution (see a projection onto the xy-plane in figure 4.1) is being used:

$$\boldsymbol{u}^* : (x, y, z, t) \mapsto \begin{pmatrix} \cos(\pi x)\sin(\pi y)e^{-2t\nu} \\ -\sin(\pi x)\cos(\pi y)e^{-2t\nu} \\ 0 \end{pmatrix}. \tag{4.1}$$

Here $\nu = \frac{1}{\mathrm{Re}} = \frac{\mu}{\rho}$, compare with (1.8). The vorticity is just $\boldsymbol{\omega}^* := \nabla \times \boldsymbol{u}^*$. This solution is particularly handy, as the right hand side

$$f^* := \frac{\partial}{\partial t}\boldsymbol{u}^* + \boldsymbol{\omega}^* \times \boldsymbol{u}^* + \frac{1}{\mathrm{Re}}\nabla \times \boldsymbol{\omega}^*$$

is curl-free: $\nabla \times \boldsymbol{f}^* = 0$. This means, it is conservative ($\exists\psi$ with $\nabla\psi = \boldsymbol{f}^*$) and can be treated as an extended pressure, see section 1.5. That means, it can be set to 0 in the simulation run, which is practical implementation wise.

For $\mathrm{Re} \to \infty$, the Taylor-Green vortex solution becomes stationary:

$$\boldsymbol{u}^* : (x, y, z, t) \mapsto \begin{pmatrix} \cos(\pi x)\sin(\pi y) \\ -\sin(\pi x)\cos(\pi y) \\ 0 \end{pmatrix}. \tag{4.2}$$

The velocity field u^* is visualized in figure 4.1.

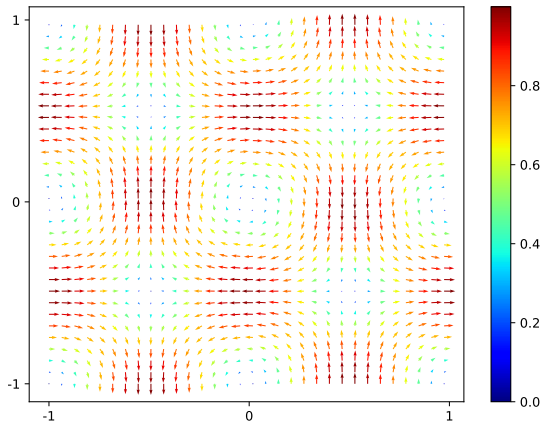

Figure 4.1: The Taylor-Green vortex solution.

The simulation domain is

$$\Omega := [-1, 1[^3$$

with a periodic boundary. The objective is to show:

$$\|\boldsymbol{u} - \boldsymbol{u^*}\|_2 \xrightarrow{h\to 0} 0, \tag{4.3}$$

$$\|\boldsymbol{v} - \boldsymbol{v^*}\|_2 \xrightarrow{h\to 0} 0, \tag{4.4}$$

$$\|\boldsymbol{u} - \boldsymbol{v}\|_2 \xrightarrow{h\to 0} 0. \tag{4.5}$$

In figure 4.2, we can see the experimental convergence results.

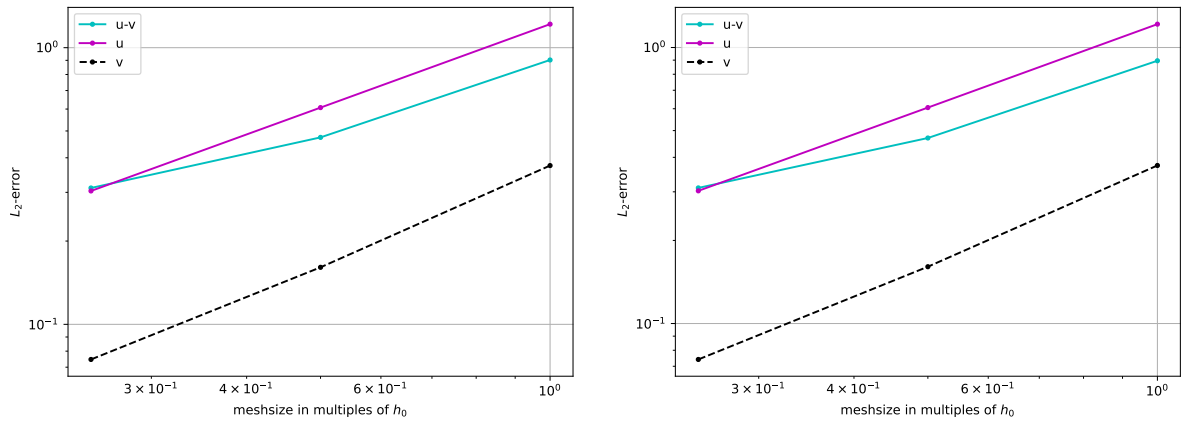

(a) Re = 500

(b) Re $\to \infty$

Figure 4.2: Convergence test of the scheme on a periodic domain, based on the Taylor-Green vortex solution with $\Delta t = 0.05$.

We clearly observe the expected convergence behaviour for all three characteristic errors. More test results can be found in [YR22].
The error $\|\boldsymbol{u} - \boldsymbol{v}\|_2$ is bounded by the sum the of the individual errors of the velocity fields. This can be shown by the triangle inequality:

$$\|\boldsymbol{u} - \boldsymbol{v}\|_2 = \|\boldsymbol{u} - \boldsymbol{v} + \boldsymbol{u}^* - \boldsymbol{u}^*\|_2 \leq \|\boldsymbol{u} - \boldsymbol{u}^*\|_2 + \|\boldsymbol{v} - \boldsymbol{u}^*\|_2. \tag{4.6}$$

Indeed, figure 4.2 shows that this property is fulfilled.

4.3 Conservation tests on periodic domains

As mentioned, the second important property of the scheme, next to convergence, is the conservation of mass, kinetic energy and helicity. As mentioned before (in sections 1.5, 2.3, 3.2, and 3.5), it is supposed that $\mathbf{f} := \mathbf{0}$ and Re $\to \infty$.

For the conservation test, the solution, from [YR22], is used:

$$\boldsymbol{u}^* : (x, y, z, t) \mapsto \begin{pmatrix} \cos(2\pi z) \\ \sin(2\pi z) \\ \sin(2\pi x) \end{pmatrix}, \tag{4.7}$$

and again $\boldsymbol{\omega}^* := \nabla \times \boldsymbol{u}^*$ and $\nabla \times \boldsymbol{f} = 0$. The velocity field is visualized in figure 4.3.

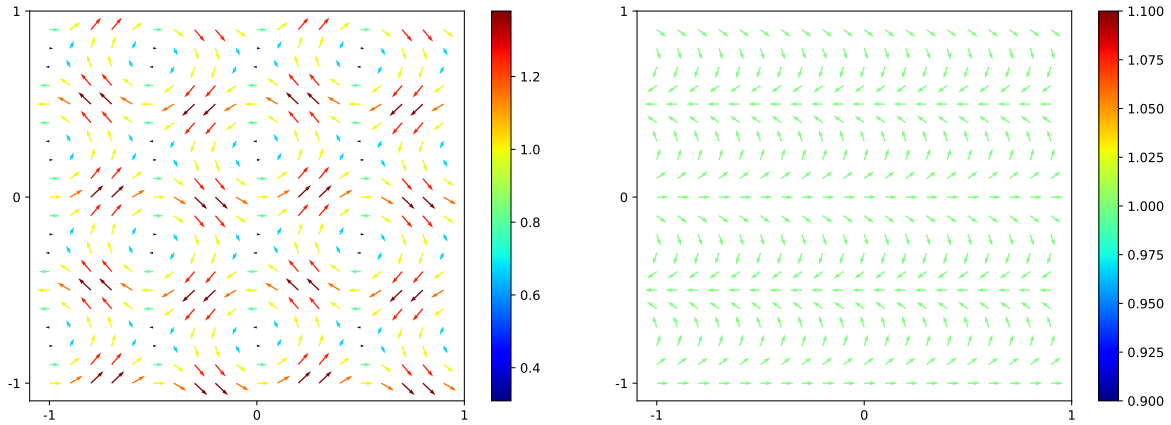

Figure 4.3: Left: xz-plane, right: xy-plane.

In this case, u^* is not a manufactured solution, but rather an initial condition. $\boldsymbol{f}$ is set to 0 and the flow field is free to evolve according to the equations. The analytical solution is unknown.

As described in section 3.2, it is expected to get

$$\mathrm{D}\vec{v}^k = 0, \tag{4.8}$$

$$\mathrm{G}^\intercal \vec{u}^{k+\frac{1}{2}} = 0, \tag{4.9}$$

$$\mathcal{K}_1^{k+\frac{1}{2}} - \mathcal{K}_1^{k-\frac{1}{2}} = 0, \tag{4.10}$$

$$\mathcal{K}_2^{k+\frac{1}{2}} - \mathcal{K}_2^{k-\frac{1}{2}} = 0, \tag{4.11}$$

$$\mathcal{H}_1^{k+\frac{1}{2}} - \mathcal{H}_1^{k-\frac{1}{2}} = 0, \tag{4.12}$$

$$\mathcal{H}_2^{k+\frac{1}{2}} - \mathcal{H}_2^{k-\frac{1}{2}} = 0 \tag{4.13}$$

for all k. The matrices in the first two lines represent the divergence operators. In figures 4.4, 4.5, and 4.6, we can see the experimental conservation results.

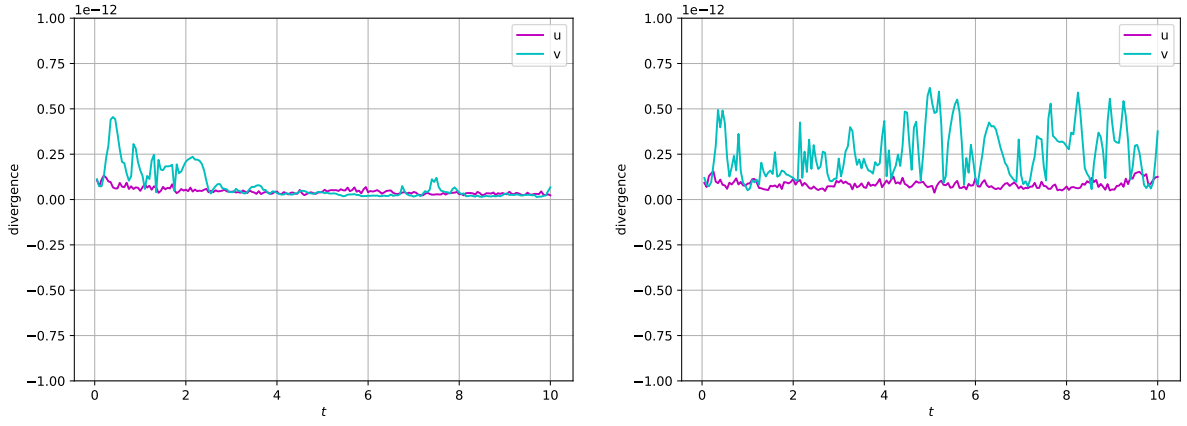

(a) Re = 100

(b) Re $\to \infty$

Figure 4.4: Mass conservation properties of periodic problem with $\Delta t = 0.05$.

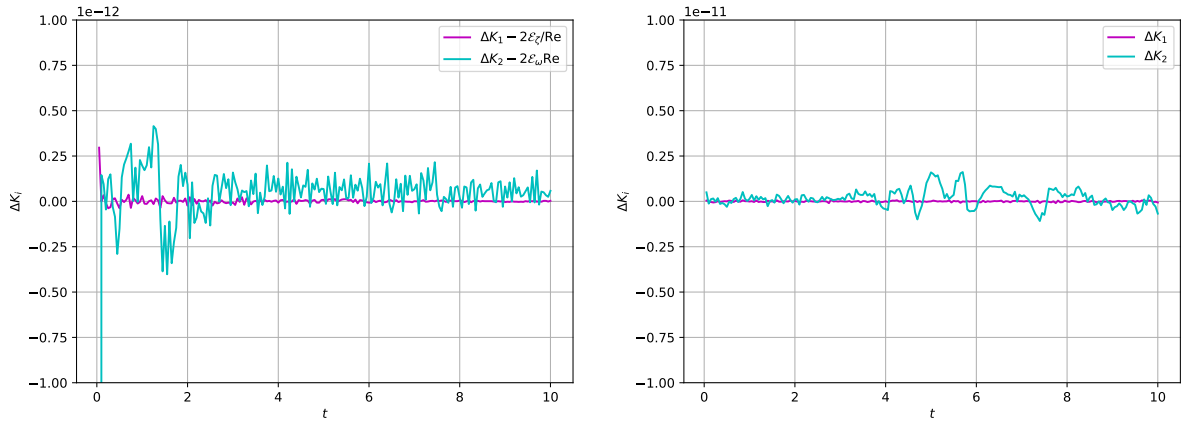

(a) Re = 100 (b) Re $\to \infty$

Figure 4.5: Energy conservation properties of periodic problem with $\Delta t = 0.05$.

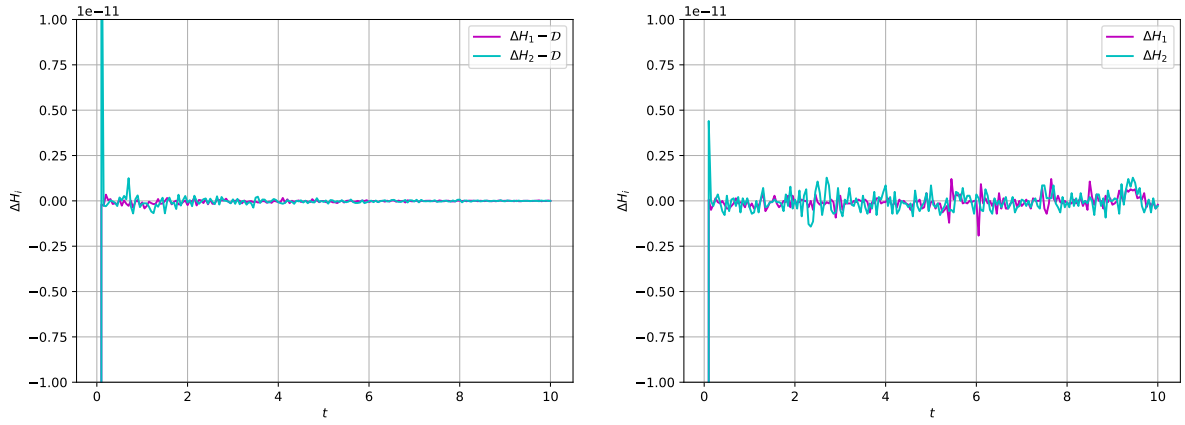

(a) Re = 100 (b) Re $\to \infty$

Figure 4.6: Helicity conservation properties of periodic problem with $\Delta t = 0.05$.

We can observe, that the data lines are at the order of 10^-11 to 10^-12, except for some initial spikes. This means all three quantities are numerically conserved by the simulation.

4.4 Convergence tests for the Dirichlet problem

In the following, the implementation of the Dirichlet problem is numerically tested.

4.4.1 Simple test case

Again, the technique of manufactured solutions was employed, see section 4.1 for an introduction. Consider

$$\boldsymbol{u}^* : (x, y, z) \mapsto \begin{pmatrix} \sin(y) \\ \sin(z) \\ 0 \end{pmatrix}. \tag{4.14}$$

From this, one gets

$$\boldsymbol{\omega}^* : (x, y, z) \mapsto \begin{pmatrix} -\cos(z) \\ 0 \\ -\cos y \end{pmatrix}, \tag{4.15}$$

and an appropriate function

$$\boldsymbol{f}^* := \boldsymbol{u}^* \times \boldsymbol{\omega}^* + \frac{1}{\mathrm{Re}} \nabla \times \boldsymbol{\omega}^*$$

enforcing the solutions above. Here, the simulation domain is the cube

$$\Omega := [0, 1]^3$$

with a periodic boundary (see section 2.2). The time step size is scaled proportionally with the mesh size.
In the following, we see the experimental results. The simulation is run for different Reynolds numbers to investigate the code behaviour in viscous and inviscid scenarios. Furthermore, not only do we compute the L^2-error of both velocity fields with respect to the analytical solution $\boldsymbol{u}^*$, but also the error between the two velocity fields, given as

$$\|\boldsymbol{u} - \boldsymbol{v}\|_2.$$

The goal is again to observe error convergence in the L^2-norm induced by the refinement of the element size h.

$$\|\boldsymbol{u} - \boldsymbol{u}^*\|_2 \xrightarrow{h \to 0} 0 \tag{4.16}$$

$$\|\boldsymbol{v} - \boldsymbol{v}^*\|_2 \xrightarrow{h \to 0} 0 \tag{4.17}$$

$$\|\boldsymbol{u} - \boldsymbol{v}\|_2 \xrightarrow{h \to 0} 0. \tag{4.18}$$

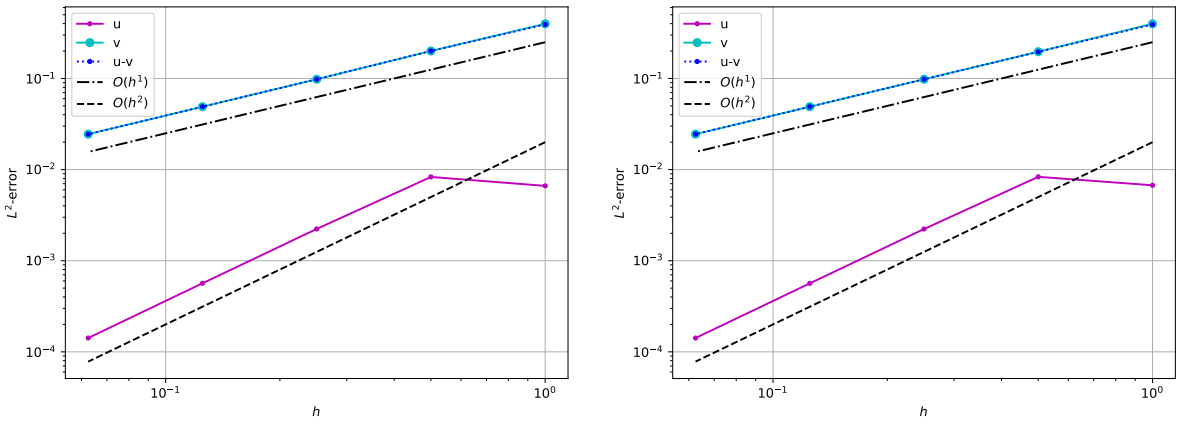

(a) Re = 1 (b) Re → ∞

Figure 4.7: Dirichlet problem with initial time step $\Delta t = 0.01$ and simple test case.

The initial time step is $\Delta t = 0.01$, and gets scaled by the factor 0.5 in each h-refinement step. The result is visualized in figure 4.7. We observe second order algebraic convergence for $\boldsymbol{u}$ and first order convergence for $\boldsymbol{v}$. This results in first order convergence of $\|\boldsymbol{u} - \boldsymbol{v}\|_2$. The reason for this unexpected second order convergence is to be investigated. Numeric values of the convergence errors are available in table 4.1.

Re	h	$\|\boldsymbol{u}-\boldsymbol{u}^*\|_2$	$\|\boldsymbol{v}-\boldsymbol{u}^*\|_2$	$\|\boldsymbol{u}-\boldsymbol{v}\|_2$	upper bound
1	1	0.006628570114628	0.398148612608578	0.391586895520635	0.404777183
1	0.5	0.008307301320286	0.200180356636513	0.200330545008355	0.208487658
1	0.25	0.002232597196012	0.098044051690552	0.097923625209320	0.100276649
1	0.125	0.000565064956576	0.048978316388722	0.048970197989106	0.049543381
1	0.0625	0.000141930771266	0.024484870179413	0.024483872950107	0.024626801
∞	1	0.006728776980671	0.398149435237438	0.391490754428929	0.404878212
∞	0.5	0.008328292452058	0.196610489356292	0.196043593196481	0.204938782
∞	0.25	0.002228741730293	0.098025217955023	0.097960519049936	0.10025396
∞	0.125	0.000564117238773	0.048978316312136	0.048970411113299	0.049542434
∞	0.0625	0.000141779654244	0.024484870147842	0.024483891923531	0.02462665

Table 4.1: Dirichlet convergence results for the simple test case and first order polynomials.

In the last column of table 4.1, the sum of the two errors is presented, providing an upper bound for $\|\boldsymbol{u}-\boldsymbol{v}\|_2$, as mentioned in (4.6):

$$\|\boldsymbol{u}-\boldsymbol{v}\|_2 \leq \|\boldsymbol{u}-\boldsymbol{u}^*\|_2 + \|\boldsymbol{v}-\boldsymbol{u}^*\|_2. \tag{4.19}$$

This property is fulfilled by the simulation.
Next, we repeat the same convergence analysis with second order polynomials. The Finite Element spaces introduced in sections 3.3 were based on the lowest order basis functions available. By increasing the number of degrees of freedom (i.e. functionals) on each element, higher order polynomials can be used for the interpolation. This results in a faster convergence.
The initial time step size is $\Delta t = 0.0001$, and gets scaled by a factor of 0.5 in each h-refinement step.
The result is visualized in figure 4.8. We observe second order algebraic convergence for $\boldsymbol{v}$, and third order for $\boldsymbol{u}$. Again, the convergence order of $\boldsymbol{u}$ is higher by one degree, which has to be investigated further. We observe second order convergence of $\|\boldsymbol{u}-\boldsymbol{v}\|_2$, according to our expectations.

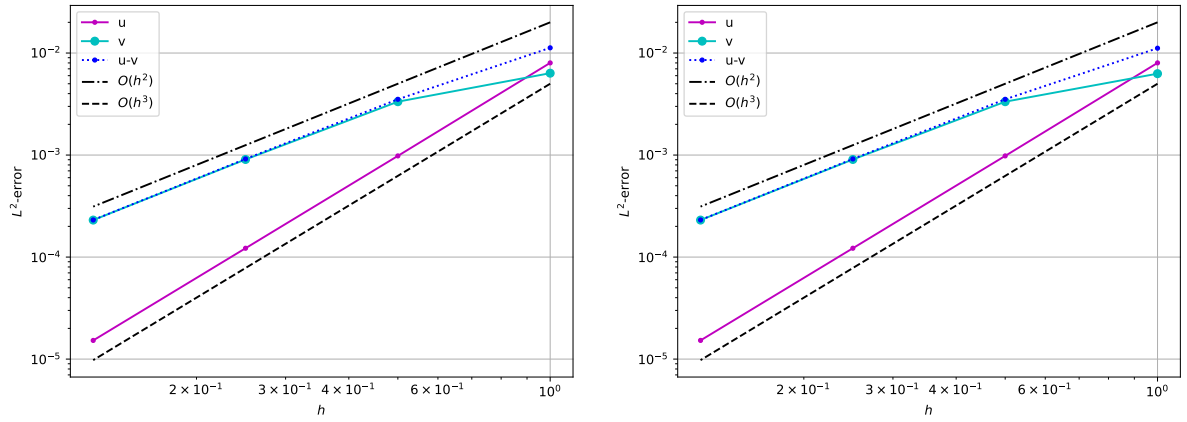

(a) Re = 1 (b) Re $\to \infty$

Figure 4.8: Dirichlet problem with $\Delta t = 0.0001$ and simple test case, polynomial order 2.

We present the numeric values of this simulation run in table 4.2. The sum of the individual errors of the velocity field again serves as an upper bound for $\|u - v\|_2$.

Re	h	$\|\boldsymbol{u} - \boldsymbol{u}^*\|_2$	$\|\boldsymbol{v} - \boldsymbol{u}^*\|_2$	$\|\boldsymbol{u} - \boldsymbol{v}\|_2$	upper bound
1	1	0.008005403333848	0.006346807240612	0.011249816066726	0.014352211
1	0.5	0.000980947844309	0.003334822183735	0.003519246033795	0.00431577
1	0.25	0.000122066370995	0.000905247685748	0.000915893255160	0.001027314
1	0.125	0.000015240892530	0.000230483767606	0.000231115426870	0.000245725
∞	1	0.008005592985507	0.006276244779475	0.011152394282438	0.014281838
∞	0.5	0.000981129525541	0.003334828940359	0.003519546289255	0.004315958
∞	0.25	0.000122103523918	0.000905248069786	0.000915993904077	0.001027352
∞	0.125	0.000015246664203	0.000230483791941	0.000231144460241	0.00024573

Table 4.2: Dirichlet convergence results for the simple test case and second order polynomials.

4.4.2 Static Taylor-Green vortex

In order to test a more complex solution, we consider the static Taylor-Green vortex. The velocity field is defined as

$$\boldsymbol{u}^* : (x, y, z, t) \mapsto \begin{pmatrix} \cos(x)\sin(y) \\ -\sin(x)\cos(y) \\ 0 \end{pmatrix},$$

and the vorticity field reads as

$$\boldsymbol{\omega}^* : (x, y, z, t) \mapsto \begin{pmatrix} 0 \\ 0 \\ -2\cos x \cos y \end{pmatrix}.$$

The corresponding forcing term producing this solution is

$$f^* := \boldsymbol{u}^* \times \boldsymbol{\omega}^* + \frac{1}{\mathrm{Re}} \nabla \times \boldsymbol{\omega}^*.$$

Similar as before, we study convergence of the three characteristic errors. The initial time step size of the simulation is $\Delta t = 0.01$, which is scaled by a factor of 0.5 in each mesh refinement step. The computation is being executed in the viscous case with $\mathrm{Re} = 1$ and in the inviscid limit case. First, we run the simulation with first order polynomials.
In the following, the convergence results are presented.

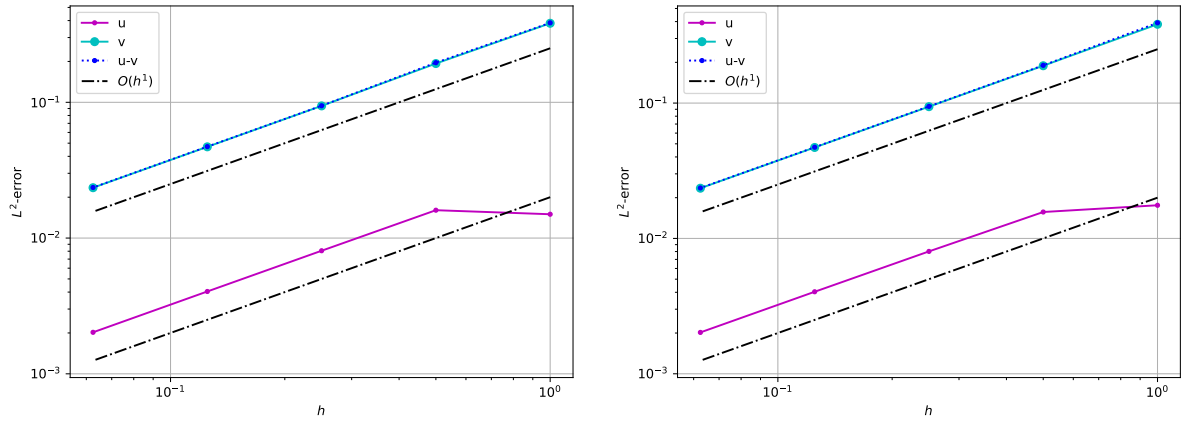

(a) Re = 1

(b) Re $\to \infty$

Figure 4.9: Dirichlet problem with $\Delta t = 0.01$ and static Taylor-Green vortex.

In figure 4.9, we can see the errors plotted over the refinement parameter. We observe first order convergence for all errors, as indicated by the trend lines.
The numerical values of the simulation run are available in table 4.3. Again, $\|\boldsymbol{u}-\boldsymbol{v}\|_2$ is bounded by the individual errors, as described in (4.19).

Re	h	$\|\boldsymbol{u}-\boldsymbol{u}^*\|_2$	$\|\boldsymbol{v}-\boldsymbol{u}^*\|_2$	$\|\boldsymbol{u}-\boldsymbol{v}\|_2$	upper bound
1	1	0.014979725687275	0.382122725318314	0.384954954889798	0.397102451
1	0.5	0.016040911244075	0.193013919771353	0.195847673579863	0.209054831
1	0.25	0.008065063706084	0.094100652643297	0.094331702420279	0.102165716
1	0.125	0.004041467773636	0.046998305809297	0.047165292758361	0.051039774
1	0.0625	0.002022055367185	0.023494669357557	0.023580711948304	0.025516725
∞	1	0.017579390530157	0.382126799975606	0.391555964937185	0.399706191
∞	0.5	0.015673010784122	0.188703214355522	0.190070277071841	0.204376225
∞	0.25	0.008019208940548	0.094067644530848	0.094489481391918	0.102086853
∞	0.125	0.004035764006117	0.046998387034079	0.047181212736714	0.051034151
∞	0.0625	0.002021373099056	0.023494679275140	0.023582727794630	0.025516052

Table 4.3: Dirichlet convergence results for the static Taylor-Green case and first order polynomials.

Next, we perform the simulation with the static Taylor-Green vortex with second order polynomials. The initial time step size is $\Delta t = 0.0001$ and the time step refinement is being performed according to the previous experiments. The results are visualized in 4.10.

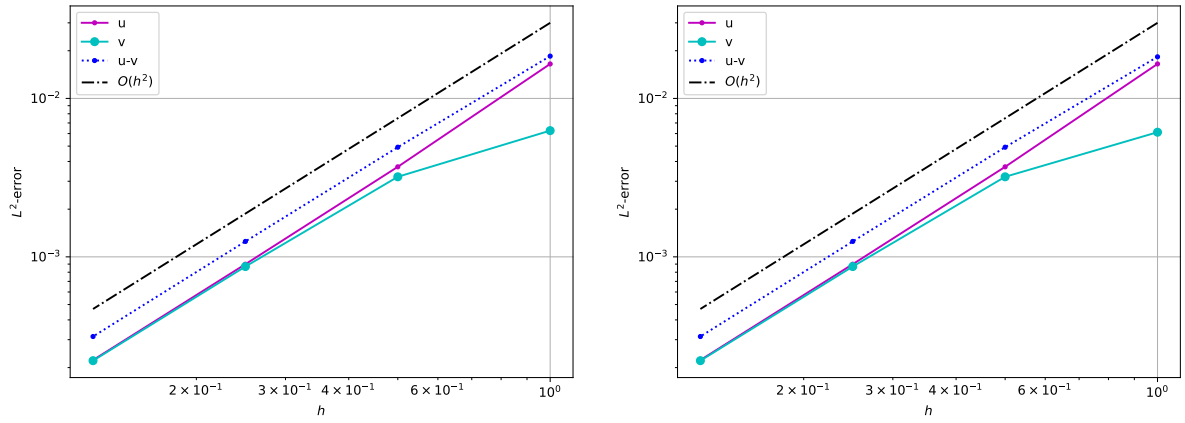

(a) Re = 1

(b) Re $\to \infty$

Figure 4.10: Dirichlet problem with $\Delta t = 0.0001$ and static Taylor-Green vortex, polynomial order 2.

This is now the first convergence test in which the error $\|\boldsymbol{u} - \boldsymbol{v}\|_2$ is not visually overlaid by one of the individual errors. The reason is that both $\|\boldsymbol{u}\|_2$ and $\|\boldsymbol{v}\|_2$ have values of similar decimal order. These values are presented in table 4.4.

Re	h	$\|\boldsymbol{u} - \boldsymbol{u}^*\|_2$	$\|\boldsymbol{v} - \boldsymbol{u}^*\|_2$	$\|\boldsymbol{u} - \boldsymbol{v}\|_2$	upper bound
1	1	0.016507721126609	0.006262822381964	0.018491314018883	0.022770544
1	0.5	0.003700770041315	0.003201201955722	0.004921792598675	0.006901972
1	0.25	0.000898723281834	0.000868691502419	0.001251439211959	0.001767415
1	0.125	0.000223024467376	0.000221164274436	0.000314153121369	0.000444189
∞	1	0.016508067364217	0.006120429946462	0.018308206754946	0.022628497
∞	0.5	0.003700867911462	0.003201215212636	0.004922216910205	0.006902083
∞	0.25	0.000898733185419	0.000868692268736	0.001251581188609	0.001767425
∞	0.125	0.000223025209084	0.000221164322487	0.000314192392966	0.00044419

Table 4.4: Dirichlet convergence results for the static Taylor-Green case and second order polynomials.

In figures 4.11, and 4.12, we have visualized the exact solution of the Taylor-Green vortex, as well as the solution computed by the scheme.

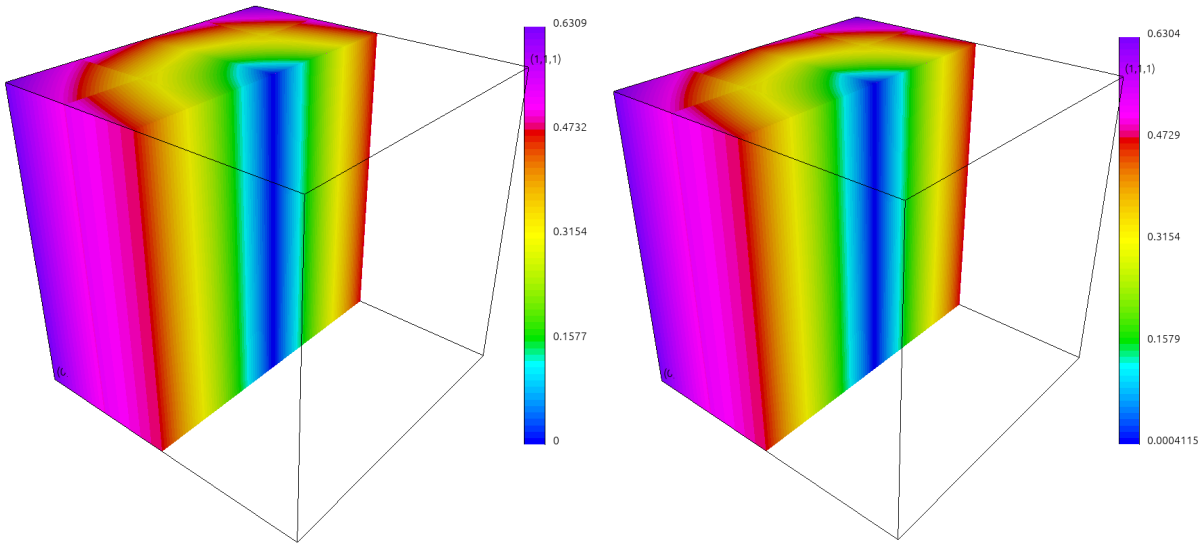

(a) Exact solution

(b) Simulated solution $\boldsymbol{u} \in H(\mathrm{curl}, \Omega)$

Figure 4.11: Comparison of the exact and simulated solution for the Taylor-Green vortex convergence test, after 3 refinement steps.

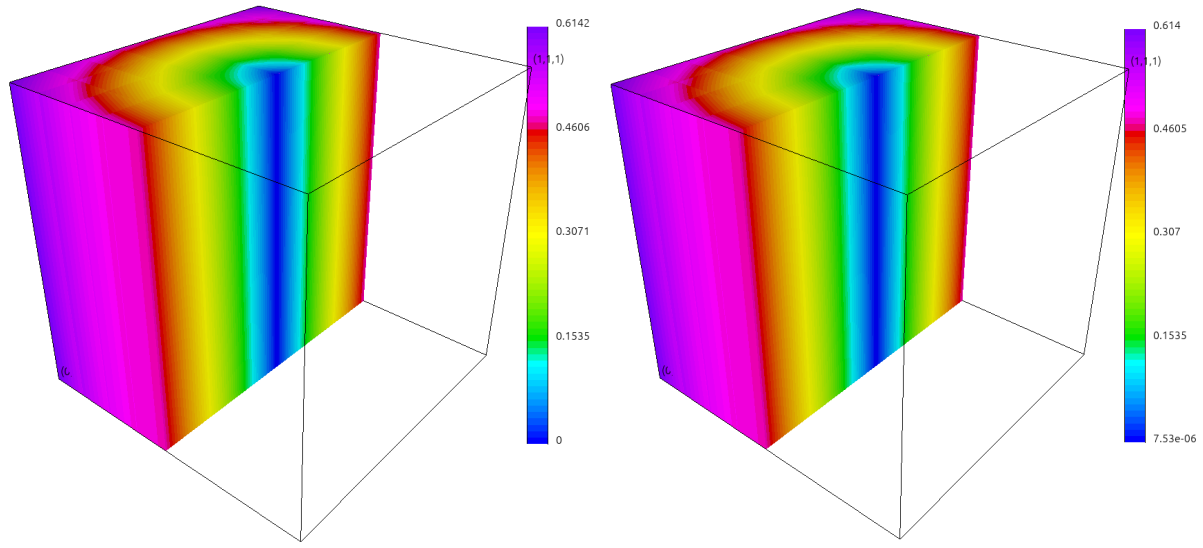

(a) Exact solution

(b) Simulated solution $\boldsymbol{u} \in H(\mathrm{curl}, \Omega)$

Figure 4.12: Comparison of the exact and simulated solution for the Taylor-Green vortex convergence test, after 4 refinement steps.

4.4.3 Dynamic, decaying Taylor-Green vortex

An example of a known time-dependent solution of the Navier-Stokes equations is the decaying Taylor-Green vortex with the velocity field

$$\boldsymbol{u}^* : (t, x, y, z) \mapsto \begin{pmatrix} \cos(x)\sin(y)e^{-2t/\mathrm{Re}} \\ -\sin(x)\cos(y)e^{-2t/\mathrm{Re}} \\ 0 \end{pmatrix},$$

and the vorticity field

$$\boldsymbol{\omega}^* : (x, y, z, t) \mapsto \begin{pmatrix} 0 \\ 0 \\ -2\cos x \cos y \exp -2t/\mathrm{Re} \end{pmatrix}.$$

The corresponding forcing term producing this solution is

$$f^* := \boldsymbol{u}^* \times \boldsymbol{\omega}^* + \frac{1}{\mathrm{Re}} \nabla \times \boldsymbol{\omega}^*.$$

Similar as before, we study error convergence. The initial time step size is again $\Delta t = 0.01$ scaled as before. The computation is being executed in the viscous case with $\mathrm{Re} = 1$ and in the inviscid limit case. We use first order polynomials.

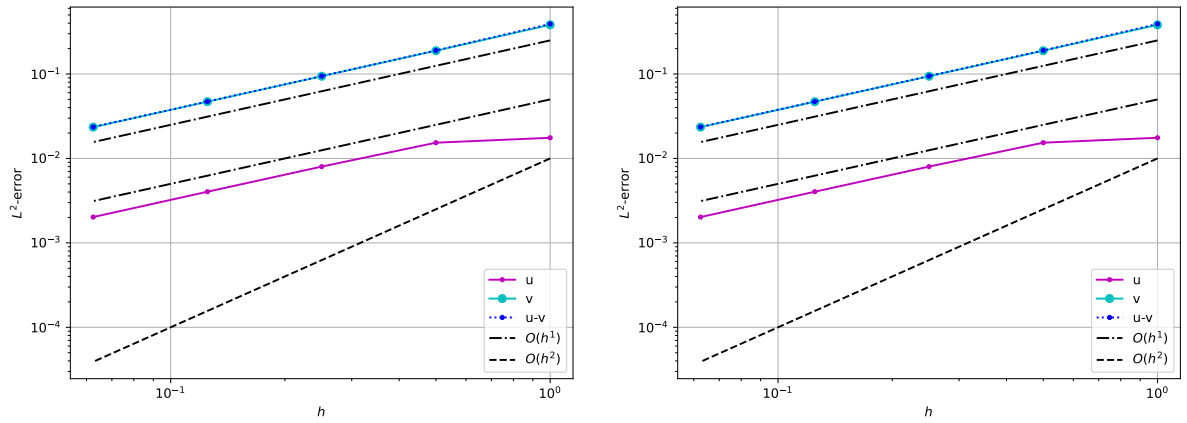

(a) $\mathrm{Re} = 1$ (b) $\mathrm{Re} \to \infty$

Figure 4.13: Dirichlet problem with $\Delta t = 0.01$ and dynamic Taylor-Green vortex.

We have first order convergence for both velocity fields, see 4.13. The numeric values are presented in table 4.5.

Re	h	$\|\boldsymbol{u} - \boldsymbol{u}^*\|_2$	$\|\boldsymbol{v} - \boldsymbol{u}^*\|_2$	$\|\boldsymbol{u} - \boldsymbol{v}\|_2$	upper bound
1	1	0.0175546909023	0.3819411198245	0.3913326371271	0.399495811
1	0.5	0.0153630713535	0.1886407945622	0.1900001043699	0.204003866
1	0.25	0.0080052172660	0.0940440506757	0.0944640528941	0.102049268
1	0.125	0.0040342338953	0.0469879726482	0.0471700743576	0.051022207
1	0.0625	0.0020209065236	0.0234897568201	0.0235772653149	0.025510663
∞	1	0.0175793905301	0.3820175156878	0.3914493130797	0.399596906
∞	0.5	0.0153649109698	0.1886789843780	0.1900427041839	0.204043895
∞	0.25	0.0080069029913	0.0940630152283	0.0944847837769	0.102069918
∞	0.125	0.0040351191423	0.0469974108627	0.0471801892679	0.05103253
∞	0.0625	0.0020212628147	0.0234944577745	0.0235824674407	0.025515721

Table 4.5: Dirichlet convergence results for the dynamic Taylor-Green case and first order polynomials.

4.5 Conservation tests for the Dirichlet problem

In this section, the conservation properties derived in sections 3.7 and 3.9 are analyzed numerically. An initial condition for the velocity and vorticity fields is utilized, together with appropriate boundary data. As mentioned in the conservation proofs on the continuous and discrete level, conservation of energy only holds in cases of vanishing boundary integrals. Intuitively speaking: we do not want transport of energy across the domain boundaries, therefore we set the (normal component of the) velocity to zero. For this, we construct a non-trivial initial velocity field. The requirements are:

- Vanishing boundary conditions
- Enough regularity
- Vorticity contraint fulfilled
- Divergence-free condition fulfilled
- Representability by elementary functions or programming routine

We start with a simple divergence-free vortex:

$$\boldsymbol{u}_0 : (x, y, z) \mapsto \begin{pmatrix} y \\ -x \\ 0 \end{pmatrix}.$$

To enforce vanishing boundary conditions with enough regularity, the velocity is multiplied by a bump-function that vanishes at a certain radius around the origin. It is given as

$$b : (x, y, z) \mapsto \cos^4(K(x^2 + y^2 + z^2)).$$

The radius where b vanishes is

$$R_K = \frac{1}{2}\sqrt{\frac{2\pi}{K}}.$$

K has to be chosen such that $\boldsymbol{u}_0$ vanishes within Ω. The resulting velocity initial condition is

$$\boldsymbol{u}_0 : (x, y, z) \mapsto \begin{cases} \cos^4(K(x^2 + y^2 + z^2)) \cdot \begin{pmatrix} y \\ -x \\ 0 \end{pmatrix} & \text{if } x^2 + y^2 + z^2 < R_K^2 \\ 0 & \text{else.} \end{cases} \tag{4.20}$$

The initial vorticity is given as

$$\boldsymbol{\omega}_0 : (x, y, z) \mapsto \begin{cases} \nabla \times \boldsymbol{u}_0 & \text{if } x^2 + y^2 + z^2 < R_K^2 \\ 0 & \text{else,} \end{cases}$$

which fulfils the vorticity constraint. $\mathbf{f}$ is set to 0 and the evolution of the flow is being observed. The analytical solution is not available.
We now want to investigate the conservation properties of the implementation. We expect a divergence-free velocity field and a conservation of kinetic energy. As the primal divergence-free condition now contains a boundary integral, see section 3.8, we now expect

$$\mathrm{D}\vec{v}^k = 0, \tag{4.21}$$

$$\mathrm{G}^\intercal \vec{u}^{k+\frac{1}{2}} - \mathrm{g}^{k-\frac{1}{2}} = 0, \tag{4.22}$$

and for the kinetic energies (in the inviscid limit case)

$$\mathcal{K}_1^{k+\frac{1}{2}} - \mathcal{K}_1^{k-\frac{1}{2}} = 0, \tag{4.23}$$

$$\mathcal{K}_2^{k+\frac{1}{2}} - \mathcal{K}_2^{k-\frac{1}{2}} = 0. \tag{4.24}$$

The simulation is run with a time step size of $\Delta t = 0.05$. The results are presented in figures 4.14 and 4.15. Both the viscous case and in the inviscid limit case, i.e. with $\mathrm{Re} \to \infty$ are being analyzed.

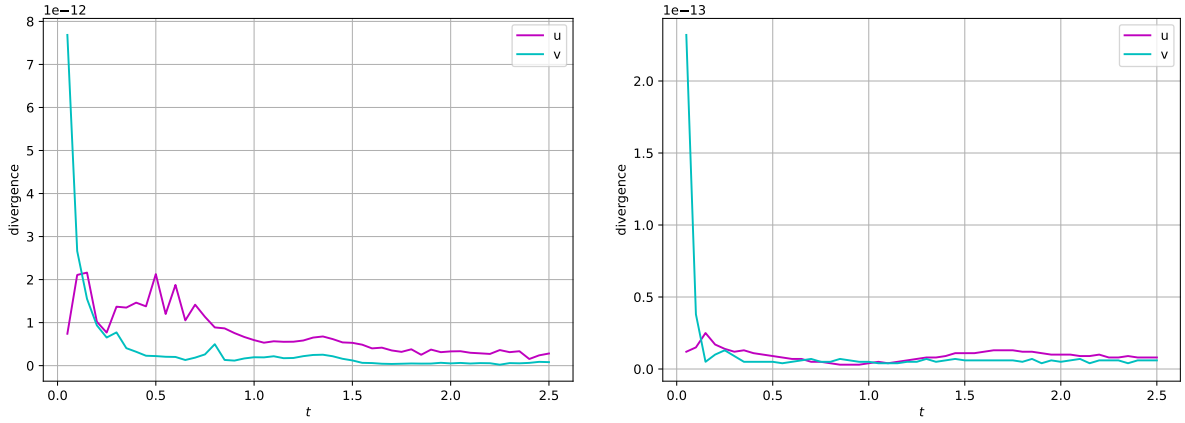

(a) $\mathrm{Re} = 1$ (b) $\mathrm{Re} \to \infty$

Figure 4.14: Mass-conservation properties of Dirichlet problem with $\Delta t = 0.05$.

As mentioned before, in the viscous case, energy is being dissipated. In the figure 4.15, this is corrected by the predicted dissipation rate, see (3.84).

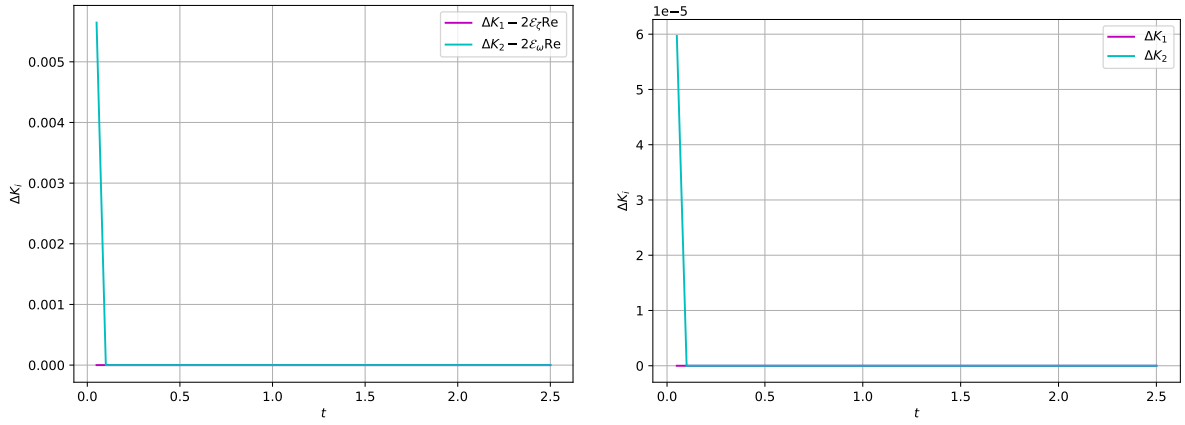

(a) $\mathrm{Re} = 1$ (b) $\mathrm{Re} \to \infty$

Figure 4.15: Energy-conservation properties of Dirichlet problem with $\Delta t = 0.05$.

As visible both the divergence-free condition and the kinetic energy conservation are being reproduced by the simulation.

4.5.1 Helicity conservation

It turns out, the previous conservation test, with the initial velocity (4.20) also conserves helicity in both the viscous and the inviscid limit case. The result is presented in figure 4.16.

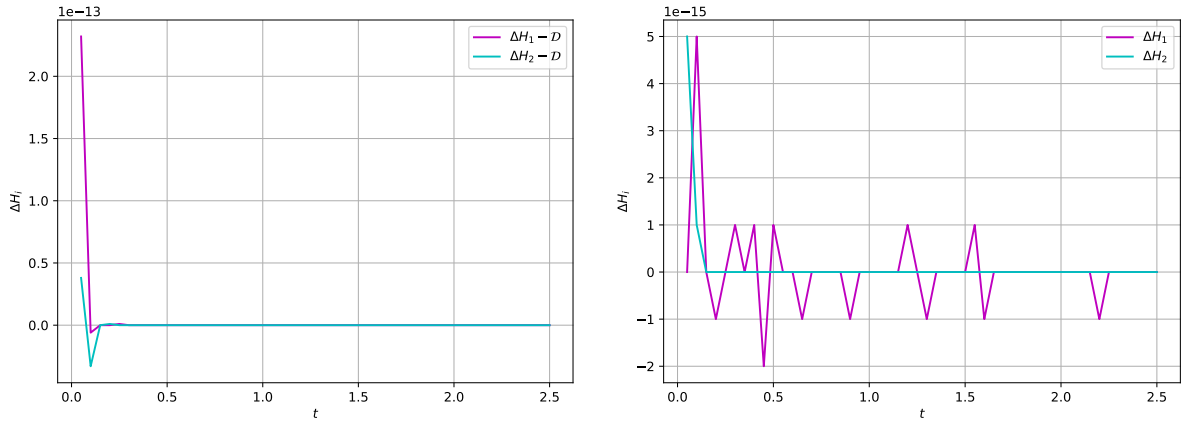

(a) $\mathrm{Re} = 1$ (b) $\mathrm{Re} \to \infty$

Figure 4.16: Helicity-conservation properties of Dirichlet problem with $\Delta t = 0.05$.

One hypothesis for the reason for this behaviour is that by choosing $\boldsymbol{u}_0$ like described above, see (4.20), the boundary values of the velocity and vorticity vanish. Therefore, we might have implicitly chosen functions that are elements of the function spaces which form a de Rham complex with essential boundary conditions, see 2.56.
This behaviour is to be investigated more thoroughly in the future.

Chapter 5

Conclusion

In this thesis, a structure-preserving dual-field scheme for the incompressible Navier-Stokes problem from [YR22] was extended to a much more realistic, non-periodic problem with Dirichlet boundary conditions. The convergence and conservation results of the original scheme for periodic domains were reproduced. Furthermore, numerical experiments for the convergence and conservation properties of the new method for non-periodic domains were presented.
The results not only show the expected convergence behaviour, but also point out several other benefits of the proposed method. Firstly, the linearization of the convective term by the means of a staggered time integrator results in two smaller system matrices instead of one large matrix. This speeds up computation time significantly. Secondly, the scheme computes two velocity fields, that can be used for error estimation. More work is required to check, if the available local difference between the two solutions can be exploited for techniques like adaptive mesh refinement.
Conservation of mass, kinetic energy, and helicity is successfully transferred into the fully discrete formulation of the problem for periodic domains. For non-periodic domains and Dirichlet boundary data, helicity is not conserved in the general case.

Bibliography

[A A18] L. Biferale A. Alexakis. "Cascades and transitions in turbulent flows". In: *Physics Reports* 767-769 (Aug. 2018). DOI: 10.1016/j.physrep.2018.08.001 (cit. on p. 12).

[Bar18] M. Bartelmann. *Theoretische Physik 1 - Mechanik*. Springer, 2018 (cit. on pp. 6, 7, 11).

[Cap15] Coppola Capuano Francesco. "Energy preserving turbulent simulations at a reduced computational cost". In: *Journal of Computational Physics* 298 (Oct. 2015). DOI: 10.1016/j.jcp.2015.06.011 (cit. on p. 12).

[Cap18] Vallefuoco Capuano Francesco. "Effects of Discrete Energy and Helicity Conservation in Numerical Simulations of Helical Turbulence". In: *Flow Turbulence and Combustion* 101 (Sept. 2018), pp. 343–364. DOI: 10.1007/s10494-018-9939-x (cit. on p. 12).

[CCE02] Qiaoning Chen, Shiyi Chen, and Gregory Eyink. "The Joint Cascade of Energy and Helicity in Three-Dimensional Turbulence". In: *Physics of Fluids* 15 (June 2002). DOI: 10.1063/1.1533070 (cit. on p. 12).

[E A04] J.L. Guermond E. Alexandre. *Theory and Practice of Finite Elements*. Springer, 2004 (cit. on p. 13).

[Fau22] M. Faustmann. *Numerical Methods for Partial Differential Equations, Lecture notes*. 2022 (cit. on pp. 13, 25).

[Hip22] R. Hiptmair. *Numerical Methods for Partial Differential Equations, Lecture notes*. 2022. URL: https://people.math.ethz.ch/~grsam/NUMPDEFL/NUMPDE.pdf (cit. on pp. 13, 22, 25).

[Mon03] P. Monk. *Finite Element Methods for Maxwell's Equations*. Oxford University Press, Apr. 2003. ISBN: 9780198508885. DOI: 10.1093/acprof:oso/9780198508885.001.0001 (cit. on pp. 13, 15).

[MW08] P. Orlandi M. Duponcheel and G. Winckelmans. "Time-reversibility of the Euler equations as a benchmark for energy conserving schemes". In: *Journal of Computational Physics* 227 (Oct. 2008), pp. 8736–8752. DOI: 10.1016/j.jcp.2008.06.020 (cit. on p. 12).

[Olv82] P. J. Olver. "A nonlinear Hamiltonian structure for the Euler equations". In: *Journal of Mathematical Analysis and Applications* 89.1 (1982), pp. 233–250. ISSN: 0022-247X. DOI: https://doi.org/10.1016/0022-247X(82)90100-7 (cit. on p. 11).

[Sch18] J. Schöberl. *Numerical Methods for Partial Differential Equations, Lecture notes*. 2018. URL: https://www.asc.tuwien.ac.at/~schoeberl/wiki/lva/numpde18/numpde.pdf (cit. on pp. 13, 14, 15, 25).

[V G12] P.A. Raviart V. Girault. *Finite Element Methods for Navier-Stokes Equations: Theory and Algorithms*. Springer Series in Computational Mathematics. Springer Berlin Heidelberg, 2012. ISBN: 9783642616235. URL: https://books.google.fr/books?id=8C7vCAAAQBAJ (cit. on pp. 13, 15).

[Val19] Capuano Vallefuoco Donato. "Discrete Conservation of Helicity in Numerical Simulations of Incompressible Turbulent Flows". In: *ERCOFTAC Series* (Jan. 2019), pp. 17–22. DOI: 10.1007/978-3-030-04915-7_3 (cit. on p. 12).

[YR22] M. Gerritsma Y. Zhang A. Palha and L. G. Rebholz. "A mass-, kinetic energy- and helicity-conserving mimetic dual-field discretization for three-dimensional incompressible Navier-Stokes equations, part I: Periodic domains". In: *Journal of Computational Physics* 451 (Feb. 2022), p. 110868. DOI: 10.1016/j.jcp.2021.110868 (cit. on pp. 11, 12, 13, 17, 25, 43, 49, 62).

[Zag06] S. Zaglmayr. "High Order Finite Element Methods for Electromagnetic Field Computation". In: (2006) (cit. on p. 24).